Electronic Thesis and Dissertation Repository

9-6-2017 2:30 PM

# A Study on Hydraulic Conductivity of Fine Oil Sand Tailings

Mingyue LIU
*The University of Western Ontario*

Supervisor
Julie Q Shang
*The University of Western Ontario*

Follow this and additional works at: https://ir.lib.uwo.ca/etd

Part of the Geotechnical Engineering Commons

## Recommended Citation

# ABSTRACT

In oil sand waste tailings pond, the gravity segregation takes place, where coarse particles settle relatively more quickly than fine particles, and a stable suspension, known as the mature fine tailings (MFT), is formed. Compression of MFT appears to be very slow, and MFT remains suspended in tailings pond for decades due to the low permeability. Large volumes of MFT continually accumulate in tailings ponds, and therefore MFT storage requires a large containment pond, which generates environmental concerns and leads to MFT management challenges. Hydraulic conductivity is one of the most important properties of MFT because it controls consolidation behaviors. Clear understandings of hydraulic conductivity and its relationship with void ratio are essential to MFT management and treatment.

This study establishes the relationship between hydraulic conductivity and a relatively wide range of void ratios for MFT through three laboratory tests, i.e. the standard oedometer test, the falling head test and the Rowe cell test. Based on the hydraulic conductivity data of this study together with the data reported in the literature, data regression models are developed to correlate the hydraulic conductivity with a wide range of void ratios (k-e relationship) for fine oil sand tailings. Empirical equations, which were proposed to predict the hydraulic conductivity for plastic soils, are evaluated their suitability and performances in terms of predicting the hydraulic conductivity for fine oil sand tailings.

*Key words*: mature fine oil sand tailings, hydraulic conductivity, void ratio, data regression.

# ACKNOWLEDGEMENTS

# TABLE OF CONTENTS

# LIST OF TABLES

**CHAPTER 3**

**CHAPTER 4**

# LIST OF FIGURES

**CHAPTER 4**

# LIST OF ABBREVIATIONS AND SYMBOLS

MFT: Mature fine tailings

USCS; Unified Soil Classification System

CT: oil sand composite/consolidated tailings

COF: cyclone overflow tailings

CFT: centrifuged fine oil sand tailings

KC: Kozeny–Carman equation

SEE: standard error of the estimate

wt%: weight percentage [%]

$k_z$: hydraulic conductivity in the vertical direction [m/s]

e: void ratio [-]

n: porosity [-]

$\gamma_w$: the unit weight of water [kN/m$^3$]

$c_v$: the coefficient of consolidation [m$^2$/s]

$m_v$: the coefficient of volume change [m$^2$/kN]

$a_v$: the coefficient of compressibility [m$^2$/kN]

g: the gravitational constant [m/s$^2$]

$\mu_w$: dynamic viscosity of water [Pa.s]

$\rho_w$: density of water [kg/m$^3$]

$G_s$: specific gravity [-]

p: portion of clay minerals

S or $A_S$: specific surface of solids [m$^2$/kg]

$e_L$: the void ratio at liquid limit [-]

$e/e_L$: the generalized state parameter [-]

$r^2$: The coefficient of determination [-]

R: the ratio of a predicted value of k ($k_{predicted}$) to a measured value of k ($k_{measured}$) [-]

*a*: mean value of R [-]

*b*: root mean square error of R [-]

# CHAPTER 1   INTRODUCTION

## 1.1 General

Oil sands mining processes produce tremendous amounts of tailings in northern Alberta, Canada. The tailings are deposited to tailings ponds, where gravity segregation takes place. During this process, sand settles more quickly than fine solids, which form a stable suspension, called mature fine tailings (MFT). MFT typically consists of 90% fines and stabilizes at a solids content of 30% (Jeeravipoolvarn 2010). Consolidation of MFT is very slow because of the tailings' low permeability (Jeeravipoolvarn 2010). Management and treatment of the MFT are major challenges facing the oil sand industry.

Hydraulic conductivity is an important physical property of MFT because it controls consolidation behaviors. Clear understandings of hydraulic conductivity and its relationship with void ratio are essential to MFT management and treatment. Owing to the excessive amount of time, and the sophisticated experimental techniques and apparatus required, studies related to investigation and measurement of the hydraulic conductivity over a wide range of void ratios for MFT are limited, and will be the focus of this study.

## 1.2 Objectives of Study

The main objective of this study is to measure the hydraulic conductivity of MFT over a relatively wide range of void ratios. The following specific objectives are devised:

- Existing experimental apparatuses and laboratory testing methods of the measurement of hydraulic conductivity for fine grained geomaterials are

summarized; particular attention is paid to the measurement methods for soft fine-grained geomaterials, which have high water content and generally present in the form of slurries.

- Available hydraulic conductivity data (k values) reported in the literature for oil sand tailings are summarized. Particular attention is paid to k values of fine grained oil sand tailings.

- Empirical equations proposed in previous studies to predict the hydraulic conductivity for plastic soils are summarized.

- The hydraulic conductivity of MFT over a wide range of void ratios is measured using three methods in laboratory tests, i.e. the standard oedometer test, the falling head test and the Rowe cell test.

- Data regression models are developed to correlate the hydraulic conductivity and a wide range of void ratios (k-e relationship) for fine oil sand tailings based on data from this study as well as data published in the literature.

- The suitability and performances of empirical equations are assessed and compared in terms of predicting hydraulic conductivity for fine oil sand tailings.

## 1.3 Thesis Outline

This thesis contains five chapters. Chapter 1 is an introduction of the thesis, including the objective of this study, thesis outline and original contributions.

Chapter 2 presents the literature review, which primarily contains three parts: a review of laboratory testing methods and relevant experimental apparatuses of the measurement of hydraulic conductivity for fine grained geomaterials; a review of

available hydraulic conductivity data for oil sand tailings; and a review of empirical equations developed for the prediction of hydraulic conductivity of plastic soils.

Chapter 3 introduces the methodology of hydraulic conductivity measurement of mature fine oil sand tailings (MFT). Geotechnical properties of MFT samples used in this study are presented. The experimental apparatuses, testing procedures and data analysis for the standard oedometer test, the falling head permeability test and Rowe cell test are described in detail. The challenges associated with the sample preparation, the test set up and execution, as well as limitations and possible sources of errors of the laboratory test methods are reported.

Chapter 4 includes the analysis and discussions of experimental results obtained from three laboratory testing methods. A hydraulic conductivity database for oil sand tailings is established based on data from this study together with data published in the literature. This database is used to develop the regression models, which correlate the hydraulic conductivity with a wide range of void ratios for fine oil sand tailings. The regression models proposed in this study can be used in the prediction and analysis of the hydraulic conductivity for fine oil sand tailings. Selected empirical equations are evaluated for their suitability and performances in predicting the hydraulic conductivity for fine oil sand tailings.

Chapter 5 presents a summary of the thesis, conclusions and a recommendation for future research.

## 1.4 Original Contributions

The original contributions of this study include:

- Measuring the hydraulic conductivity for MFT over a wide range of void ratios using three experimental devices

- Establishing a hydraulic conductivity database for oil sand tailings

- Developing data regression models for MFT and oil sand tailings

- Evaluating the suitability and performance of previous empirical equations in terms of predicting hydraulic conductivity for fine oil sand tailings

# CHAPTER 2   LITERATURE REVIEW

## 2.1 Introduction

Oil sands tailings are by-products of the bitumen extraction process used in mining operations. The tailings directly produced from oil sands processing are called whole tailings.

The tailings slurry, which is discharged into a tailings pond for storage, contains approximately 40% solids. Upon deposition, the tailings segregate, coarse solids settle quickly, forming beaches. The remaining water, bitumen, and fines accumulate in the center of tailings pond. Fine tailings remain suspended in the water and form a stable suspension containing about 30 % solids and are known as mature fine tailings (Xu et. al 2008). Compression of mature fine tailings (MFT) is extremely slow and MFT remains in a fluid-like state for decades given the tailings' low permeability (Jeeravipoolvarn 2010). The management of tailings largely depends on the consolidation behavior of MFT. Large volumes of MFT require multiple large containment ponds, which generates environmental issues and leads to MFT management challenges due to limited capacity of tailings pond.

The hydraulic conductivity is one of the most important physical properties of geomaterials as it controls seepage and the rate of consolidation. In soil mechanics, the hydraulic conductivity is defined as a coefficient of proportionality of Darcy's law, which links the discharge velocity with the hydraulic gradient. Darcy's law can be

expressed with the following equation (Das 2013):

$$v = ki \tag{2.1}$$

where $v[L/T]$ discharge velocity, $i$ is hydraulic gradient, and $k[L/T]$ is hydraulic conductivity. Hence, the hydraulic conductivity can be measured through the volume rate of flow, $q[L^3/T]$, and cross-sectional area, $A[L^2/T]$, given by the following equation:

$$q = kiA \tag{2.2}$$

It should be noted that hydraulic conductivity is a measure of the rate of flow for a particular fluid through a porous medium and its value varies as function of the fluid and the porous medium. Permeability, also termed intrinsic permeability, is a property of the medium itself and is not related to the fluid flowing through the fabric. The hydraulic conductivity and permeability can be related by the following equation (Adams 2011):

$$k = \frac{K\rho g}{\mu} \tag{2.3}$$

where $k$ $[L/T]$ is the hydraulic conductivity, $K[L^2]$ is the intrinsic permeability, $\rho$ $[M/L^3]$ is the density of the fluid, $g$ $[L/T^2]$ is the gravitational constant, and $\mu$ is the dynamic viscosity $[M/LT]$ which reflects one of the fluid properties.

Clear understanding of hydraulic conductivity and its relationship with void ratio are essential to the investigation of the MFT consolidation behavior and oil sand tailings

6

management. According to Terzaghi's one-dimensional consolidation theory, the coefficient of consolidation, $C_v$ [$L^2T^{-1}$] can be related to the hydraulic conductivity, k [$LT^{-1}$], by the following equation (Das 2013):

$$C_v = \frac{k}{m_v \gamma_w} \quad (m^2/s) \qquad (2.4)$$

where $\gamma_w$ [9.8 kN/m$^3$, $ML^{-2}T^{-2}$] is the unit weight of water, and $m_v$ ($M^{-1}LT^2$) is the coefficient of volume change. This theory was developed based on the assumptions of incompressible soil properties, i.e. a linear stress-strain relationship, a constant hydraulic conductivity, and infinitesimal strain. Hence the coefficient of consolidation, Cv, is assumed to be a constant during the consolidation process.

However, Terzaghi one-dimensional consolidation theory is not applicable to soft fine-grained geomaterials, like MFT. The compressibility and hydraulic conductivity of MFT are highly non-linear. Significant settlements occur when it is subjected to small stress increments from continuous deposition (Ahmed 2013). Therefore, Cv cannot be considered as a constant and consolidation of MFT cannot be considered as a small strain problem, especially with high water content.

More accurate methods for predicting the consolidation behavior of soft fine-grained geomaterials are based on large-strain consolidation theory (or finite strain consolidation theory), which releases the restrictions and allows for non-linear material properties. Large strain consolidation theory can be presented in several forms, for example: (Guo 2017).

7

$$\frac{1}{\gamma_w}\frac{d}{d_s}\left[\frac{\gamma_s-\gamma_w}{1+e}k+\frac{1}{1+e}k\frac{d\sigma'}{ds}\right]+\frac{\partial e}{\partial t}=0 \qquad (2.5)$$

Where k [L/T] is the hydraulic conductivity, $\sigma'$ is the effective stress [$ML^{-1}T^{-2}$], $\gamma_w$ is the unit weight of water, $kN/m^3$, $\gamma_s$ is the unit weight of soil solid, $kN/m^3$, and e is the void ratio. Obtaining the coefficient of consolidation, $C_v$, from Equation 2.5, requires an explicit relationship between the hydraulic conductivity and void ratio (k-e), as well as between the stress and strain ($\sigma'$-e), which is beyond the scope of this study.

To date, studies related to the investigation and measurement of hydraulic conductivity over a wide range of void ratios (k-e relationship) for MFT have been very limited.

In this chapter, a review of laboratory testing methods for the measurement of hydraulic conductivity is presented; particular attention is paid to the measurement methods for soft fine-grained geomaterials having high water content and generally present in the form of slurries. Pros and cons, as well as the suitability of these methods, are discussed. In Section 2.3, the available hydraulic conductivity data (k values) for oil sand tailings reported in the literature are summarized to constitute a hydraulic conductivity database. In Section 2.4, empirical equations, which were proposed to predict the hydraulic conductivity for plastic soils, are summarized and classified into two categories based on the form of the equations. These equations correlate the hydraulic conductivity with the void ratio and/or other properties of soil, such as Atterberg limits.

## 2.2 Laboratory Methods and Apparatuses of the Hydraulic Conductivity Measurement

Many techniques and methods have been developed and reported in previous studies to measure the hydraulic conductivity of soils in the laboratory. In this section, existing experimental apparatuses and testing methods of the hydraulic conductivity measurement in the laboratory are summarized. For fine-grained soils with high-water content, conventional measurement techniques are inadequate or even not suitable for determining the hydraulic conductivity. Therefore, special attention is paid to experimental apparatuses and methods designed for soft fine-grained geomaterials that have a high compressibility and low permeability.

The hydraulic conductivity of soils can be measured by direct or indirect methods. In sections 2.2.1 and 2.2.2, two types of methods are introduced, and a comparison between the direct and indirect methods is presented in Section 2.2.3.

### 2.2.1 Direct Methods

### 2.2.1.1 Constant Head Test

The constant head test has been carried out in various apparatuses, such as the constant head permeameter, the oedometer cell, the slurry consolidometer, the large strain consolidation cell and the Rowe cell, to directly measure the hydraulic conductivity of geomaterials. In this section, these appartuses are introduced in detail. It should be noted that the test performed in constant head permeameter is a standarad

test followed by standard ASTM D2434, except which the test performed in other apparatuses mentioned above are non-standard tests.

The principle of the constant head test performed in various apparatuses is the same, and the hydraulic conductivity can be calculated using the following equation:

$$k_z = \frac{QL}{Aht} \ (m/s) \tag{2.6}$$

where $k_z$ (m/s) is the hydraulic conductivity in the vertical direction, A is the soil sample cross-sectional area ($m^2$), h (m) is the constant total head, t (s) is the measured time, Q ($m^3$) is the total quantity of water collected over time t, and L(m) is the sample height.

- **Constant Head Permeameter**

A typical arrangement for performing the constant head test using the conventional constant head permeameter is shown in Figure 2.1. The arrangement is suitable for measuring the hydraulic conductivity of coarse grained soils with high permeability. A detailed description of the constant head test performed in this apparatus is given in the ASTM D2434 - Standard Test Method for Permeability of Granular Soils. For fine-grained soils, the water tank is replaced by the Mariotte bottle, as shown in Figure 2.2, to apply the constant head during the test. The Mariotte bottle is designed to apply very small heads so it is most useful for soils with relatively low permeability (Olson et. al. 1981).

- **Oedometer Cell**

Some oedometer cells are equipped with the means to perform the constant head test while the sample is under load, as shown in Figure 2.3. The essential features of such oedometer cells are a bottom inlet, which can be connected to a standpipe; sealing rings to prevent water escaping around the specimen and containing ring; and an upper overflow outlet (Head 1982).

The constant head test performed in such an oedometer cell is more suitable for soils with intermediate permeability, such as silts. However, this method cannot be used for soft fine-grained geomaterials with high initial water content because large deformations occur during the consolidation stage, so the small sample thickness is not adequate for consolidation.

- **Slurry Consolidometer**

Figure 2.4 shows the slurry consolidometer, which was developed in the Geotechnical Centre at the University of Alberta, to carry out large strain consolidation tests (Jeeravipoolvarn 2005). The slurry consolidometer is about 30 cm in height and 20 cm in diameter, which allows large deformation during the consolidation and allows the constant head test to be directly performed at the end of each consolidation loading step. This apparatus is equipped with a clamping device, which consists of a horizontal steel bar (50 mm by 50 mm) fastened to two vertical frame rods, to prevent settlements caused by the applied hydraulic gradients when performing permeability tests on slurry-like soils (Suthaker 1995).

The constant head test performed in the slurry consolidometer has been adopted in previous studies by Suthaker (1995), Jeeravipoolvarn (2005) and Miller (2010) to measure the hydraulic conductivity of fine oil sand tailings. The advantage of this apparatus is the development of a top cap clamping system, which permits the permeability test to be conducted on slurry samples without further consolidation induced by seepage forces. However, the disadvantage is obvious. The slurry consolidometer is not equipped with the means of applying back pressure to the sample, which means it cannot ensure the sample being fully saturated, cannot give a rapid pore water pressure reponse, and cannot ensure that the primary consolidation phase is completed (Head 1986).

- **Large Strain Consolidation Cell**

Figure 2.5 (a) shows the large strain consolidation cell adopted by Qiu (2001). This apparatus was used to carry out the consolidation test and permeability test (the constant head test) for four tailings, i.e., copper mine tailings, gold mine tailings, coal wash plant tailings and oil sand composite/consolidated tailings (CT). According to Qiu, tailings samples taken from mine sites were unsaturated, and thus a special laboratory technique was adopted to saturate tailings samples. First, tailings samples were carefully placed into a de-airing cylinder, as shown in Figure 2.5 (b). Then the de-airing cylinder was placed on a vibrating table while a vacuum of 60 kPa was applied for at least 2 hours to draw off any gas entrapped in the specimen. To avoid entrapping air when a sample was placed in the large strain consolidation cell, a vacuum tube was used to connect the de-airing cylinder and consolidation cell, as shown in Figure 2.5 (c). The sample was placed

into the large strain consolidation cell while suction (vacuum pressure) was applied to both the de-airing cylinder and the cell.

The experimental arrangement, including the large strain consolidation cell, the de-airing cylinder, and the vacuum tube, can improve the saturation degree of sample, but cannot apply a back pressure to the sample, similar to the slurry consolidometer.

- **Rowe Cell**

The Rowe cell, also known as the hydraulic consolidation cell, was developed by P. W. Rowe and his research group to overcome the disadvantages of the conventional oedometer apparatus when performing consolidation tests on low-permeability soils (Head 1986). This apparatus allows the constant head test to be directly conducted, either as an independent test or after the consolidation test on a sample of a known vertical effective stress. Rowe cells are available in three different nominal diameters: 76mm, 150mm and 250 mm.

A typical general arrangement of the apparatuses for a Rowe cell test is diagrammatically shown in Figure 2.6. In a Rowe cell, a sample is loaded hydraulically by water pressure acting on a convoluted flexible diaphragm, and this differs from the conventional oedometer test using a mechanical lever system. This hydraulic loading system is capable of testing large diameter samples, i.e, up to 250 mm in diameter, and allows large deformations during consolidation. Owing to the hydraulic loading system, the sample is less susceptible to vibration effects; in addition, the applied hydraulic pressure can be very low to as high as 1000 kPa, even with a large diameter (Head 1986).

The sample can be loaded either by applying a uniform pressure over its surface, i.e. the free strain test, or through a rigid plate which maintains the loaded surface plane, i.e. the equal strain test. More importantly, the Rowe cell has the ability to control drainage conditions. Both vertical and horizontal drainage conditions can be imposed on the sample. The Pore water pressure can be measured during consolidation at any time and with immediate response, and thus the primary consolidation can be monitored from the pore pressure readings. Rowe cells are equipped with the means of applying back pressure. An elevated back pressure can ensure a sample is fully saturated, rapid pore water pressure reponse, and completion of primary consolidation (Head 1986).

The Rowe cell has been adopted in previous studies to measure the hydraulic conductivity and compression behaviour of fine-grained geomaterials, including marine clays and other ultra soft soils (Bo 1998, 2003, 2010)

### 2.2.1.2 Falling Head Test

The falling head test has been carried out in the falling head permeameter as well as in the oedometer cell to directly measure the hydraulic conductivity of fine-grained geomaterials. In this section, these appartuses are introduced in detail. It should be noted that the test performed in falling head permeameter is a standard test followed by ASTM D5856, and the test performed in oedometer cell is an non-standard test.

For measuring the hydraulic conductivity of soils with intermediate and low permeability, i.e. silt and clays, the falling head test is often used (Head 1982). The

principle of the falling head test performed in various apparatuses is basically the same, i.e. a soil sample is connected to a standpipe which provides both the head of water and the means of measuring the quantity of water flowing through the sample (Head 1982). Denoting the cross-sectional area of the standpipe by a (m$^2$), sample length by L (m), sample cross-sectional area by A (m$^2$), time duration by t (s), and $h_1$ (m) and $h_2$ (m) are initial and final hydraulic head differences, respectively, the vertical hydraulic conductivity k (m/s) can be determined using the following equation (Budhu 2007):

$$k = \frac{aL}{At} \ln \frac{h_1}{h_2} \text{ (m/s)} \tag{2.7}$$

- **Falling Head Permeameter**

Figure 2.7 shows a typical arrangement for performing the falling head test using the falling head permeameter. This arrangement is suitable for measuring the hydraulic conductivity of fine-grained soils. A detailed description of the falling head test performed in this apparatus is given in ASTM D5856 Standard Test Method for Measurement of Hydraulic Conductivity of Porous Material Using a Rigid-Wall, Compaction-Mold Permeameter (ASTM D5856).

In order to reduce testing time, the falling head test of fine-grained soils is often performed using high hydraulic gradients. However, high gradients induce large seepage forces that may consolidate soft and compressible samples, such as fine oil sand tailings, thereby reducing their hydraulic conductivity as the test proceeds and causing erroneous results. Therefore, when performing the test in a falling head permeameter, it is

important to apply an appropriate hydraulic gradient to the sample without causing significant consolidation, particularly for soft fine-grained samples with high water contents, and to avoid prolonged testing time.

- **Oedometer Cell**

The falling head test can be performed in the oedometer cell at various stages during a consolidation test after the completion of the primary consolidation. An oedometer cell arranged for the falling head test with an upward flow is shown in Figure 2.8, which is similar to the constant head test performed in the oedometer cell. The test is started by opening the pinch clip (shown in Figure 2.8) and running the clock when the level in the burette reaches the first desired level. The next step is to record the time taken to the level in the burette to fall to the second desired level. This step is repeated two or three times. The hydraulic conductivity can be calculated using Equation 2.2.

### 2.2.1.3 Flow Pump Test

Olsen first proposed the flow pump technique for measuring the hydraulic conductivity of fine-grained soils (Olsen 1966). The flow pump test is the opposite concept of the constant head test. Figure 2.9 shows a schematic diagram of a flow pump test, in which a flow pump is incorporated into a conventional triaxial test system to allow water to flow in or out from the base of a soil sample at a small and constant rate. According to Fernandez (1985), the flow pump test generates a constant flow rate through the sample and the induced head drop across the sample is used to calculate the hydraulic conductivity using Darcy's law.

The advantage of the flow pump test is the hydraulic conductivity can be obtained more rapidly at substantially smaller gradients (Olsen 1985). This advantage is more apparent when testing soft fine-grained geomaterials, where errors from high hydraulic gradients caused sample consolidation can be avoided or minimized. The disadvantage of this test is the high initial cost for equipment; whereas it may be offset by testing time saved in commercial laboratories (Aiban, 1989).

**2.2.2 Indirect Method**

The hydraulic conductivity of geomaterials can be measured either directly or indirectly in the laboratory. The indirect method refers to the hydraulic conductivity back-calculated from consolidation parameters, i.e. the coefficient of consolidation and the coefficient of volume change, based on Terzaghi's one-dimensional consolidation theory using Equation 2.4.

The coefficient of consolidation, $c_v$, and the coefficient of volume change, $m_v$, are obtained from the standard oedometer test, which has been widely used in geotechnical laboratories as a basic laboratory test. The standard oedometer test is performed based on the standard test method for one-dimensional consolidation properties of soils using incremental loading (ASTM D2345). However, the test is not applicable for soft fine-grained geomaterials that have high water content and generally are in the form of slurries. Two major problems can invalidate the hydraulic conductivity measurement for soft fine-grained geomaterials. The first is that large deformations may occur during consolidation, thus the small sample thickness is not adequate for consolidation. The

second problem is that such materials present non-elastic properties during the test, which violate the assumptions of Terzaghi's theory and result in errors in the back-calculation of the hydraulic conductivity.

According to Olson and Daniel (1981), the standard oedometer test was developed for soil that is in a relatively solid phase with a shear strength no less than 2 kPa, which places limitations on the applicability of the test. The other limitation is that the oedometer cell is not equipped with the means to measure the excess pore water pressure, the dissipation of which controls the consolidation process; therefore, the approach to the completion of primary consolidation is based solely on the change of sample height (Gofar and Kassim 2006).

### 2.2.3 Discussion and Conclusions

In Section 2.2, direct and indirect methods for hydraulic conductivity measurement are introduced. Direct methods include the constant head test, the falling head test, and the flow pump test. The indirect method refers to the hydraulic conductivity back-calculation from the consolidation parameters based on Terzaghi's one-dimensional consolidation theory.

The constant head test and the falling head test are widely used in geotechnical laboratories owing to their simplicity and the availability of equipment at a reasonable cost (Aiban and Znidarcic 1989, Suthaker 1995). The constant head test can be performed in the constant head permeameter, the oedometer cell, the slurry

consolidometer, the large strain consolidation cell, and the Rowe cell. Comparing these apparatuses, the constant head permeameter and the oedometer cell are not applicable to conducting the constant head test on soft fine-grained geomaterials. The slurry consolidometer and the large strain consolidation cell, both of which were designed for mine tailings, allow large deformation during the consolidation and allow the constant head test to be directly conducted at the end of each consolidation loading step. However, these two apparatuses are not equipped with the means to apply the back pressure during the test. The Rowe cell is superior to other apparatuses not only because it can be used for soft fine-grained geomaterials, but also because it is capable of applying back pressure.

The falling head test can be performed in the falling head permeameter and the oedometer cell. Comparing these two apparatuses, the falling head permeameter is commonly used in geotechnical laboratories to measure the hydraulic conductivity of fine-grained geomaterials. As mentioned previously, the oedometer cell is not suitable for carrying out permeability tests for soft fine-grained geomaterials, either the constant head test or the falling head test.

The other direct method, i.e. the flow pump test, has rarely been used due to the complexity of equipment and complicated calculation process needed for determining hydraulic conductivity.

The indirect method can be used for fine-grained geomaterials that obey the assumptions involved in Terzaghi's infinitesimal consolidation theory. However, this

method is unacceptable in measuring the hydraulic conductivity of geomaterials with high compressibility and low permeability when Terzaghi's consolidation theory is not valid.

Based on the above discussions, it can be concluded that the constant head test performed in the Rowe cell is well suited for measuring the hydraulic conductivity of soft fine-grained geomaterials, such as mature fine oil sand tailings, over a wide range of void ratios. Thus, the Rowe cell is adopted in this study to perform the constant head test. In addition, the falling head test performed in a conventional falling head permeameter is also adopted in this study as another direct method to compare results obtained by using the Rowe cell and to determine the measurement range of hydraulic conductivity with this method. The standard oedometer test has been used in this study as an indirect method to determine the hydraulic conductivity of the mature fine tailings at relatively low water content and void ratio and to estimate the measurement range of hydraulic conductivity with this method.

## 2.3 Database of the Hydraulic Conductivity of Oil Sand Tailings

The available hydraulic conductivity data for oil sand tailings reported in the literature are summarized in this section to constitute a database.

Suthaker (1995) investigated the consolidation behavior of fine oil sand tailings and the factors affecting this behavior. The slurry consolidometer, as shown in Figure 2.4, was adopted in this study to conduct the one-dimensional multi-step loading

consolidation test and the constant head test. The constant head test with an upward flow was carried out at the end of each consolidation increment. The permeant fluid used in the constant head test was tailings pond water. In the study, the hydraulic conductivity of fine oil sand tailings with three initial solids contents (20%,25%, and 30%) over the void ratio range from 1 to 8 was measured. The 20% and 25% initial solids content fine oil sand tailings consisted of approximately 2% fine sand, 43% silt and 55% clay, while the 30% initial solids content fine tailings had 5% sand, 49% silt, and 46% clay. The specific gravity of samples varied from 2.1 to 2.5. The author indicated that this variation is attributable to the variable amount of bitumen, which has a specific gravity of 1.03. The average unit weight of fine oil sand tailings was about 12 kN /m$^3$. The liquid limit of tailings samples varied between 40% and 60% and the plasticity index varied between 20% and 35%. Based on the Unified Soil Classification System (USCS), the fine tailings samples were classed as high plasticity clay (CH). The hydraulic conductivity data obtained from this study are plotted in Figure 2.10, which shows that the hydraulic conductivity decreased by about four orders of magnitude when void ratio decreased from 8 to 1. The author also suggested that the initial solids content did not affect the hydraulic conductivity of fine oil sand tailings.

Qiu (2001) measured the hydraulic conductivity and other engineering properties for oil sand composite/consolidated tailings (CT) from Syncrude Canada Ltd. CT essentially is a mix of coarse sands and mature fine tailings, with a coagulant added to produce non-segregating tailings that can settle and consolidate quickly (Jeeravipoolvarn 2010). CT samples used in this study consisted of about 76% sand, 15%

silt, and 9% clay. Fines content for CT samples accounted for 24%. The specific gravity

of CT was 2.6. Based on the USCS, CT samples is classed as non-plastic silty sand

(SM). In this study, a large strain consolidation apparatus, as shown in Figure 2.5, was

used to carry out the one-dimensional multi-step loading consolidation test and the

constant head test. The hydraulic conductivity was directly measured at the end of each

consolidation increment by applying a constant head difference across the sample to

measure the upward flow through the sample. The results obtained from this study are

presented in Figure 2.10. The hydraulic conductivity values range from $2.2 \times 10^{-9}$ m/s to

$6.3 \times 10^{-9}$ m/s for CT samples within the void ratios varying between 0.47 and 1.14

range, which is consistent with the results (2.5 to $8.5 \times 10^{-9}$ m/s) presented by Liu et al.

(1994).

Jeeravipoolvarn (2010) measured the geotechnical properties of the cyclone

overflow tailings (COF). After the extraction of bitumen, oil sands tailings are passed

through cyclones, which produce coarse and fine tailing streams, known as COF.

According to Jeeravipoolvarn (2010), COF is a source of new fines and one of the

contributions to new MFT. The initial void ratio and water content of COF samples were

5.66 and 223.6%, respectively. COF samples had 8% sand, 40% silt, and 52% clay. The

fines content for COF samples accounted for 92%. The specific gravity of the COF was

2.53. The liquid limit and plastic limit of samples were 50% and 21%, respectively.

Based on USCS , COF samples should be classed as clay with high plasticity (CH). The

experimental apparatus, the testing method and testing procedures used in this study

were the same as those used in Suthaker's study (1995). The hydraulic conductivity data

of COF over the range of void ratios from 0.8 to 4 are shown in Figure 2.10.

Miller (2010) carried out a comprehensive study to evaluate the properties and processes influencing the rate and magnitude of volume decrease for fine oil sand tailings resulting from different bitumen extraction processes (caustic versus non-caustic). In this study, the fine content of tailings samples ranged from 96% to 100%. The specific gravity of samples varied from 2.48 to 2.55. The liquid limit of samples varied between 50% and 60% and plasticity limit varied between 21% and 31%. Based on USCS , fine oil sand tailings samples used in this study should be classed as clay with high plasticity (CH). The experimental apparatus, the testing method and testing procedures used in this study were the same as those used in Suthaker's study (1995) and Jeeravipoolvarn's study (2010). The hydraulic conductivity data obtained from this study are presented in Figure 2.10, where it can be found that the hydraulic conductivity decreased by five orders of magnitude when the void ratio decreased from 10 to 1.

Owolagba (2013) investigated the dewatering behavior of centrifuged oil sand fine tailings. After centrifugation, the water content of centrifuged fine oil sand tailings (CFT) decreased to 63wt% from 240wt%. The specific gravity of the CFT was 2.39. CFT samples contained approximately 95% material finer than 0.075 mm and 52% material finer than 0.002 mm. The liquid limit and plastic limit of CFT samples were 41% and 20%, respectively. Based on USCS , CFT samples used in this study should be classed as clay with low plasticity (CL). In this study, a fixed ring consolidometer testing system, as shown in Figure 2.8, was used to perform the one-dimensional consolidation test and

23

the falling head test. The one dimensional consolidation test was performed in accordance with the ASTM Standard D2435-11.The hydraulic conductivity was measured after each load increment using the falling head method along with an upward flow through the sample. The hydraulic conductivity data of centrifuged fine oil sand tailings over the range of void ratios from 0.5 to 1.5 are shown in Figure 2.10.

The available hydraulic conductivity data published in previous studies are summarized in this section and presented in Figure 2.15. Since the hydraulic conductivity controls the rate of consolidation and there is less hydraulic conductivity data available in the literature, it is necessary to obtain more hydraulic conductivity data for oil sand tailings in future works.

## 2.4 Predictive Models

The hydraulic conductivity of geomaterials is one of the most significant and widely used geotechnical parameters in many applications (Mbonimpa 2002). Due to the excessive amount of time, and the sophisticated experimental techniques and apparatus required for the measurement of hydraulic conductivity of fine-grained soil, especially for soft fine-grained geomaterials with high water content, empirical equations have been developed to predict and estimate the hydraulic conductivity of fine-grained soils from properties such as Atterberg limits and void ratio. In this section, a review of empirical equations proposed in the literature is presented. These equations are classified into two categories based on equation formats and geotechnical parameters.

24

**2.4.1 Class 1: Based on Kozeny-Carman Equation and its Extensions**

- **Kozeny–Carman equation (1937)**

A well-known relationship between the hydraulic conductivity and the properties of pores of geomaterials was proposed by Kozeny and later modified by Carman. The resulting equation is known as the Kozeny–Carman (KC) equation. This equation was developed after considering a porous material as an assembly of capillary tubes. It yielded the hydraulic conductivity as a function of the porosity, the specific surface of solids, and the parameter C (Chapuis 2003).

The following equation was one of the forms of the KC equation, (Chapuis 2012)

$$k = C \frac{g}{\mu_w \rho_w} \frac{e^3}{S^2 G_s^2 (1+e)} \tag{2.8}$$

where C is a constant which depends on the porous space geometry, g is the gravitational constant (m/s$^2$), $\mu_w$ is the dynamic viscosity of water (kg/(s·m)), $\rho_w$ is the density of water (kg/m3), $G_s$ is the specific gravity, S (m$^2$/kg) is the specific surface of solids, and e is the void ratio. According to Chapuis (2012), the KC equation is not convenient to use because the determination of specific surface (S) of geomaterials is difficult and not commonly measured in geotechnical laboratories.

- **Chapuis (2003)**

Chapuis (2003) developed the following equation that can be used for any soil, either plastic soil or non-plastic soil, based on the well- known KC equation,

25

$$\log(k_{sat}) = 0.5 + \log(\frac{e^3}{G_S^2 S^2 (1+e)}) \tag{2.9}$$

where $k_{sat}$ (m/s) is the saturated hydraulic conductivity, $G_s$ is the specific gravity, and S (m$^2$/kg) is the specific surface. Chapuis (2012) reported that Equation 2.5 predicts a $k_{sat}$ value between one-third and three times the $k_{sat}$ value obtained with a high-quality laboratory test performed on fully saturated samples.

In order to apply Equation 2.5, it is necessary to measure the specific surface of geomaterials in a laboratory or estimate it through experimental correlations. The laboratory methods for measuring the specific surfaces of fine-grained soils involve adsorption of either a gas or a polar liquid but are not frequently used in geotechnical laboratories (Chapuis 2012). Several experimental correlations have been proposed between the specific surface of geomaterials and basic soil properties, such as consistency limits (Muhunthan 1991). Four frequently used methods for estimating the specific surface of plastic soils are summarized as below.

Locat (1984) indicated that the use of quantitative mineralogy and specific surface area can interpret index properties of clay soils. In this study, the specific surface area of clay soils from nine sites in Eastern Canada was measured using the methylene blue method. Afterward, the measured specific surface area for all samples was related to the plasticity index as shown in Figure 2.11. The coefficient of determination ($r^2$) for this correlation is 0.85. The author suggested that the plasticity index relates well with the specific surface for clay soils. (Locat 1984)

Mbonimpa (2002) established the following simple relationship between the specific surface and liquid limit by using the data published by Locat et al. (1984), Sridharan et al. (1986), Muhunthan (1991), Sitharam et al. (1995), and Tanaka and Locat (1999),

$$S = 0.20 w_L^{1.45} \qquad (2.10)$$

where S ($m^2$/g) is specific surface, $w_L$ is liquid limit in percentage. This equation is valid for materials with the specific surface within the range of 21 $m^2$/g to 433 $m^2$/ g, and their liquid limit within the range of 25% to 127%.

Chapuis (2003) reported that the specific surfaces of most clay soils can be assessed from their liquid limit. The author proposed a linear correlation between $S^{-1}$ and $w_L^{-1}$ using data from plastic soils published by De Bruyn et al. (1957), Farrar and Coleman (1967), Locat et al. (1984), Sridharan et al. (1986, 1988), and Muhunthan (1991).

$$\frac{1}{S} = \frac{1.3513}{w_L} - 0.0089 \qquad (2.11)$$

where S ($m^2$/g) is specific surface and $w_L$ (%) is liquid limit. The $r^2$ of this equation is 0.88. Chapuis (2012) pointed out that Equation 2.7 predicts an S value usually within ±25 % of the measured value when $w_L^{-1} > 0.0167$, i.e. $w_L < 60$ %; the predictions of this equation are less accurate for clays with $w_L > 60$ %, especially those contains trace bentonite and organic clays. The equation is invalid for high plasticity clay with $w_L > 110$ %.

Dolinar (2009) proposed that the specific surface of non-swelling clay soil can be expressed in the following equations from the Atterberg limits or the plasticity index, and the weight portion of clay minerals in the soil,

$$S = (w_L - 31.91p) / 0.81 \qquad (2.12)$$

$$S = (w_p - 23.1p) / 0.27 \qquad (2.13)$$

$$S = (I_P - 8.74p) / 0.54 \qquad (2.14)$$

where $S$ ($m^2/g$) is specific surface, $w_L$ (%), $w_p$ (%) and $I_P$ (%) are the liquid limit, plastic limit and plasticity index, respectively. The equations (Equations 2.8, 2.9 and 2.10) are only valid for inorganic soils at an ambient temperature of 20 °C.

- **Mbonimpa (2002)**

Mbonimpa (2002) proposed a set of simple equations, based on pedologic material properties, to predict the hydraulic conductivity for granular and plastic soils., as an extension of the KC equation. The author suggested that the fundamental equation for hydraulic conductivity, k, can be formulated by combining the different influence factors as follows:

$$k = f_f \, f_v f_s \qquad (2.15)$$

where $f_f$ ($L^{-1}T^{-1}$) represents the function of pore fluid properties, $f_v$ ($L^3L^{-3}$) represents the function of the void space, and $f_s$ ($L^2$) represents the function of the solid grain surface characteristics. Then, using the experimental results taken from his study and from the

28

literature, the author proposed the following pedotransfer functions that can be used for

quickly estimating k value for plastic soils,

$$k_{sat} = C_P \frac{\gamma_w}{\mu_w} \frac{e^{3+x}}{1+e} \frac{1}{\rho_s^2 w_L^{2\chi}} \qquad (2.16)$$

where $k_{sat}$ (cm/s) is saturated hydraulic conductivity, $C_P$ ($g^2/m^4$) is a constant and equal

to 5.6 for plastic soils, $\gamma_w$ ($kN/m^3$) is the unit weight of water, $\mu_w$ (kg/(s·m)) is the dynamic

viscosity, $\chi$ is an empirical material parameter (1.5), $\rho_s$ ($kg/m^3$) is density of solid grain,

$w_L$ (%) is the liquid limit, and the parameter x is defined by

$$x = 7.7 w_L^{-0.15} - 3 \qquad (2.17)$$

Equation 2.12 is an extension of the KC equation and does not require the specific

surface of soils, which means it equation is more convenient to use than the KC equation

and the equation proposed by Chapuis (2003). Thus, Equation 2.12 will be used to assess

its suitability and relative performances in terms of predicting the hydraulic conductivity

for fine oil sand tailings in this study.

**2.4.2 Class 2: Based on Atterberg Limits and Index Properties of Geomaterials**

It has long been recognized that the compressibility and hydraulic conductivity of

fine-grained soils, especially for soils that are deposited as slurries, are closely related

to Atterberg limits (Carrier 1984, Morris et al. 2000). Because Atterberg limits can be

determined rapidly using basic geotechnical laboratory equipment and small quantities

of samples, it would be very convenient to use Atterberg limits to predict the hydraulic conductivity of geomaterials. In this section, empirical equations based on Atterberg limits used to predict the hydraulic conductivity for fine-grained soils are summarized.

- **Nishida (1969)**

Nishida (1969) indicated that the hydraulic conductivity of clay can be approximately estimated from its void ratio and plasticity index. In this study, the author started from the following linear relationship, which was formed based on data from experiments,

$$e = \alpha + \beta \log_{10} k \tag{2.18}$$

where α and ß are empirical constants. Based on experimental results carried out in this study, the author found that the value of α is nearly equal to 10 times the value of ß, and the coefficient ß has a linear relationship with the plasticity index, as shown below,

$$\beta = 0.01(I_P) + \gamma \tag{2.19}$$

where $I_P$ (%) is the plastic index. γ is a constant depending on the kind of clay, which takes the value of 0.3 for an oven-dried clay and 0.05 for a fine-grained soil. Then, the following equation was proposed:

$$e = (0.01\, I_P + 0.05)(10 + \log k_{sat}) \tag{2.20}$$

where $k_{sat}$ (cm/s) is the saturated hydraulic conductivity and e is the void ratio.

- **Samarasinghe (1982) and Sridharan and Nagaraj (2005)**

Samarasinghe (1982) proposed the following equation to predict the hydraulic conductivity of clay soils.

$$k_{sat} = C \frac{e^x}{1+e} \tag{2.21}$$

where $k_{sat}$ (m/s) is the saturated hydraulic conductivity, e is the void ratio, C (m/s) and x are permeability parameters. According to Sridharan and Nagaraj (2005), x is about 5 for clay and C can be calculated using the plasticity index, $I_P$ (%).

$$C = 0.00104 I_P^{-5.2} \tag{2.22}$$

However, Samarasinghe (1982) stated that for large void ratio variations, no single hydraulic conductivity -void ratio relationship is valid for all soils.

- **Carrier (1984)**

Carrier (1984) measured the hydraulic conductivity using various test methods for a total of 61 samples, of which 22 are phosphatic, 13 are dredged materials, and 26 are remoulded natural clays. Then, the author proposed the following equation to predict the hydraulic conductivity of remoulded clays.

$$k_{sat} = \frac{0.0174 I_P^{-4.29}}{(1+e)} [e - 0.027(w_P - 0.242 I_P)] \tag{2.23}$$

where $k_{sat}$ (m/s) is the saturated hydraulic conductivity, e is the void ratio, $w_P$ (%) i the plastic limit, and $I_P$ (%) is the plasticity index.

- **Nagaraj (1993, 1994) and Prakash (2002)**

Nagaraj (1991) reported that all clays have almost the same hydraulic conductivity value at their limit liquid. Nagaraj (1993) generalized the prediction of hydraulic conductivity in terms of the void ratio at the liquid limit and proposed the following equation:

$$\frac{e}{e_L} = 2.38 + 0.233 \log(k_{sat}) \tag{2.24}$$

where $e/e_L$ is defined as the generalized state parameter, e is the void ratio, $e_L$ is the void ratio at liquid limit, and $k_{sat}$ (m/s) is the saturated hydraulic conductivity.

Nagaraj (1994) proposed an updated model (Equation 2.21) to relate the generalized state parameter, $e/e_L$. The updated model is applicable for normally consolidated soil as well as overconsolidated soils,

$$\frac{e}{e_L} = 2.162 + 0.195 \log(k_{sat}) \tag{2.25}$$

However, Stepkowsa (1996) pointed out that the equations proposed by Nagaraj, i.e. Equations 2.20 and 2.21, are not applicable to sludges materials, and explained the reason being the difference in their microstructures.

Prakash (2002) proposed an equation similar to Equations 2.20 and 2.21,

$$\frac{e}{e_L} = 2.23 + 0.204 \log(K_{sat}) \tag{2.26}$$

where $e/e_L$ is defined as the generalized state parameter, e is the void ratio, $e_L$ is the void

ratio at liquid limit, and $k_{sat}$ (m/s) is the saturated hydraulic conductivity.

Equations 2.20, 2.21 and 2.22 imply that at the liquid limit, i.e. $e/e_L=1$, the $k_{sat}$ value takes a constant value whatever the clay.

- **Suthaker (1995)**

Suthaker (1995) carried out large strain consolidation tests (Jeeravipoolvarn 2005) on fine oil sand tailing using the slurry consolidometer, as introduced in section 2.2.1. This test allows large deformation during the consolidation and allows the hydraulic condutivity of fine oil sand tailings to be directly measured at the end of each consolidation loading step. Based on the experimental results, the author proposed the following equation to describe the relationship between the hydraulic conductivity and void ratio for fine oil sand tailings.

$$k = 6.16 \times 10^{-9} e^{4.468}$$ (2.27)

where k (cm/s) is hydraulic conductivity and e is the void ratio.

- **Sivappulaiah (2000)**

Sivappulaiah (2000) carried out one-dimensional consolidation tests on bentonite - sand mixtures to measure the hydraulic conductivity using Terzaghi's consolidation theory. Then, based on experimental results, the author proposed four methods for predicting the hydraulic conductivity from void ratio and liquid limits.

Method 1: Equation 2.24 can be used to predict the value of hydraulic conductivity at liquid limits greater than 50%.

$$\log k_{sat} = e(53.06 w_L^{-0.846}) - 11.8 \qquad (2.28)$$

where $k_{sat}$ (m/s) is the saturated hydraulic conductivity, e is the void ratio, and $w_L$ (%) is the liquid limit. The $r^2$ of this equation is 0.71.

Method 2: Equation 2.25 is valid for soils with a liquid limit greater than 50%. The $r^2$ of this equation is 0.81.

$$\log(k_{sat}) = \frac{e - 0.0535 w_L - 5.286}{0.0063 w_L + 0.2516} \qquad (2.29)$$

where $k_{sat}$ (m/s) is the saturated hydraulic conductivity, e is the void ratio, and $w_L$ (%) is the liquid limit.

Method 3: Equation 2.26 is similar to Equations 2.20, 2.21 and 2.22, in which the generalized state parameter, $e/e_L$, relates to log k. Equation 2.25 is valid for soils with liquid limits ranging from 50% to 100%.

$$\frac{e}{e_L} = 1.16 + 0.242 \log(k_{sat}) \qquad (2.30)$$

where $k_{sat}$ (m/s) is the saturated hydraulic conductivity, and e is the void ratio. The $r^2$ of this equation is 0.722.

Method 4: This method relates $\log e/e_L$ to log k.

$$\log_{10}\left(\frac{e}{e_L}\right) = 0.237 \log_{10} k + 0.29 \qquad (2.31)$$

where k (m/s) is the hydraulic conductivity, and e is the void ratio. The $r^2$ of this equation is 0.74. The author suggested that Method 2 is preferred compared to the other three methods because it gives a higher correlation coefficient.

**Morris et al. (2000, 2003)**

Morris et al. (2000) proposed Equation 2.28 based on the index properties of mine tailings to estimate the hydraulic conductivity. Equation 2.28 was developed based on data from New South Wales and Queensland coal tailings, Western Australian bauxite tailings, and Florida phosphate tailings. These data were obtained through a variety of test methods and consist mostly of laboratory data, and field data for bauxite tailings.

$$\frac{e}{e_L} = 29.80[k_{sat}(1 + e)]^{0.177} - 0.09527 \tag{2.32}$$

where $k_{sat}$ (m/s) is the saturated hydraulic conductivity, e is the void ratio, and $e_L$ is the void ratio at the liquid limit. The $r^2$ of this equation is 0.8.

Morris et al. (2003) proposed a new correlation (Equation 2.29) for fine-grained dredged materials based on the liquid limit alone. Data representing 18 American and 10 Australian dredged materials were used in the study to develop Equation 2.29. According to Morris et al. (2003), the new correlation is both simpler and statistically stronger than comparable earlier correlations.

$$\frac{e}{e_L} = 12.55[k_{sat}(1 + e)]^{0.109} - 0.372 \tag{2.33}$$

where $k_{sat}$ (m/s) is the saturated hydraulic conductivity, e is the void ratio, and $e_L$ is the void ratio at the liquid limit. The corresponding $r^2$ is 0.874. The authors also pointed out that sandy (SC or SM) materials do not conform to Equation 2.29, and whether materials with high organic contents conform to this equation is uncertain.

- **Bo (2003)**

Bo (2003) conducted one-step loading and step-loading compression tests for ultra-soft soil using a Rowe cell to investigate the compression behavior in the ultra-soft stage. Based on experimental results, the author established a correlation between the hydraulic conductivity and void ratio under vertical and horizontal drainage conditions.

$$k = \exp(\frac{e - 8.291}{0.3155})$$
(2.34)

where k (m/s) is the hydraulic conductivity, e is the void ratio.

- **Somogyi (1979) and Berilgen (2006)**

Somogyi (1979) suggested that the variation of hydraulic conductivity during one-dimensional compression can be described in the following form:

$$k = Ce^D$$
(2.35)

where k (m/s) is the hydraulic conductivity, e is the void ratio, and C (m/s) and D are empirical coefficients.

Berilgen (2006) carried out seepage induced consolidation tests on clays in a slurry consistency. The data obtained from this study, together with information already in the literature, were used to investigate relationships between index properties and hydraulic conductivity. The author suggested that the coefficients C and D are correlated with the plasticity index and the liquidity index in the following forms:

$$C = \exp[-5.51 - 4\ln(I_P)] \tag{2.36}$$

$$D = 7.52\exp(-0.25I_L) \tag{2.37}$$

where $I_P$ (%) is plasticity index and $I_L$ (%) is liquidity index.

- **Dolinar (2009)**

Dolinar (2009) started from the power equation (Equation 2.31) proposed by Somogyi (1979), and pointed out that C and D are soil-dependent parameters, which reflect the tortuosity of the flow path and the cross-sectional characteristics of the flow conduit, depending on the shape and the size of the particles.

In this study, the hydraulic conductivity of non-expansive clays was measured using the falling-head test in an oedometer consolidation cell. Then, the following equations were proposed:

$$C = 4.08 \times 10^{-6} A_S^{-3.03} \tag{2.38}$$

$$D = 2.30 A_S^{0.234} \tag{2.39}$$

$$k = 4.08 \times 10^{-6} A_S^{-3.03} e^{2.30 S^{0.234}} \tag{2.40}$$

where $A_S$ (m$^2$/g) is the specific surface. Combining Equation 2.36 with Equation 2.10, the following equation is proposed to predict the hydraulic conductivity of fine-grained soils containing non-swelling clay minerals,

$$k_{sat} = \frac{6.31 \cdot 10^{-7}}{(I_P - 8.74p)^{3.03}} e^{2.66(I_P - 8.74p)^{0.234}} \tag{2.41}$$

where $k_{sat}$ (m/s) is the hydraulic conductivity, e is the void ratio, $I_P$ (%) is plasticity index, and p is the portion of clay minerals ($0 \leq p \leq 1$).

## 2.5 Summary

In this chapter, direct and indirect methods, as well as experimental apparatuses used for measuring the hydraulic conductivity of geomaterials are reviewed in detail. It is concluded that the constant head test performed in the Rowe cell is well suited for measuring the hydraulic conductivity of soft fine-grained geomaterials over a wide range of void ratios, hence it is adopted in this study to measure the hydraulic conductivity of MFT. A hydraulic conductivity database of oil sand tailings is established, which provides useful information for future studies in terms of the investigation of consolidation behaviors of oil sand tailings. Empirical equations developed in the literature to predict the hydraulic conductivity of fine-grained soils are summarized. These equations are classified into two categories, i.e. Class 1, Kozeny-Carman Equation and its Extensions; and Class 2, Equations based on Atterberg Limit Properties.
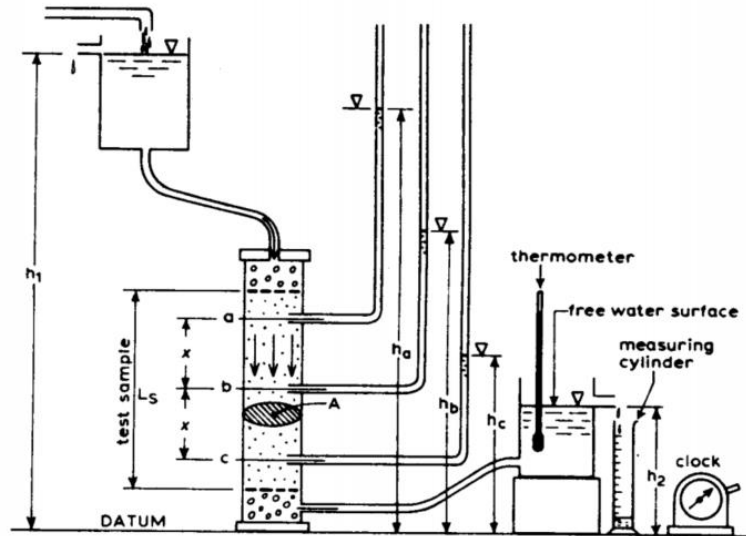
Figure 2. 1 Constant head test in the constant head permeameter
with downward flow (Head 1982)
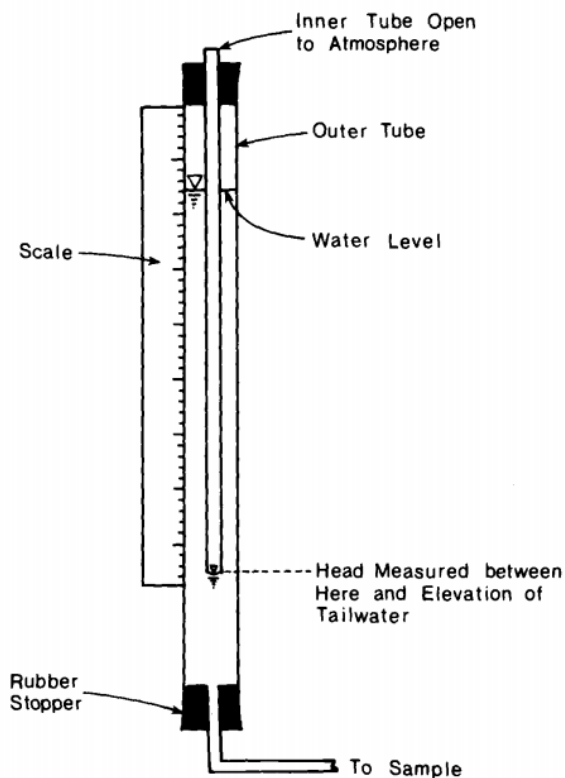


Figure 2. 2 Mariotte bottle (Olson et. al. 1981)
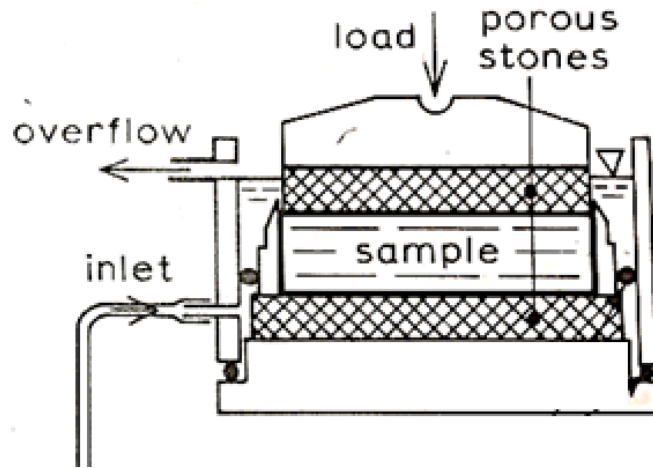
Figure 2. 3 Constant head test in oedometer cell (modified from Head 1982)
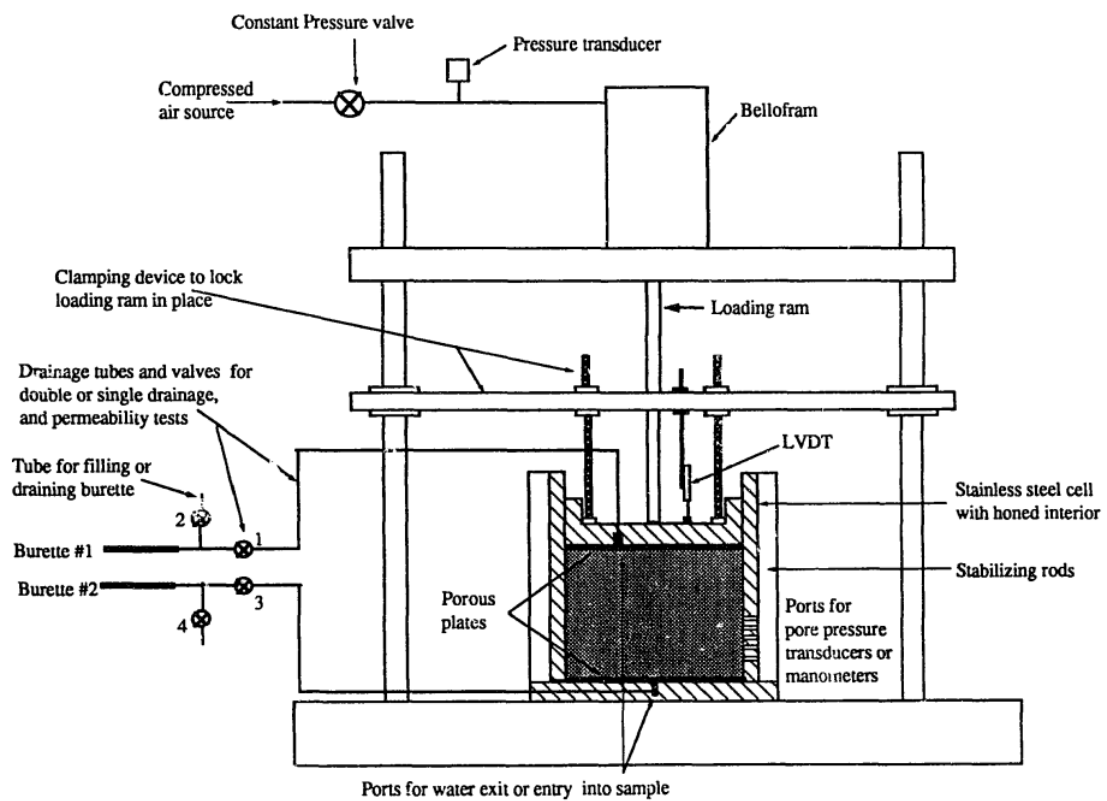


Figure 2. 4 Slurry consolidometer (Suthaker 1995)
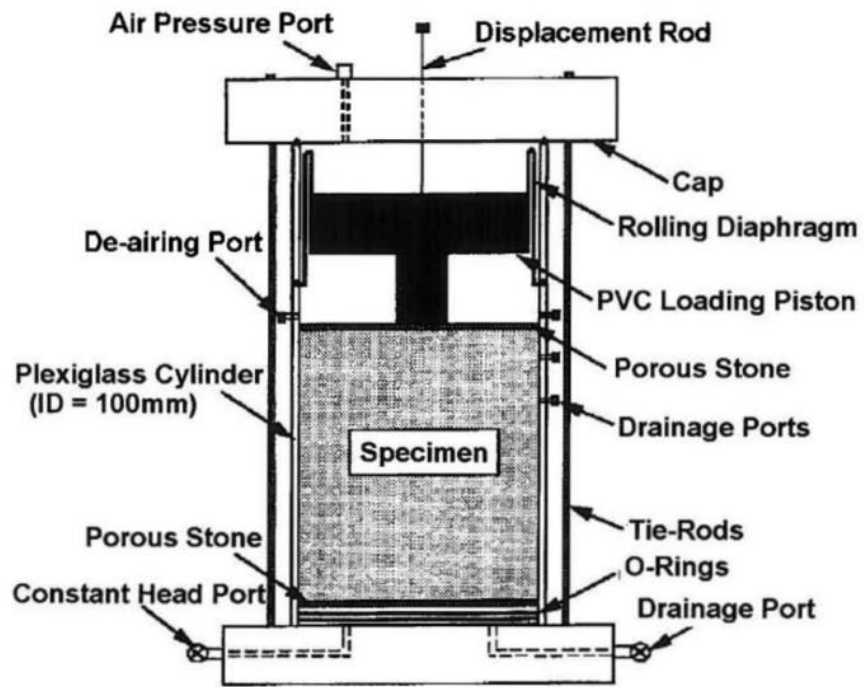
(a)
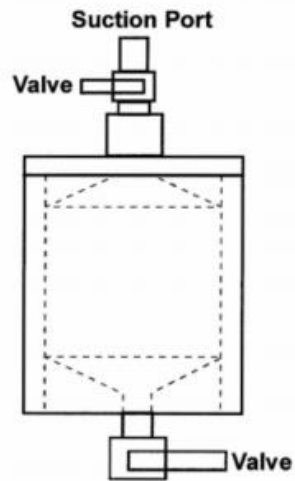


(b)
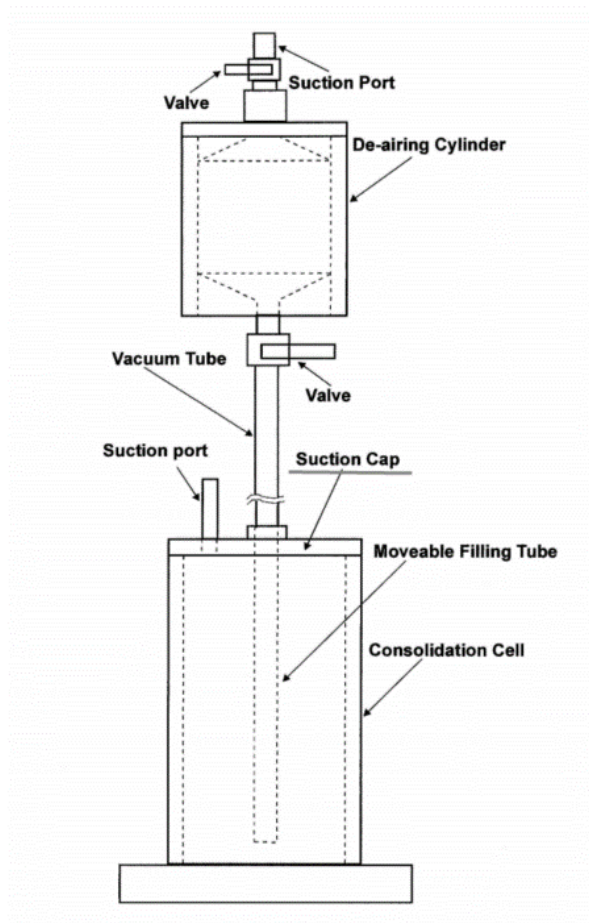
(c)

Figure 2. 5 (a) The large strain consolidation apparatus (b) The de-airing cylinder

(c) The tailings placement technique. (Qiu 2001)
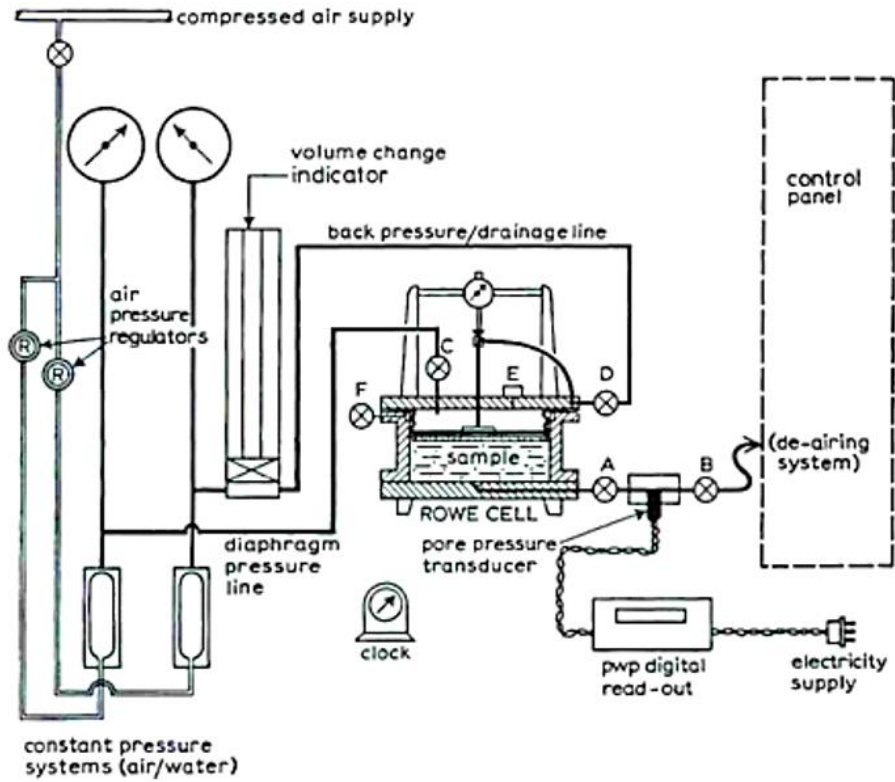
Figure 2. 6 The schematic diagram of a typical Rowe cell (modified form Head 1986)
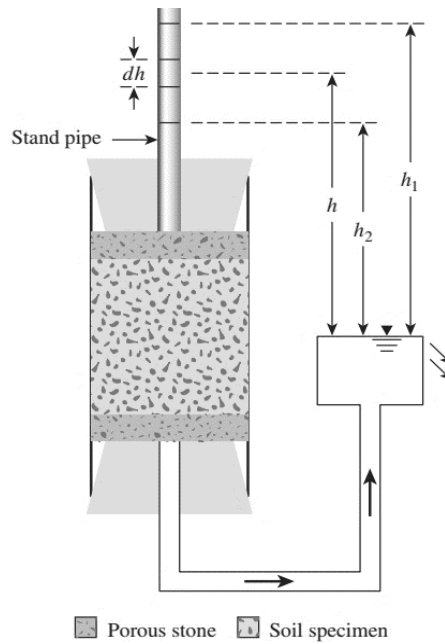


Figure 2. 7 Falling Head Permeameter (Das, 2013)
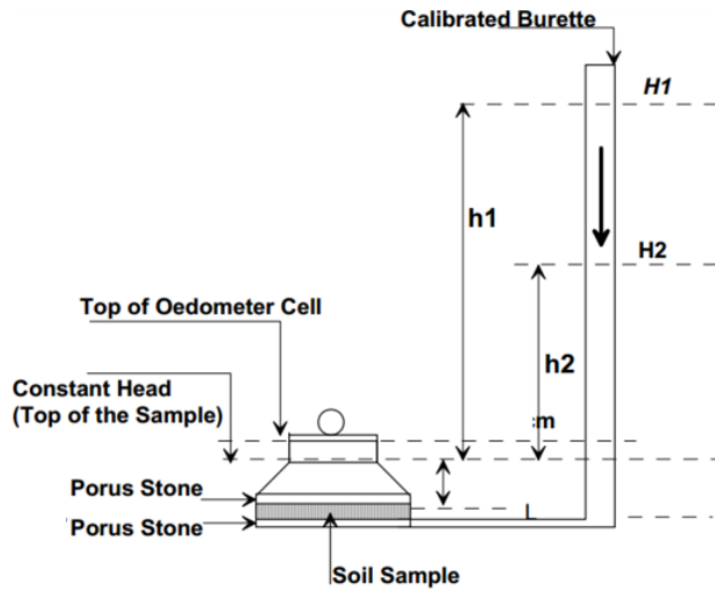
Figure 2. 8 Falling head test in oedometer consolidation cell (Owolagba 2013)
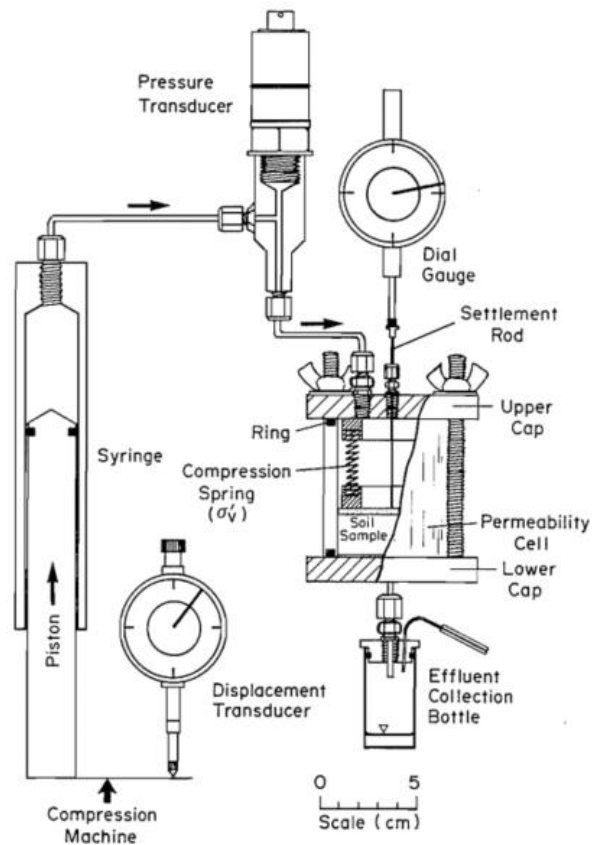


Figure 2. 9 Flow pump test (Fernandez, 1991)
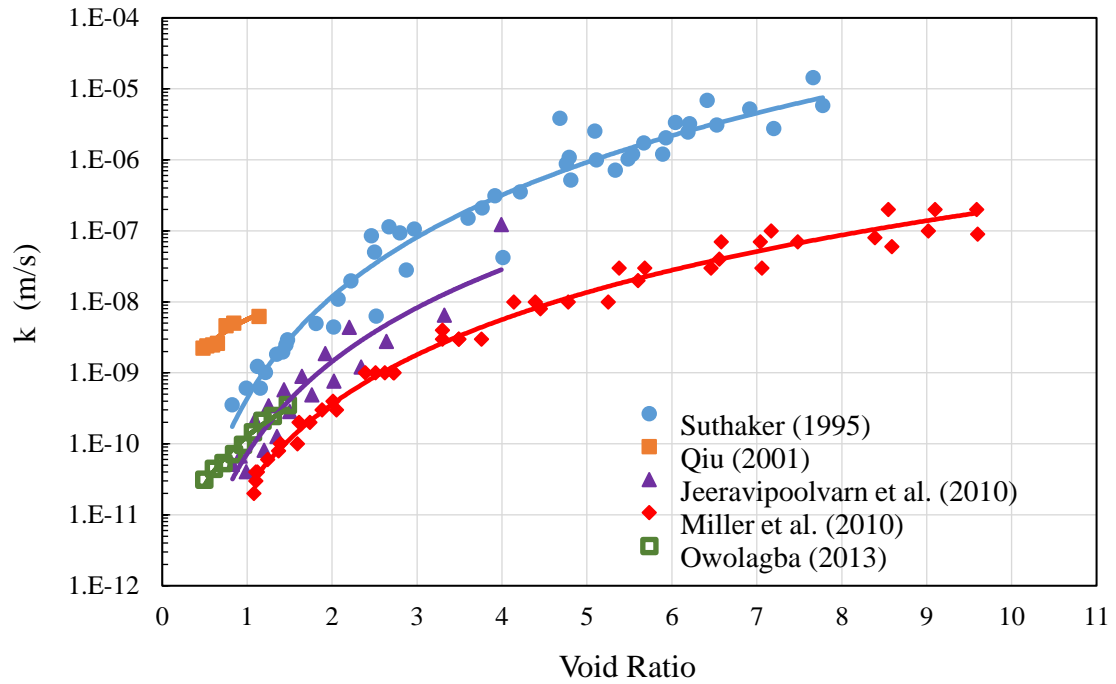
Figure 2. 10 Hydraulic conductivity database of oil sand tailings
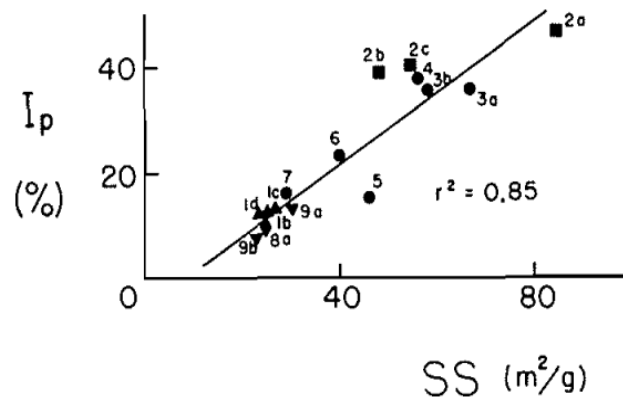


Figure 2. 11 Specific surface versus plasticity index for clay soils (Locat 1984)

# CHAPTER 3   METHODOLOGY OF HYDRAULIC CONDUCTIVITY MEASUREMENT OF FINE OIL SAND TAILINGS

## 3.1 Introduction

Establishing the relationship between a relatively large range of void ratios and hydraulic conductivity for fine oil sand tailings is one of the objectives of this study. As discussed in Chapter 2, the hydraulic conductivity of soils can be determined either indirectly and measured directly in the laboratory (Suthaker 1995). However, the characteristics of the fine oil sand tailings posts restrictions on the test methods that could be chosen. The measurement of hydraulic conductivity for fine oil sand tailings and other soft fine-grained geomaterials, which have high water content and generally in the form of slurries, is particularly challenging because these geomaterials have a large void ratio, high compressibility, low permeability, which result in nonlinear and lengthy consolidation.

The oedometer test, which is the standard test for measuring the consolidation characteristics of natural soils, was adopted in this study as an indirect method to estimate the hydraulic conductivity of fine oil sand tailings at relatively low water content and void ratio. As discussed in Chapter 2, direct measurement methods perform better than indirect methods for fine grained soils, particularly on soils with water contents above the liquid limits. Two direct measurement methods were adopted in this study, i.e., the falling head test and the Rowe cell test. The falling head test has been widely used in geotechnical laboratories for direct measurement of the hydraulic

conductivity of fine grained soils owing to its simplicity and availability of equipment at a reasonable cost (Aiban and Znidarcic 1989, Suthaker 1995). This test was used to measure the hydraulic conductivity of fine oil sand tailings at relatively high water content and void ratio. The Rowe cell has many advantages, as discussed in Chapter 2. It allows large deformations in the consolidation stage and allows the hydraulic conductivity measurement of the sample at the end of primary consolidation of each loading increment. The results obtained from the Rowe cell test are used to compare with results obtained from the oedometer test and falling head test.

In this chapter, the characterization of fine oil sand tailings used in this study is presented. Then three laboratory test methods of measuring the hydraulic conductivity of mature fine oil sand tailings are described in detail, including the experimental apparatus, testing procedures, and data analysis methods of the test results. The challenges associated with the sample preparation, the test set up and execution; as well as limitations and possible sources of errors are discussed at the end of each laboratory test method section.

## 3.2 Properties of fine oil sand tailings

The samples used in this study are the mature fine oil sand tailings (MFT) recovered from the tailings pond in Fort McMurray, Alberta, Canada, courtesy of Syncrude Canada Ltd. and Imperial Oil Canada. The properties of mature fine tailings are listed in Table 3.1. The specific gravity ($G_s$) is 2.51, and the liquid limit and plastic limit of mature fine tailings (MFT) are 51.6% and 29.1%, respectively. The plastic index, considered a measure of plasticity of geomaterials, is 22.5. The organic matter,

which is mainly attributed to residual bitumen in MFT, is 14.7wt%. Based on the Unified Soil Classification System (USCS), the mature fine tailings is classified as a silt with high plasticity (MH). The mature fine oil sand tailings have high water contents and large void ratios in tailings ponds. The natural water content is 171.3% when the mature fine tailings (MFT) samples were received (Guo 2012).

## 3.3 Standard Oedometer Test

The oedometer test, also known as the one-dimensional consolidation test, is used to determine the consolidation parameters for soils. The hydraulic conductivity of soils can also be derived from the test results. In the standard oedometer test (ASTM D2435), the soil sample is confined laterally and drained vertically while it is subjected to a sequence of incremental vertical loads; and each load increment is maintained until the excess pore water pressure is essentially dissipated.

Two standard oedometer tests (Oedo-1and Oedo-2) were carried out, and the initial water content and void ratio of both test samples were approximately 65% and 1.6, respectively. The next sections introduce the experimental apparatus used in the tests, the testing procedures, and data analysis methods for the standard oedometer test.

### 3.3.1 Experimental Apparatus

The consolidation test unit, consisting of a fixed ring consolidometer and a loading device, was used in this test. The test sample was confined in a stainless-steel consolidation ring of 15.2 mm in height and 49.7 mm in diameter. A linear displacement transducer mounted to the arm on the support post of the loading frame, as shown in Figure 3.1, was used to measure the deformation of the test sample during the

48

consolidation process. The linear displacement transducer and the readout unit were manufactured from Schaevitz Equipment LTD.

### 3.3.2 Testing Procedures

The standard oedometer tests were performed according to ASTM D2435-11, the standard test method for one-dimensional consolidation properties of soils using incremental loading (ASTM D2345). The test samples were first preconsolidated in the permeameter chamber by applying various loads on the sample and opening the drainage port at the bottom rim of the permeameter, as shown in Figure 3.2, in order to reach a lower water content. The preconsolidation pressure was less than the first loading increment in the subsequence oedometer test. The test sample was preconsolidated in the permeameter until it could sustain at least 2 kPa axial pressure. After completing preconsolidation, the sample was trimmed to the consolidation ring. It should be noted that the maximum water content of mature fine tailings sample used in the oedometer test is approximately 65%, which was ascertained by trial. At water contents higher than 65%, corresponding to a void ratio of 1.6, the oedometer test may not be suitable for the hydraulic conductivity measurement because the too soft sample can not be properly trimmed to a consolidation ring. In addition, very large nonlinear deformation can occur during consolidation for a soft sample, which results in errors in the back-calculation based on Terzaghi's one dimensional consolidation theory.

A standard incremental load was applied to two standard oedometer tests (Oedo-1and Oedo-2) in the following sequence: 5kPa, 10kPa, 25 kPa, 50 kPa, 100 kPa, 200 kPa and 400 kPa. The displacement readout was recorded and collected at 16 time

intervals: 6s, 15s, 30s, 1min, 2min, 4min, 8min, 15min, 30min, 1h, 2h, 4h, 6h, 24h, 48 and 72h. The sample deflection versus time was recorded during the test to monitor the progress of primary consolidation and to decide the time to apply to the next load increment. For MFT samples used in oedometer tests, the loading increment of 72 hours was proved to be reasonable.

### 3.3.3 Data Analysis

To back calculate the hydraulic conductivity from consolidation parameters, the coefficient of consolidation and the coefficient of volume change are assumed constant over each loading increment, and using the following equation that is derived from Terzaghi's one-dimensional consolidation theory (Budhu 2008),

$$k_z = \gamma_w c_v m_v$$  (3.1)

where, $k_z$ (L/T) is the hydraulic conductivity in the vertical direction, $\gamma_w$ (M/T$^2$L$^3$) is the unit weight of water (9.8 kN/m$^3$), $C_v$ (L$^2$/T) is the coefficient of consolidation, which is determined from two commonly used curve fitting methods, i.e. Cassagrande's logarithmic time method and Taylor's square root time method (Gofar and Kassim 2006), and $m_v$ (LT$^2$/M) is the coefficient of volume change or modulus of volume compressibility. After obtaining the values $C_v$, and $m_v$, the values of $\gamma_w$, $C_v$, and $m_v$ were substituted to Equation 3.1. The hydraulic conductivity values of mature fine tailings were obtained, and then the relationship between the hydraulic conductivity and void ratio for the mature fine oil sand tailings was established.

### 3.3.4 Discussion

The standard oedometer test, as a basic laboratory test, has been widely used in

50

geotechnical laboratories. However, based on the standard ASTM-D2435, the oedometer test was not applicable for the slurry-like soil such as the mature fine oil sand tailings with high water content, because of its large void ratio and high compressibility during self-consolidation stages (Proskin et al. 2010). The standard oedometer test was developed for the soil that is in a relatively solid phase with a shear strength of no less than 2 kPa (Olson and Daniel 1981). The other limitation is that the oedometer used in this study cannot measure the excess pore water pressure, therefore, the completion of primary consolidation is based solely on the change of sample height (Gofar and Kassim 2006).

In addition, the maximum initial water content of the MFT sample that can be used in the standard oedometer test is approximately 65%, which was estimated by trials, corresponding to a void ratio of 1.6. As discussed previously, at water contents higher than 65%, two major difficulties can invalidate the oedometer test for determining the hydraulic conductivity. For samples with higher void ratios, other measurement methods must be adopted.

## 3.4 Falling Head Test

The falling head permeability test, also known as the falling head test, is one of the most commonly used laboratory tests for the direct measurement of hydraulic conductivity (ASTM D5856). The falling head test is usually used for fine-grained soils with intermediate and low permeability. The mature fine tailings used in this study fits in this category. Another method, i.e. The constant head test (ASTM D5856) is used for coarse grained soils with high permeability. These two methods are widely used in

geotechnical laboratories owing to simplicity and availability of equipment at a reasonable cost (Aiban and Znidarcic 1989, Suthaker 1995).

The falling head tests with the downward flow and constant tail water elevation were carried out in this study on MFT samples of a wide range of void ratios, from approximately 1.5 to 7.0. A detailed description of the falling head test is given in ASTM D5856 Standard Test Method for Measurement of Hydraulic Conductivity of Porous Material Using a Rigid-Wall, Compaction-Mold Permeameter (ASTM D5856).

### 3.4.1 Experimental Apparatus

A rigid wall permeameter from Hoskin Scientific LTD. and an open standpipe fitted with a meter stick were used in this test. The permeameter chamber with 150 mm in height and 76.3 mm in inner diameter was used to place the sample. This permeameter allows for observation of the sample height from the transparent plexiglass wall. Water flowing through MFT samples from the standpipe connected to the influent port at the top plate of the permeameter and then to the funnel which was connected to the drainage port at the bottom rim of the permeameter, as the schematic diagram shown in Figure 3.3. This arrangement allows the downward hydraulic gradient to be applied to the test sample. The standpipe and funnel were connected to the permeameter both by rubber tubes. The funnel was clamped to the meter stick and used to maintain a constant tailwater level. The realistic view of the arrangement of the falling head test with the downward flow is shown in Figure 3.4.

### 3.4.2 Testing Procedures

The falling head tests were performed according to ASTM D5856 Standard Test

Method for Measurement of Hydraulic Conductivity of Porous Material Using a Rigid-Wall, Compaction-Mold Permeameter, Method B - Falling head, constant tailwater elevation (ASTM D5856). The sample with the natural water content of 171.3% was first preconsolidated in the permeameter chamber to reach a predetermined water content for the falling head tests by applying incremental vertical loads on the top of the sample and opening the drainage port of the permeameter, as shown in Figure 3.5. Another method of sample preparation was that the sample was first mixed with de-aired water and curing for 24 hours. The sample height was measured and recorded during consolidation. The sample height versus elapsed time was recorded and was plotted against log time, as shown in Figure 3.6. This step allows the falling head test to be conducted under a stable void ratio of the sample.

In the falling head test, the following values were recorded: the initial and final heads, denoted by $h_1$ and $h_2$, respectively (shown in Figure 3.3); the time t corresponding to $h_1$ to $h_2$; and the temperature, T, of the tail water in the funnel. The height of the sample was measured and recorded at the start and end of each permeation trial. Four or five permeation trials were conducted consecutively to obtain at least four values of hydraulic conductivity in one falling head test. At the end of the test, the permeameter was dismantled and the final water content of the test sample was determined.

### 3.4.3 Data Analysis

The hydraulic conductivity is calculated from the falling head test by using the following equation (Holtz and Kovacs, 1981):

$$k_T = 2.303 \frac{aL_{av}}{At} \log_{10} \frac{h_1}{h_2} \quad \text{(cm/s)} \tag{3.2}$$

where $k_T$ (cm/s) is the hydraulic conductivity in the vertical direction carried out at T°C, a (cm$^2$) is the cross-sectional area of the standpipe, $L_{av}$ (cm) is the average value of the sample height at the beginning and end of each permeation trial. A (cm$^2$) is the cross-sectional area of the test sample, $h_1$ (cm) and $h_2$ (cm) are initial and final hydraulic head difference, respectively, t (s) is the time duration for the head difference dropping from $h_1$ to $h_2$. Then the $k_T$ value was corrected to a baseline temperature of 20°C by using the following equation (Budhu 2007):

$$k_{20} = k_T (\frac{\mu_T}{\mu_{20}}) = k_T R_T \tag{3.3}$$

where $\mu_T$ and $\mu_{20}$ are the viscosities of water at T°C and 20°C, respectively. T is the temperature at which the permeation trial was made, and $R_T$ is the temperature correction factor that was calculated using the following equation:

$$R_T = 2.42 - 0.475 \ln(T) \tag{3.4}$$

After calculating the average value of hydraulic conductivity, $k_{20}$, which was obtained from each permeation trial in one falling head test, the relationship of the test sample between the hydraulic conductivity and void ratio was obtained.

### 3.4.4 Discussions

The falling head test has been widely used in geotechnical laboratories owing to its simplicity and the availability of equipment at a reasonable cost (Suthaker 1995), as well as the simplicity of interpretation of test data.

For the soil sample with low permeability, it is usually necessary to apply larger

hydraulic gradients in the laboratory to accelerate the test, while a high hydraulic gradient produces high seepage force that can consolidate soft and compressible samples, which results in reducing the sample hydraulic conductivity as the test proceeds. Therefore, the major challenge for the falling head test was applying an appropriate hydraulic gradient to the samples without causing significant consolidation and to avoid prolonged testing time. The sample height should be continuously monitored during the test. Once an obvious change of the sample height occurs the test should be terminated.

Due to limitations of the experimental conditions, two possible sources of errors for this test are identified: 1) The test can only measure the inflow rate, which may lead to an error in obtaining the hydraulic conductivity value, especially for soft fine-grained soils in which consolidation and permeability may occur together (Chapuis 2012); 2) Evaporation from the standpipe or the tail water funnel may occur, which would lead to overestimation of the hydraulic conductivity values.

In addition, the minimum water content of the MFT samples that can be achieved by consolidating the sample in the permeameter is approximately 60%. Therefore, in this study, the falling head test can measure the hydraulic conductivity of MFT samples with water contents higher than 60%, corresponding to a void ratio of 1.5.

## 3.5 Rowe Cell Test

The Rowe cell, also known as the hydraulic consolidation cell, was developed by P. W. Rowe and his research group to overcome the disadvantages of the conventional oedometer apparatus when performing consolidation tests on low permeability soils

55

(Head 1986). A detailed description of the experimental apparatus and ancillary devices, testing procedures, and data analysis methods for the Rowe cell test are presented in this section.

The schematic diagram of a typical Rowe cell is shown in Figure 3.7 (a). The main feature of the Rowe cell is its hydraulic loading system. In the Rowe cell, a sample is loaded hydraulically by water pressure acting on a convoluted flexible diaphragm, which differs from the mechanical lever system used in the conventional oedometer. This allows for testing large diameter samples, i.e, up to 250 mm diameter for commercial purposes, and allows for large deformations in consolidation. With the hydraulic loading system, the loading pressure, including very low pressures, can be easily applied (Head 1986). In contrast to the conventional oedometer apparatus, the Rowe cell allows the direct measurement of hydraulic conductivity, either as an independent test or after the consolidation test on a sample with a known vertical effective stress. More importantly, the Rowe cell has abilities to control drainage conditions, to measure pore water pressure during the consolidation stage, and to apply back pressure throughout the test, as introduced in Chapter 2.

In this study, four Rowe cell tests, i.e. RC 1, RC 2, RC 3 and RC 4, were carried out to measure the hydraulic conductivity of MFT over a wide range of void ratios, from approximately 1 to 6. This range partially overlaps with the ranges of the standard oedometer test and falling head test. Each Rowe cell test includes step loadings consolidation tests and permeability tests. A permeability test was performed during the consolidation test sequence at the end of each loading stage.

56

### 3.5.1 Experimental Apparatus

The following apparatuses were used in this study for Rowe cell tests:

- A Rowe cell

- A Brainard. Kilman pressure control panel (B.K panel)

- A vertical pressure transducer

- A pore water pressure transducer

- A linear displacement transducer

- A volume change indicator

- A data logger

A Rowe cell produced by ELE International, UK, of 150 mm nominal diameter was used in this study, as shown in Figure 3.7 (b). The cell has an internal diameter of 150.4 mm with a smooth plastic lining, as shown in Figure 3.8 (b). The cell consists of three parts: the cell top, the cell body, and the cell base, as shown in Figure 3.8. The cell top is fitted with a convoluted flexible diaphragm made of synthetic rubber, which is used to transmit a uniform water pressure to the sample underneath. The cell top is also fitted with an inlet valve, denoted by valve C as shown in Figure 3.7 (a), connecting to a hydraulic pressure on a sample. An aluminum alloy hollow spindle passes through a seal in the center of the cell top. The lower end of this spindle passes through the center of the diaphragm at which it is sealed and fixed by two thin washers. The upper end of it is connected to a drainage valve, denoted by valve D, via a flexible tube, as shown in Figure 3.7 (a). The drainage valve D is fitted to the edge of the cell top. An air bleed screw, denoted by E as shown in Figure 3.7 (a), is placed on the top of the cell top. The

cell body has a flange at each end with bolt holes for securing the cell top and base, as shown in Figure 3.8 (b). A small hole at the upper end of the cell body is an outlet leading and connected to a valve, denoted by valve F as shown in Figure 3.7 (a). A smooth plastic lining is bonded onto the inside face of the cell body to reduce the friction between the sample and cell wall. A small circular pore stone is inserted in the center of the cell base. This is the main pore water pressure measuring point, and leads to valve A (as shown in Figure 3.7 (a)) on the outer edge of the cell base. Valve A is connected to the pore water pressure transducer. (Head 1986)

Two large pore stones obtained from Hoskin Scientific LTD of 150 mm in diameter and 13 mm in thickness are used with the Rowe cell, as shown in Figure 3.9.

A Brainard-Kilman pressure control panel (B.K panel) is used to provide three independently controlled pressures required for the Rowe cell test: the vertical pressure, and two separate back pressures. The realistic view and schematic diagram of the B.K panel are shown in Figures 3.10 and 3.11, respectively. The three pressure systems are fitted on the B.K panel on positons 1, 2 and 3, respectively, as shown in Figure 3.11. The B.K pressure control panel has an accuracy of 1kPa (B.K. panel operation manual).

The vertical pressure transducer, which has a better accuracy of 0.1 kPa compared with the B.K pressure control panel, measured the real-time pressure applied on the sample. The pore water pressure was measured by the pore water pressure transducer, which has an accuracy of 0.1 kPa. A linear displacement transducer was used to measure vertical displacements of the sample during the test. It has a maximum travel of 25 mm and has the accuracy of 0.001 mm. The above transducers were manufactured by

58

Dynisco Ltd.

The volume change indicator (SHAPE Instrument Ltd.), as shown in Figure 3.12, was used to measure the volume of the outflow water during the consolidation test and permeability test. It was incorporated into the drainage line of the Rowe cell test arrangement by connecting with valve D. The volume change indicator used in this study has the maximum capacity of 100ml and has the accuracy 0.01ml. All the measured data, including vertical pressure, pore water pressure, deflections of the testing sample and the volume of the outflowing water, were recorded by the data logger (SCIEMETRIC INC).

### 3.5.2 Testing Procedures

For the MFT samples having a water content much higher than the liquid limit, it is necessary to start with applying a low consolidation pressure and gradually increase in a few increments. In this study, four Rowe cell tests were performed.

In the first Rowe cell test (RC 1), the sample with an initial water content of 176.9% was consolidated under four loading increments with a back pressure. The incremental vertical loading was applied in the following sequence: 7 kPa, 12 kPa, 17 kPa and 43 kPa. The corresponding back pressure for each loading step was applied in the following sequence: 5 kPa, 7 kPa, 10 kPa and 33 kPa. Thus, the theoretical effective stresses of the sample after the completion of each loading consolidation were as follows: 2 kPa, 5 kPa, 7 kPa and 10 kPa. The above pressures applied in the RC 1 test are summarized in Table 3.2. After the completion of primary consolidation under each loading, one-way drainage permeability tests were carried out on the samples of known

59

effective stress in the Rowe cell with the vertical upward flow. Two constant back pressures were applied to the sample to provide a constant differential pressure between the sample base and top, while the sample was subjected to a vertical pressure as in the previous consolidation step. The differential pressures applied to the sample at each permeability test are also summarized in Table 3.2.

In the second Rowe cell test (RC 2), the sample with an initial water content of 129.7% was consolidated by incremental loading. A back pressure of 10 kPa was maintained during the test. The incremental vertical loads were: 12 kPa, 13 kPa, and 15 kPa. Thus, the theoretical effective stresses on the sample after the completion of consolidation in each stage were: 2 kPa, 3 kPa, and 5 kPa. At the end of each consolidation stage, the permeability test was carried out under a constant differential pressure. Pressures applied in the RC 2 test are summarized in Table 3.3.

In the third Rowe cell test (RC 3), the sample with an initial water content of 210.4% was consolidated under four loading increments with a back pressure of 5 kPa. The incremental vertical loads were: 7 kPa, 8 kPa, 9 kPa and 10 kPa. The theoretical effective stresses on the sample after the completion of consolidation in each stage were: 2 kPa, 3 kPa, 4 kPa and 5 kPa. At the end of each consolidation stage, a permeability test was carried out under a constant differential pressure. Pressures applied in the RC 3 test are summarized in Table 3.4.

In the fourth Rowe cell test (RC 4), the sample with an initial water content of 76.7% was consolidated in four increments with a back pressure of 10 kPa. The incremental vertical loads were: 15 kPa, 20 kPa, 30 kPa and 50 kPa. The theoretical effective

stresses on the sample after the completion of consolidation in each stage were: 5 kPa, 10 kPa, 20 kPa and 40 kPa. At the end of each consolidation stage, a permeability test was carried out under a constant differential pressure. Pressures applied in the RC 4 test are summarized in Table 3.5.

In this study, the Rowe cell tests were carried out primarily based on Hydraulic Cell Consolidation and Permeability Test in the *Manual of Soil Laboratory Testing* (Head 1986), while some steps were modified to accommodate the B.K pressure system. A detailed description of the test executions is introduced in the following steps.

**Step 1. Cell assembly**

The cell body was first bolted to the cell base, as shown in Figure 3.13. MFT samples were poured into the cell to a depth of 15-30 mm with a uniform surface. Then, the cell top was placed on the cell body, and the diaphragm flange of the cell top was seated onto the cell body flange without entrapping air or causing ruckling or pinching, as shown in Figure 3.14. The view of the correctly seated diaphragm flange on the cell body flange is shown in Figure 3.15. After completing the cell assembly, the valve C (Rowe cell) was connected to a water supply to completely fill the space above the diaphragm with water. (Head 1986)

**Step 2. Rowe cell connection with B.K pressure system**

The arrangement of the Rowe cell and connections with a B.K Pressure control panel are shown in Figure 3.16. The valve C (Rowe cell) was connected with valve Q1 (B.K panel) through a flexible tube, as shown in Figure 3.18. This line provided vertical hydraulic pressures on the sample throughout the Rowe cell test. The valve A (Rowe

cell) was connected with valve Q2 (B.K panel) through a flexible tube, as shown in Figure 3.18. This line provided one of the back pressure to the sample during permeability test but kept closed during consolidation stage. The valve D (Rowe cell) was connected to the volume change indicator, which was then connected to the valve Q3 (B.K panel), as shown in Figure 3.16. This line was the drainage line in which water flowed out of the sample through valve D (Rowe cell) to the volume change indicator; which provides another back pressure to the sample throughout the Rowe cell test. The above three lines were fully saturated with freshly de-aired water and de-aired by flushing with de-aired water to ensure saturation.

Then, the vertical pressure transducer, pore water pressure transducer, displacement transducer and volume change indicator were connected to the data-logger. The readings showing on the data logger were calibrated to be consistent with the readings showing on the B.K pressure panel.

**Step 3. Checking Saturation**

The degree of saturation of MFT samples can be related to the pore pressure ratio, i.e. $\delta u / \delta \sigma$, where $\delta u$ is the pore pressure response to an increment of the total vertical stress $\delta \sigma$ without drainage (Head 1986). It should be noted that this ratio is not the exact pore pressure parameter B, which is defined as the pore pressure response to the increments of isotropic stress not vertical stress. However, the similar method was used to check the saturation of the sample in this study. Saturation is usually acceptable when the ratio $\delta u / \delta \sigma$ reaches approximately 0.9 (Head 1986). The detailed execution of checking saturation degree of samples is introduced as follows.

A very small vertical pressure, $p_0$, which was less than the first increment consolidation pressure, was applied to the sample without drainage (valve D closed). The initial vertical pressure, $p_0$, and the initial pore pressure, $u_0$, were recorded by the data logger when $p_0$ and $u_0$ reach a stable value. Then, the vertical pressure was increased from the initial pressure $p_0$ to a value that gave the required first increment pressure $p_1$, typically an increase of 3 to 5 kPa on the sample, without drainage. The pore pressure $u_1$ was recorded when it reached a stable value. The initial ratio, $\delta u/\delta \sigma$, was calculated as:

$$\frac{\delta u}{\delta \sigma} = \frac{u_1 - u_0}{p_1 - p_0} \qquad (3.5)$$

The initial ratios ($\delta u/\delta \sigma$) of the MFT samples used in this study were larger than 0.92, which means the samples satisfy the test saturation requirement. After checking the saturation condition of the sample, the vertical pressure was set back to the initial pressure $p_0$.

**Step 4. Consolidation Test**

The vertical pressure was set to the first increment consolidation pressure on the B.K panel with valve C (Rowe cell) closed. The back pressure was set to a desired value corresponding to the first incremental loading with valve D (Rowe cell) closed. The data logger was first to run to record the initial vertical deflection reading and the initial volume change indicator readings, corresponding to time equal to zero.

The consolidation stage was started by opening valves C and D to apply vertical pressure and back pressure on the sample and allow water to be expelled from the sample. Once opened valves C and D allowed water to drain from the sample, the

63

applied stress was transferred from the pore water to the soil skeleton, increasing the effective stress, while the total applied vertical stress was held constant. The following data were recorded by the data logger at an appropriate time intervals.

- Vertical settlement

- Pore water pressure

- Volume-change indicator on outlet back pressure line

- Diaphragm pressure for checking purpose

As the consolidation stage proceeded, the following graphs were created.

- Settlement ($\Delta H$ mm) against log time (min)

- Outflow volume change ($\Delta V$ mm) against log time (min)

- Pore water pressure against time (min)

The permeability test was performed when the primary consolidation was completed based on instruction listed above, i.e. the pore pressure approached the back pressure. For most practical purposes, 95% dissipation of the excess pore pressure is sufficient (Head 1986). The percentage pore pressure dissipation, denoted by U%, is given by the following equation:

$$U = \frac{u_0 - u}{u_0 - u_b} \times 100\%$$

$$(3.6)$$

where, u is the pore water pressure at a time considered, $u_b$ is the back pressure applied in the consolidation stage, and $u_0$ is the pore water pressure at the start of consolidation.

**Step 5. Permeability test**

One-way drainage permeability tests were carried out on the samples of known effective stress in the Rowe cell with the vertically upward flow. Three independently

controlled constant pressure systems were used for the permeability test. One system was connected to valve C (Rowe cell) to maintain the pressure as applied in the previous consolidation step. The other two back pressures were connected to valve A and D, respectively, as shown in Figure 3.16. The arrangement of the Rowe cell for the one-way drainage permeability test is shown in Figure 3.17, and this arrangement allows water to vertically flow upward through the sample by applying different inlet (p2) and outlet (p1) pressures between the sample base and top, while the sample was subjected to a vertical pressure as the in previous consolidation step.

The differential pressure between the inlet and outlet was adjusted by trial and error to establish a reasonable rate of flow through the sample. In this study, 1 or 2 kPa differential pressure, $\Delta p$, between the inlet and outlet was used (shown in Tables 3.2 to 3.5), which was ascertained from the trials. The procedure for the permeability test in the Rowe cell is described as follows:

The outlet pressure P2 was maintained the same as the back pressure applied in the consolidation stage. The inlet pressure P1 was adjusted by starting with a pressure equal to P2 and increasing progressively, but this pressure must never exceed the vertical pressure. The differential pressures $\Delta p$ applied in the permeability tests are shown in Tables 3.2- 3.5.

The volume of the cumulative outflow water Q (ml) and the elapsed time t (s) were recorded by the data logger. As the permeability test proceeded, the graph of the cumulative outflow water Q (ml) on ordinate against the elapsed time t (minute) on abscissa was plotted. The test was continued until a steady rate of flow was reached, i.e.

the graph presented a linear segment. In this study, permeability tests generally lasted 1.5 to 2 hours to allow enough linear segment on the graph to emerge. The permeability test was stopped by closing valves A and D.

**Step 6. Further consolidation tests and permeability tests**

Additional tests at the higher effective stress level were carried out by either raising the vertical pressure only or by raising vertical pressure and back pressure both but with different increments to the predetermined value. In this study, the samples were consolidated 3 or 4 times at the subsequent loading levels by increasing the vertical pressure and back pressure to the desired value, as summarized in Tables 3.2- 3.5.

The procedures described in Step 4--Consolidation Test were repeated. After setting up the vertical pressure and back pressure to the next loading level on the B.K pressure control panel, valves C and D were opened simultaneously to allow water to be expelled from the sample under a new consolidation pressure. When the primary consolidation was completed, the permeability test was carried out by repeating the procedures as described in Step 5 on a sample under a new void ratio and effective stress level.

After the samples were consolidated 3 or 4 times, the Rowe cell was disassembled and the final water content was measured.

**3.5.3 Data analysis**

The hydraulic conductivity can be directly measured by the Rowe cell tests. The graph of the cumulative outflow water Q (ml) against the elapsed time t (minute) was plotted, in which the slope of the linear segment of the graph was used to calculate the

rate of flow, q (ml/minute), i.e. q = δQ/δt (ml/minute). The pressure difference Δp across

the soil sample was equal to (p2 – p1). The hydraulic conductivity of the sample can be

calculated by using the following equation based on Darcy's Law, (Head 1986)

$$k_V = \frac{q_V}{60Ai} \quad \text{(m/s)} \tag{3.7}$$

where $k_v$ is the hydraulic conductivity in vertical direction (m/s), $q_v$ is the rate of vertical

flow (ml/minute) obtained from the slope of the linear part of the graph of the

cumulative outflow water Q against the elapsed time t, A is the sample cross-sectional

area ($mm^2$), approximately 18,000$mm^2$, and i is the hydraulic gradient. A pressure

difference of 1 kPa is equivalent to a water head 1/9.81m≈102 mm (Head 1986). Thus,

the hydraulic gradient i can be calculated from the following equation:

$$i = \frac{102}{H} \times \Delta P \tag{3.8}$$

where, Δp (kPa) is the pressure difference between the inlet pressure $p_2$ and outlet

pressure $p_1$, and H is the height of the sample (mm). Substituting Equation 3.8 into

Equation 3.7, the hydraulic conductivity, $k_v$, can be expressed as:

$$k_V = \frac{q_V}{60Ai} = \frac{q_V H}{60A \times 102\Delta P} = \frac{q_V H}{6120A\Delta P} \tag{3.9}$$

The hydraulic conductivity values calculated from Equation 3.9 were corrected to

the equivalent values at 20°C by using the temperature correction factor $R_T$, as

introduced in Section 3.4.3.

The void ratio corresponding to each hydraulic conductivity value of the sample

was back-calculated from the final void ratio after obtaining the final water content.

### 3.5.4 Discussion

The most important feature of the Rowe cell is that it allows the consolidation and permeability tests to be directly and successively conducted, which provides data covering a wide range of void ratios or strains (Gofar and Kassim 2006). The Rowe cell test can be used for the measurement of the hydraulic conductivity of the MFT samples, partially overlapping with the ranges of the standard oedometer tests and falling head tests. In addition, the advanced hydraulic loading system, and the abilities to control drainage and to measure pore water pressure, as well as to apply the back pressure to the sample, contribute to more reliable results compared to other methods.

### 3.6 Summary

This chapter describes in detail the experimental apparatus, testing procedures and data analysis for the standard oedometer test, the falling head test and Rowe cell test used in this study to measure the hydraulic conductivity of mature fine oil sand tailings. In the standard oedometer test, the incremental loads were applied to the samples, and vertical settlements were measured throughout the test. Due to the limitations of the test, the ASTM-D2435 standard oedometer test was not applicable for the MFT samples with the initial water content and void ratio higher than 65 % and 1.6, respectively.

The falling head test was chosen as one of the direct measurement methods to determine the hydraulic conductivity of the mature fine oil sand tailings. The major difficulty encountered during the test was adjusting an appropriate hydraulic gradient to the MFT samples to avoid the prolonged testing time and to avoid consolidation. Then, two possible sources of errors for this test were recognized because of limitations

of the experimental conditions.

The Rowe cell test overcomes the disadvantages inherent in the standard oedometer test and falling head test for measuring the hydraulic conductivity of the mature fine tailings. The Rowe cell test is capable of testing the sample covering a large range of void ratios, which partially overlaps the range of both standard oedometer and falling head tests. Comparing three laboratory test methods, the Rowe cell test is more complex than the other two tests in terms of the experimental apparatus assembly and connection, as well as test execution. In addition, the advanced control features, the ability to measure pore water pressure and the ability to apply back pressure on the sample contribute to more reliable test results obtained with Rowe cell tests.

Table 3. 1 Properties of mature fine tailings (modified from Guo 2012)

| | | |
|---|---|---|
| Specific gravity, $G_s$ | | 2.51 |
| Organic matter (%) | | 14.7 |
| Atterberg limits | Plastic limit, PL (%) | 29.1 |
| | Liquid limit, LL (%) | 51.6 |
| | Plasticity index, PI (%) | 22.5 |
| Grain size | $D_{10}$ (μm) | 0.85 |
| | D50 (μm) | 7.15 |
| | D90 (μm) | 27.9 |
| | Sand (%) | 0.00 |
| | Silt (%) | 80.00 |
| | Clay (%) | 20.00 |
| Unified Soil Classification | | MH |

Table 3. 2 Summary of Rowe cell test 1 (RC 1)

| | Vertical Pressure (kPa) | Outlet Back Pressure P2 (kPa) | Inlet Back Pressure P1 (kPa) | Effective stress after consolidation σ' (kPa) | Differential Pressure Δp (kPa) |
|---|---|---|---|---|---|
| C-1[a] | 7 | 5 | n/a | 2 | n/a |
| P-1[b] | 7 | 5 | 6 | 2 | 1 |
| C-2 | 12 | 7 | n/a | 5 | n/a |
| P-2 | 12 | 7 | 9 | 5 | 2 |
| C-3 | 17 | 10 | n/a | 7 | n/a |
| P-3 | 17 | 10 | 12 | 7 | 2 |
| C-4 | 43 | 33 | n/a | 10 | n/a |
| P-4 | 43 | 33 | 35 | 10 | 2 |

a. C refer to consolidation test;

b. P refers to permeability test

Table 3. 3 Summary of Rowe cell test 2 (RC 2)

| | Vertical Pressure (kPa) | Outlet Back Pressure P2 (kPa) | Inlet Back Pressure P1 (kPa) | Effective stress after consolidation σ' (kPa) | Differential Pressure Δp (kPa) |
|---|---|---|---|---|---|
| C-1[a] | 12 | 10 | n/a | 2 | n/a |
| P-1[b] | 12 | 10 | 11 | 2 | 1 |
| C-2 | 13 | 10 | n/a | 3 | n/a |
| P-2 | 13 | 10 | 12 | 3 | 2 |
| C-3 | 15 | 10 | n/a | 5 | n/a |
| P-3 | 15 | 10 | 12 | 5 | 2 |

a. C refer to consolidation test;

b. P refers to permeability test

Table 3. 4 Summary of Rowe cell test 3 (RC 3)

| | Vertical Pressure (kPa) | Outlet Back Pressure P2 (kPa) | Inlet Back Pressure P1 (kPa) | Effective stress after consolidation σ' (kPa) | Differential Pressure Δp (kPa) |
|---|---|---|---|---|---|
| C-1[a] | 7 | 5 | n/a | 2 | n/a |
| P-1[b] | 7 | 5 | 6 | 2 | 1 |
| C-2 | 8 | 5 | n/a | 3 | n/a |
| P-2 | 8 | 5 | 6 | 3 | 1 |
| C-3 | 9 | 5 | n/a | 4 | n/a |
| P-3 | 9 | 5 | 6 | 4 | 1 |
| C-4 | 10 | 5 | n/a | 5 | n/a |
| P-4 | 10 | 5 | 6 | 5 | 1 |

a.  C refer to consolidation test;

b.  P refers to permeability test

Table 3. 5 Summary of Rowe cell test 4 (RC 4)

| | Vertical Pressure (kPa) | Outlet Back Pressure P2 (kPa) | Inlet Back Pressure P1 (kPa) | Effective stress after consolidation σ' (kPa) | Differential Pressure Δp (kPa) |
|---|---|---|---|---|---|
| C-1[a] | 15 | 10 | n/a | 5 | n/a |
| P-1[b] | 15 | 10 | 12 | 5 | 2 |
| C-2 | 20 | 10 | n/a | 10 | n/a |
| P-2 | 20 | 10 | 12 | 10 | 2 |
| C-3 | 30 | 10 | n/a | 20 | n/a |
| P-3 | 30 | 10 | 12 | 20 | 2 |
| C-4 | 50 | 10 | n/a | 40 | n/a |
| P-4 | 50 | 10 | 12 | 40 | 2 |

a.  C refer to consolidation test;

b.  P refers to permeability test

Figure 3. 1 The consolidation test unit



| (a) | (b) |

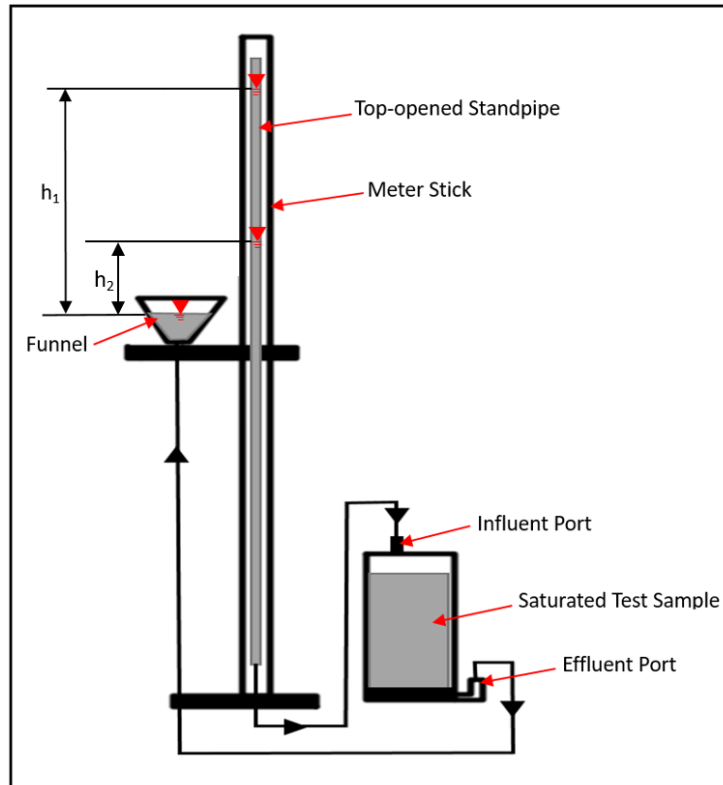Figure 3. 2 Preconsolidation of sample in permeameter before the oedometer test

Figure 3. 3 Schematic of Falling Head Test



Figure 3. 4 Falling head test apparatus

(a)



(b)

Figure 3. 5 (a) Preconsolidation of sample in permeameter

before the falling head test
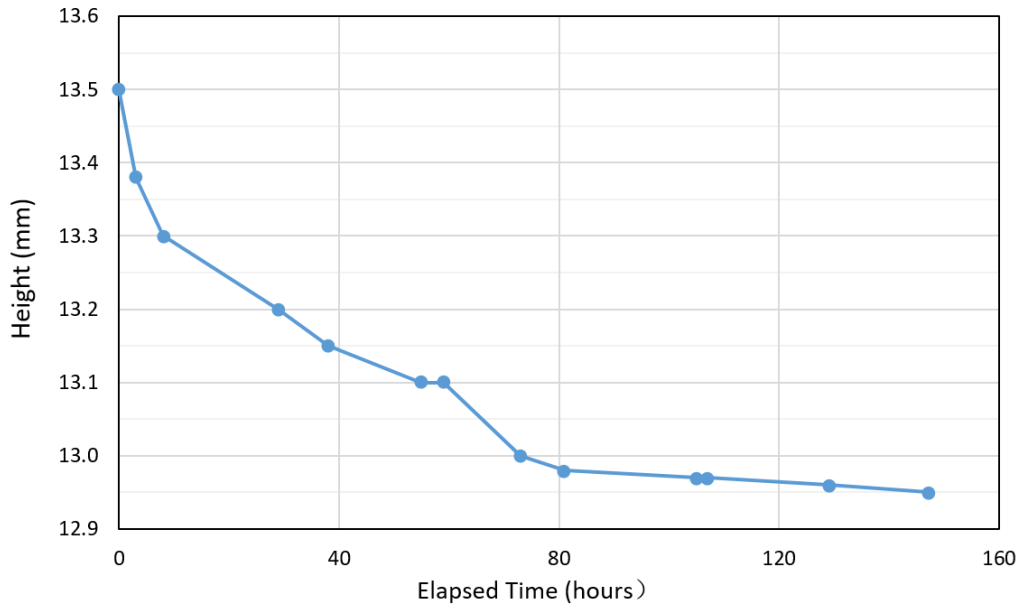
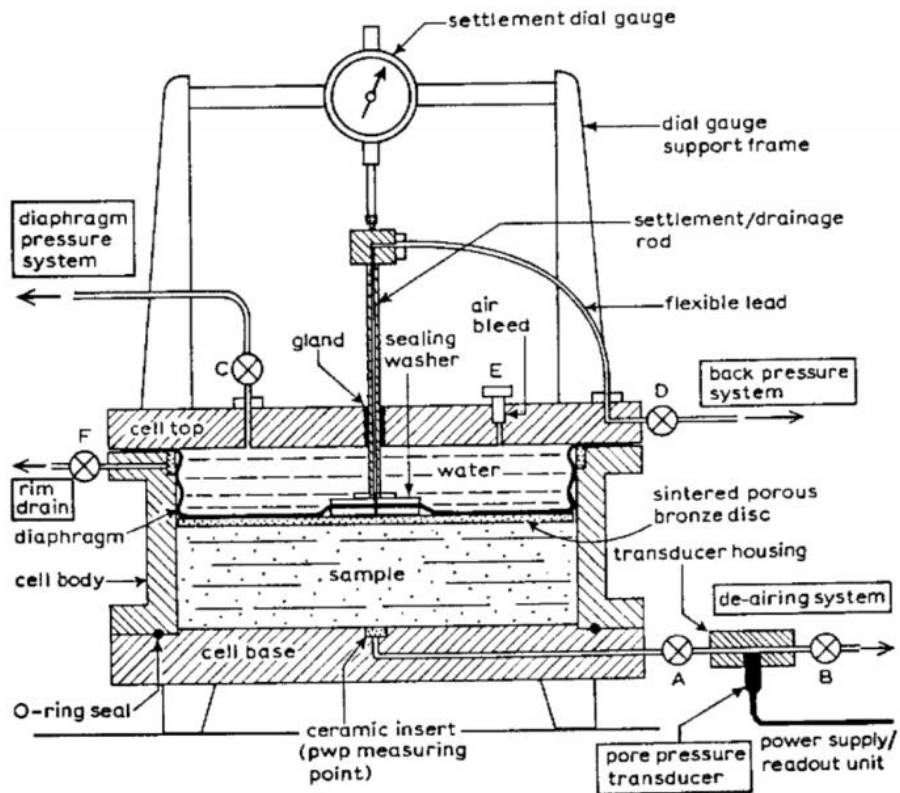(b) Weights used to preconsolidate the sample

Figure 3. 6　Sample height versus time during preconsolidation
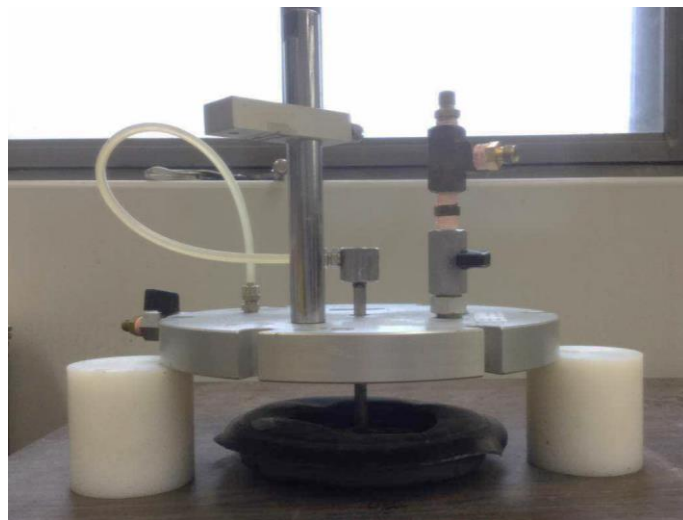


(a)

(b)

Figure 3. 7 (a) Schematic of Rowe cell (Head 1986) (b) Rowe cell used in this study



(a)

(b)



(c)

Figure 3. 8 (a) Rowe Cell Cover; (b) Rowe Cell Body; (c) Rowe Cell Base



Figure 3. 9 Two porous stones used in Rowe cell test
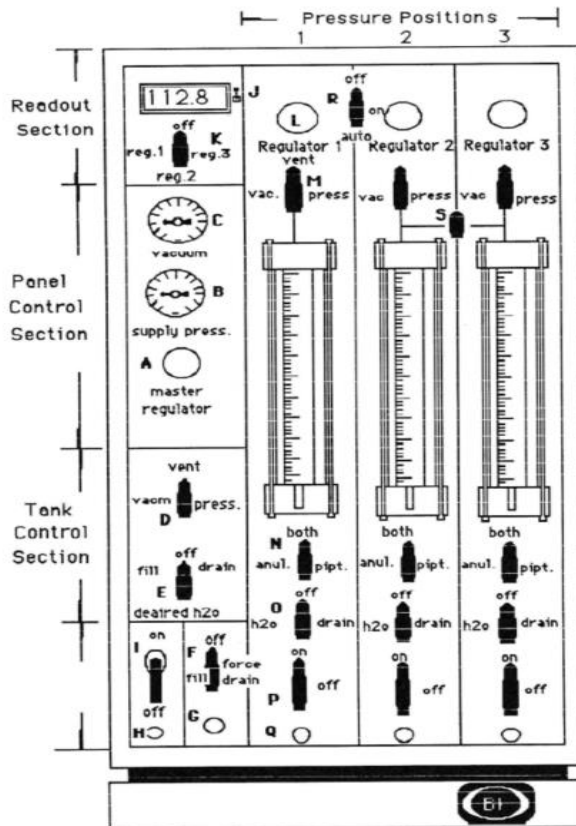
Figure 3.10 B.K Pressure control panel



Figure 3. 11 Schematic of B.K. Pressure control panel (B.K. panel operation manual)

Figure 3. 12 Volume change indicator

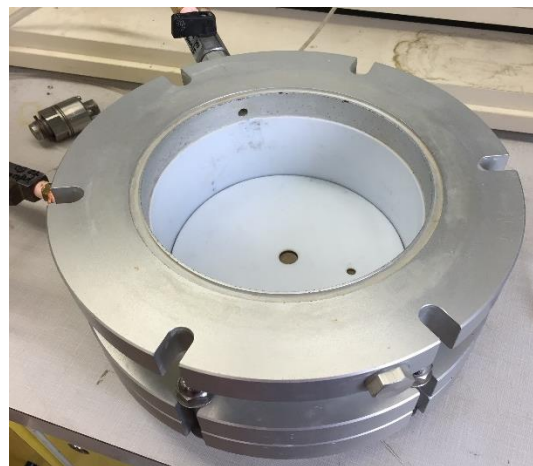

Figure 3. 13 Lower cell body bolted to the cell base
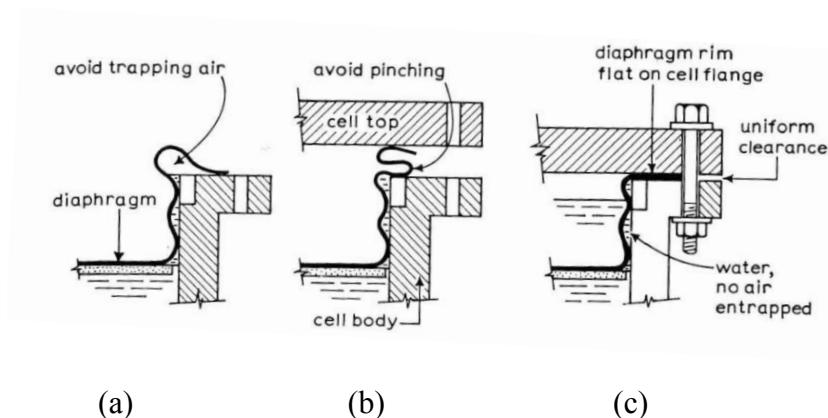


(a)                (b)                (c)

Figure 3. 14 Seating the diaphragm: (a) avoid trapping air under flange (b) avoid ruckling and pinching (c) diaphragm correctly seated (Head 1986)
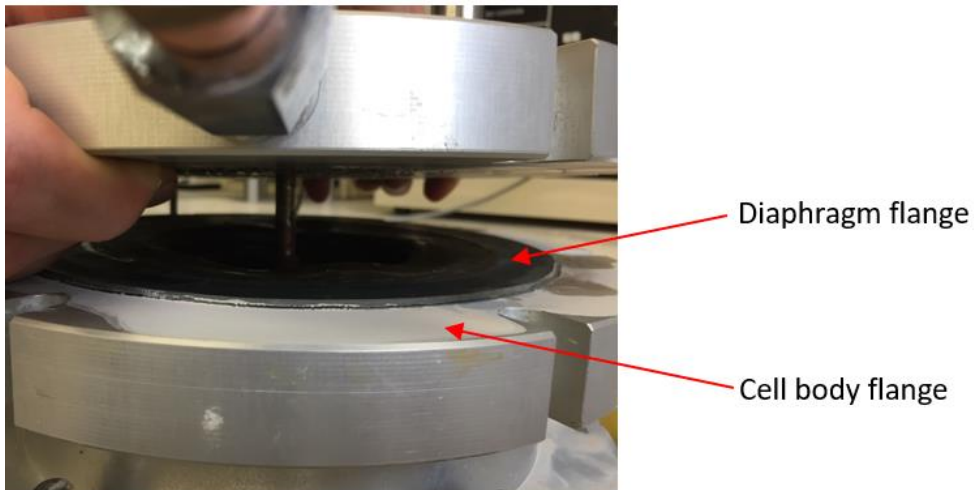
Figure 3. 15 The realistic view of the diaphragm flange correctly seating on the cell body flange
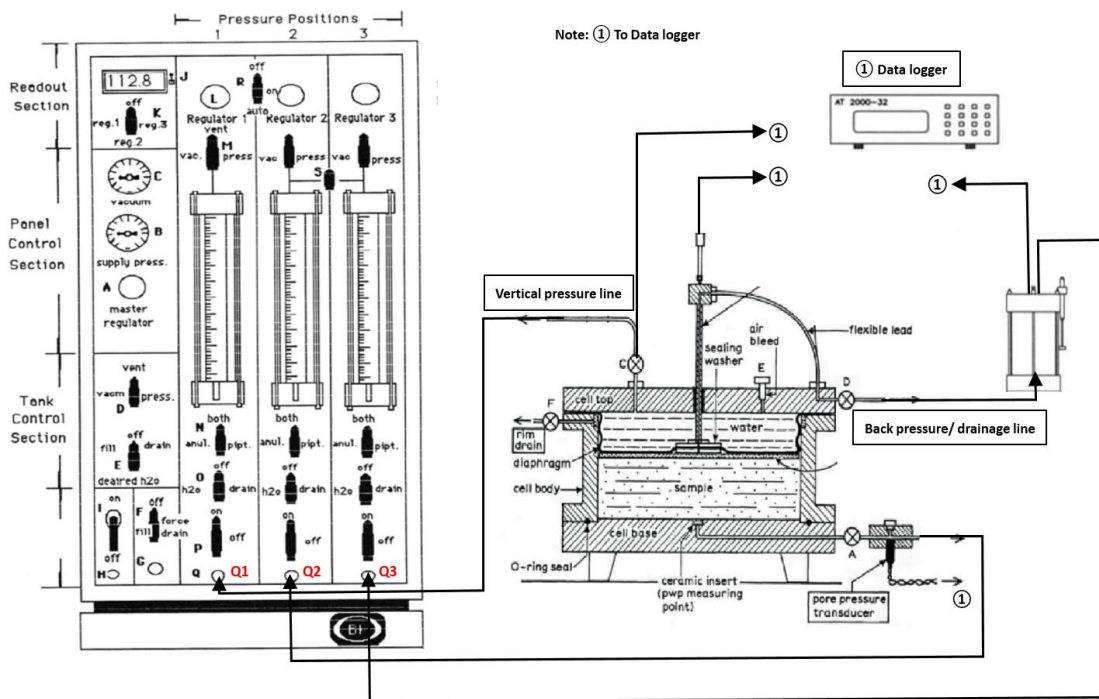


Figure 3. 16 The arrangement of the Rowe cell and connections with B.K Pressure control panel (modified from Head 1986 and B.K. panel operation manual)
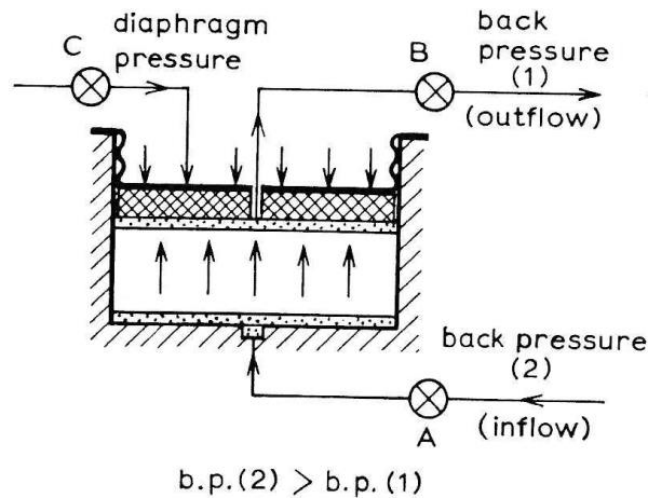
Figure 3. 17 Upward flow condition for permeability test

in the Rowe cell (Head 1986)

# CHAPTER 4    RESULTS AND DISCUSSIONS

## 4.1 Introduction

This chapter focuses on presenting the experimental results and discussion. First, the hydraulic conductivity data produced in three laboratory tests, i.e., the standard oedometer test, the falling head test and the Rowe cell test, are presented in Section 4.2. The results obtained from the Rowe cell tests are then compared with the results from the oedometer tests and falling head tests. The measurement range of the hydraulic conductivity for the mature fine oil sand tailings (MFT) in these tests is also presented and discussed. In Section 4.3, a hydraulic conductivity database for oil sand tailings is presented. A comparison of the hydraulic conductivity data is discussed in detail. In Section 4.4, two data regression models are established to correlate the hydraulic conductivity with a wide range of void ratios for fine oil sand tailings. The first model is developed based on the experimental results in this study, and the second model is developed based on the database presented in Section 4.3. Regression models proposed in this section can be used in the prediction and analysis of the hydraulic conductivity and consolidation behaviors for fine oil sand tailings. In Section 4.5, eight equations for predicting the hydraulic conductivity of fine-grained soils selected from the literature (summarized in Chapter 2) are assessed for their suitability and performances in terms of predicting the hydraulic conductivity for fine oil sand tailings using the data in the database presented in Section 4.3.

**4.2 Laboratory Test Results**

This study is an experimental research on the measurement of hydraulic conductivity of mature fine oil sand tailings. As introduced in Chapter 3, three laboratory tests were performed. In particular, the oedometer test was carried out to measure the hydraulic conductivity of the mature fine oil sand tailings (MFT) at a relatively low void ratio; the falling head test was used to measure the hydraulic conductivity of MFT samples at a relatively high void ratio; and the Rowe cell test was used to measure the hydraulic conductivity of MFT samples partially overlapping with the ranges of the standard oedometer tests and falling head tests.

**4.2.1 Results of Standard Odometer Test**

Two standard oedometer tests (Oedo-1 test and Oedo-2 test) were conducted on the MFT samples with the initial water content and void ratio 65% and 1.6, respectively. The final water content of MFT samples used in Oedo-1 test and Oedo-2 test after completing the tests were 29.0 % and 28.7%, respectively. Both MFT samples were subjected to consolidation pressures of 5kPa, 10kPa, 25 kPa, 50 kPa, 100 kPa, 200 kPa and 400 kPa during the test. The consolidation pressure was applied for 72-hour for each increment. The hydraulic conductivity values of the MFT samples were indirectly calculated from the test results by following the procedures described in Chapter 3.

Table 4.1 present a summary of results obtained with the Oedo-1 test and Oedo-2 test, including the void ratio (e), the coefficient of consolidation ($C_v$), the coefficient of volume change ($m_v$), the coefficient of compressibility ($a_v$), and hydraulic conductivity (k) for each loading increment. The coefficient of consolidation, $C_v$, for each loading

increment was determined using the Cassagrande's logarithmic time fitting method (Casagrande and Fadum 1940). The log time-settlement curves under each loading obtained from the Oedo-1 test and Oedo-2 test are plotted in Figure 4.1 (a)-(g). The coefficient of compressibility, $a_v$, for each loading increment was obtained from the graph of the void ratios versus consolidation pressure, as shown in Figure 4.2.

The hydraulic conductivity data versus void ratios of the mature fine oil sand tailings obtained from two oedometer tests are presented in Figure 4.3. It can be observed that the results obtained from the two tests are consistent, which indicates that the experiments are repeatable; the values from the Oedo-2 test are slightly higher than values from the Oedo-1 test. The hydraulic conductivity values range from 9.32 x $10^{-12}$ (m/s) to 1.22 x $10^{-9}$ (m/s) for the void ratio varying from 0.778 to 1.52. As shown in Figure 4.3, the relationship between the logarithm of hydraulic conductivity and void ratio can be described as a linear correlation. The following linear regression equation can be proposed:

$$\log k = 1.863e - 12.471 \,(\text{m/s}) \tag{4.1}$$

where k (m/s) is hydraulic conductivity and e is the void ratio. The coefficient of determination ($r^2$) of this equation is 0.969, which indicates that the regression line fits well with the data. Equation 4.1 can be rewritten as a power law function between k and e:

$$k = (3.38 \times 10^{-13}) \times 10^{1.863e} \;\;(\text{m/s}) \tag{4.2}$$

**4.2.2 Results of Falling Head Permeability Test**

The falling head tests with the downward flow and constant tail water elevation

were carried out in this study on MFT samples of void ratios from 1.5 to 7.0. The hydraulic conductivity data obtained from the test versus void ratio are presented in Figure 4.4. A best fitted curve for the results is also plotted in Figure 4.4 and can be expressed in the following power law function:

$$k = 2 \times 10^{-9} e^{1.853} \quad (m/s) \tag{4.3}$$

where k (m/s) is hydraulic conductivity and e is the void ratio. The coefficient of determination ($r^2$) of this equation is 0.813. The hydraulic conductivity values of the MFT samples vary from $1.48 \times 10^{-9}$ (m/s) to $6.8 \times 10^{-8}$ (m/s). As shown in Figure 4.4, at a particular void ratio, the deviation of the measured hydraulic conductivity is within half an order of magnitude, indicating the results are consistent.

### 4.2.3 Results of Rowe cell test

Four Rowe cell tests, i.e. tests RC 1, RC 2, RC 3 and RC 4, were carried out to measure the hydraulic conductivity of MFT samples over void ratios from 1 to 6. Table 4.2 presents the initial water content, initial sample height, final water content and final sample height of four Rowe cell tests. Tables 4.3-4.6 present a summary of results obtained from tests RC 1, RC 2, RC 3 and RC 4, respectively. The hydraulic conductivity data and their corresponding void ratios of MFT samples obtained with four Rowe cell tests are summarized in Table 4.7 and shown in Figure 4.5. The hydraulic conductivity decreased by about three orders of magnitude when the void ratio decreased from 5 to 1. Specifically, the hydraulic conductivity of the MFT samples within the range of void ratio 1.09 to 4.96 varies from $3.72 \times 10^{-10}$ (m/s) to $9.18 \times 10^{-8}$ (m/s). A best fitted curve for the results is plotted in Figure 4.5 and can be expressed in

the following power law function:

$$k = 2 \times 10^{-10} e^{4.0295} \quad \text{(m/s)} \tag{4.4}$$

where k (m/s) is the hydraulic conductivity and e is the void ratio. The coefficient of

determination ($r^2$) of this equation is 0.98, which indicates a strong agreement between

the measured data and the regression curve.

### 4.2.4 Discussions and Summary

The standard oedometer test and the falling head permeability test were adopted in

this study as indirect and direct measurement methods, respectively, to determine the

hydraulic conductivity of fine oil sand tailings. The Rowe cell test was adopted in this

study to overcome the disadvantages inherent in the standard oedometer test and the

falling head permeability test in terms of measuring the hydraulic conductivity of the

mature fine tailings. The Rowe cell allows the consolidation and permeability tests to

be directly and successively conducted, and provides data covering a wide range of void

ratios or strains.

Figure 4.6 presents the hydraulic conductivity versus void ratio (k-e) of the MFT

samples measured in this study with three different methods. The followings are

observed from Figure 4.6:

a) The hydraulic conductivity of MFT samples decreases approximately four

orders of magnitude when the void ratio decreases from 7 to 0.5;

b) The standard oedometer test and the Rowe cell test were performed on the MFT

samples with void ratios less than 1.5. The results of the Rowe cell tests were

higher than the results of the standard oedometer tests, mainly because the

latter were back-calculated based on Terzaghi's one dimensional consolidation theory, which may underestimate the values of hydraulic conductivity. Tavenas et al. (1983) also indicated that the back-calculated values of the hydraulic conductivity underestimated the measured values by up to six times for soft clays, attributing such differences to the assumptions of Terzaghi's consolidation theory.

c) The Rowe cell tests and falling head tests produce similar trends for the k-e relationship. Within the range of void ratio from 1.5 to 3, two tests produce consistent results. In contrast, at void ratios larger than 3, the results of Rowe cell tests were slightly higher than the results of falling head test within one order of magnitude.

Figure 4.7 shows the measurement ranges of the hydraulic conductivity in this study using the three laboratory tests. It is clear from Figure 4.7 that the Rowe cell test covers the largest measurement range (approximately three orders of magnitude) of hydraulic conductivity of MFT samples. The falling head test enables the measurement of the hydraulic conductivity covering two orders of magnitude, and the oedometer test can only measure the hydraulic conductivity of MFT samples with low void ratio within one and a half orders of magnitude.

The change of void ratio with effective stress ($\sigma'$- e) is shown in Figure 4.8, which depicts the compressibility of the mature fine oil sand tailings. The data plotted in Figure 4.8 are taken from the standard oedometer tests and the Rowe cell tests in this study. The void ratios are scattered at low effective stress ($\sigma' < 10$ kPa), but tend to

converge into a narrow band when the effective stress reaches 10 kPa. This indicates that different initial void ratios affect the compressibility in low effective stress and this effect becomes small when the effective stress on the MFT sample is larger than 10 kPa. Suthaker (1995) and Jeeravipoolvarn (2005) also stated that the compressibility of the fine tailings is controlled by the initial void ratio of the sample. Additionally, Figure 4.8 shows that a marked reduction in void ratio with little change in effective stress occurs in the first log cycle and shows that notable effective stress gain of MFT samples commenced at the void ratio of approximately 1.5.

**4.3 A Comparison of the hydraulic conductivity data of oil sand tailings**

The available hydraulic conductivity data for a variety of oil sand tailings reported in the literature (summarized in Section 2.3) together with the data obtained in this study constitute a hydraulic conductivity database for oil sand tailings. This database, which will be used to develop the regression models in the next section, includes the data of Suthaker (Suthaker 1995); Qiu (Qiu 2001); Jeeravipoolvarn (Jeeravipoolvarn 2010); Miller (Miller 2010) and the experimental results in this study. The database is presented in Figure 4.9, in which the followings can be observed:

a)  There is a considerable spread between the upper and lower boundaries of hydraulic conductivity data

b)  A good agreement between the results of this study and Jeeravipoolvarn's research (Jeeravipoolvarn 2010) was observed, particularly at void ratios less than 3.

c)  The hydraulic conductivity data reported by Qiu (2001) show the highest

values that range from 2.2 x $10^{-9}$ m/s to 6.3 x $10^{-9}$ m/s at low void ratios from 0.47 to 1.14, which is considerably different with data presented in other studies.

d) Without considering the data presented by Qiu (2001), the hydraulic conductivity data are within two orders of magnitude at void ratios less than 3. However, at void ratios larger than 3, the data spread over two orders of magnitude and the widest spread occurs between the results of Suthaker (1995) and Miller (2010). The results of this study fall between the above two studies but are closer to Miller's results.

The measurement deviations and unavoidable experimental errors during the tests may cause differences in hydraulic conductivity data. Besides that, as indicated in Table 4.8, the following factors may also contribute to such differences: the type of oil sand tailings used in these studies, geotechnical index properties of the samples, particle size, mineral composition, organic or bitumen content in the samples, and the permeant fluid used in the test.

The oil sand tailings samples presented in Table 4.8 were all produced in northern Alberta, Canada. The samples used in Qiu's research (2001) were oil sand composite tailings (CT). CT essentially is a mix of coarse sands and mature fine tailings, with a type of coagulant added to produce non-segregating behavior tailings that can settle and consolidate quickly (Jeeravipoolvarn 2010). The samples used in Jeeravipoolvarn's research (2010) were untreated cyclone overflow (COF). Untreated COF can be referred to as fine tailings and is a source of new fines and one of the contributions to

new MFT (Jeeravipoolvarn 2010). In Miller's research (2010), Ore A and Ore B (Table 4.8) refer to oil sands ore originating from the Syncrude mine and Suncor mine, respectively; C and NC refer to caustic and non-caustic fine tailings, which are two different tailings resulting from different bitumen extraction processes.

As shown in Table 4.8, the specific gravity (Gs) of the samples varies from 2.1 to 2.6. According to Suthaker (1995), this variation is attributable to the variable amount of bitumen, which has a specific gravity of 1.03. The liquid limit varies from 40% to 60%, and the plastic limit varies from 21% to 31%. Differences between the liquid limit and plastic limit for these samples (shown in Table 4.8) were not significant. The clay minerals of these oil sand tailings are kaolinite and/or illite, which reflects the average clay mineralogy of the clay-shale strata in the McMurray Formation in northern Alberta (Suthaker 1995).

Fines content shown in the grain size distribution column refers to the content of particles with sizes less than 75 μm. Except for the CT (Qiu 2001), fines contents of the samples were above 90%, whereas the CT was dominated by sand sized particles. Suthaker (1995) and Jeeravipoolvarn (2005) reported that, in the mixes of fine oil sand tailings and sand, the hydraulic conductivity is controlled by the fines content and decreases with increasing fines content. An increase in sand content leads to increased hydraulic conductivity. As CT has the largest sand content and a non-plastic cohesionless characteristic, the hydraulic conductivity values published by Qiu were higher than others by up to two and a half orders of magnitude.

The bitumen contents, which is the bitumen mass divided by the mass of mineral

solids plus bitumen (Miller 2010), in various samples are given in Table 4.8. The hydraulic conductivity of fine oil sand tailings is influenced by bitumen content and decreases with a higher bitumen content (Suthaker 1995). As shown in Table 4.8, the samples of this study had the highest bitumen content, followed by the COF. The bitumen contents of samples used in Suthaker's research and Miller's research were significantly lower than in other samples. Relatively low bitumen content may explain why the hydraulic conductivity values reported by Suthaker are higher than that reported by this study and Jeeravipoolvarn. However, more investigations are suggested.

The process water used in tests, as shown in Table 4.8, is another possible reason causing the differences in hydraulic conductivity data. Different process water has different ion types and the concentration of ions is different, which affects the double-layer of clay particles and further affects the hydraulic conductivity of fine oil sand tailings. Miller (2010) states that pore water chemistry in fine oil sand tailings, which varies greatly depending on the extraction process, type of the process water and the oil sands ore, impacts their compressibility and hydraulic conductivity, particularly at high void ratios (low effective stress). Miller also refers to the double layer theory of clay particles to further explain this idea. In addition, the effect of pore water chemistry is expected to be significant at high void ratios, which explains why the range of hydraulic conductivity values, as shown in Figure 4.9, was greater at high void ratios. However, because the specific information, such as ion types, the concentration of ions and the specific composition of process water, are not available in the literature, more investigations are suggested.

**4.4 Regression Models for Fine Oil Sand Tailings**

Owing to the excessive amount of time, and the sophisticated experimental techniques and apparatus required, studies on measuring the hydraulic conductivity of soft fine-grained geomaterials, such as fine oil sand tailings, are usually based on very limited data. Several equations have been proposed to predict and estimate the hydraulic conductivity for fine-grained soils from easily measured data, such as Atterberg limits and void ratio. In these equations, the hydraulic conductivity is expressed as a function of the porosity (i.e., void ratio) and selected properties of soils (Dolinar 2009). These equations are applicable to most types of fine-grained soils, but they have rarely used for fine oil sand tailings.

In this section, the hydraulic conductivity database presented in Section 4.3 is used to obtain reliable k - e relationships or ranges of relationships. Two data regression models are proposed to establish the correlation between the hydraulic conductivity and a wide range of void ratios of fine oil sand tailings (k-e relationship). The first set of models is developed based solely on the experimental results in this study, thus it is more suitable for the mature fine tailings used in this study or similar geomaterials. The second set of models is developed based on the database presented in Section 4.3. Data published by Qiu (2001) are excluded as that study did not use fine oil sand tailings. The second set of models is applicable for the prediction or analysis of the hydraulic conductivity and consolidation behaviors of various fine oil sand tailings from different locations.

The practical significance of establishing the k-e regression models is to investigate

the consolidation behaviors of fine oil sand tailings, which undergo large settlements during consolidation (Suthaker 1995), based on large strain consolidation theories. These theories require explicit relationships between hydraulic conductivity and void ratio, as well as a relationship between void ratio and effective stress (Gibson et al. 1967). In addition, from a practical point of view, the models can be used to quickly estimate the hydraulic conductivity in preliminary design stages for tailings disposal projects without excessive time or prohibitive testing costs.

### 4.4.1 Regression Models Based on the Experimental Results of this Study

The first set of regression models was developed based on the experimental results in this study. Experimental results presented in previous studies show that the hydraulic conductivity is strongly dependent of soil porosity and various correlations were proposed between the hydraulic conductivity and void ratio (Deng, Y. F. et. al 2011). Conventionally, such correlations can be expressed in the following form:

$$k = Ce^D \text{ (m/s)} \tag{4.5}$$

where k (m/s) is the hydraulic conductivity, e is the void ratio, and C (m/s) and D are empirical coefficients. Equation 4.5 was first proposed by Somogyi (1979) to define the hydraulic conductivity changes during a one-dimensional compression of soils. This form coincides with the findings published by other researchers (Carrier and Beckman 1984; Krizek and Somogyi 1984; Al-Tabba and Wood 1987; Suthaker 1995; Pane and Schiffman, 1997; Dolinar 2009).

For the mature fine tailings tested in this study, the experimental results presented in Figure 4.6 indicate that the power law equation, as the same form as that in Equation

4.5, can be employed to describe the variation of the hydraulic conductivity with the void ratio. A best fitted curve for the results plotted in Figure 4.6 can be expressed in the following function:

$$k = 1 \times 10^{-10} e^{3.987} \text{ (m/s)} \tag{4.6}$$

where k (m/s) is the hydraulic conductivity and e is the void ratio. The coefficient of determination ($r^2$) of this equation is 0.833. Figure 4.10 shows the hydraulic conductivity data versus porosity of the mature fine tailings tested in this study. As shown in this figure, the relationship between the logarithm of hydraulic conductivity (log k) and porosity (n) can be described as a linear correlation. The following linear regression equation can be proposed by using the OLS method:

$$\log k = 8.815n - 14.57 \text{ (m/s)} \tag{4.7}$$

where k (m/s) is hydraulic conductivity and n is the porosity, calculated as e/(1+e). This expression is similar to the regression Equation 4.1 obtained from the oedometer test. $r^2$ of this equation is 0.89, which indicates good agreement between the measured data and the regression curve. The upper bounds and lower bounds are also drawn in Figure 4.10 based on a confidence interval of 95%. Equation 4.7 can be rewritten as a power law function as follows:

$$k = 10^{-14.57} \times 10^{8.815n} \text{ (m/s)} \tag{4.8}$$

Equations 4.6, 4.7 and 4.8 are the regression equations based on the experimental results in this study and can be specifically used for studies related to the mature fine tailings similar to those used in study.

### 4.4.2 Regression Models Based on the Database of Oil Sand Tailings

The second set of regression models was developed based on the database (as presented in Section 4.3). Data published by Qiu (2001) were excluded because the samples are not fine oil sand tailings. Figure 4.11 shows a linear correlation between the logarithm of hydraulic conductivity (log k) and the void ratio (e). This linear correlation is in the form of:

$$\log k = 0.447e - 9.826 \ (\text{m/s}) \tag{4.9}$$

where k (m/s) is hydraulic conductivity and e is the void ratio at which k is required. $r^2$ of this equation is 0.6. The upper bounds and lower bounds are also drawn in Figure 4.11 based on a confidence interval of 95%. Equation 4.9 can be rewritten as a power law function as follow:

$$k = 10^{-9.826} \times 10^{0.447e} \ (\text{m/s}) \tag{4.10}$$

Figure 4.12 shows a power law relationship between the hydraulic conductivity and void ratio. The following equation is proposed to describe this relationship with an $r^2$ of 0.67.

$$k = 2 \times 10^{-10} e^{3.58} (\text{m/s}) \tag{4.11}$$

Figure 4.13 shows a linear correlation between the logarithm of hydraulic conductivity and porosity. The following equation is proposed to describe this linear correlation with an $r^2$ of 0.75:

$$\log k = 9.46n - 15.05 (\text{m/s}) \tag{4.12}$$

Equation 4.12 can be rewritten as a power law function as follow:

$$k = 10^{-15.05} \times 10^{9.46n} \ (\text{m/s}) \tag{4.13}$$

where k (m/s) is hydraulic conductivity and n is the porosity.

Figure 4.14 shows a power law relationship between the hydraulic conductivity and porosity. The following equation is proposed to describe this relationship with an $r^2$ of 0.74.

$$k = 9 \times 10^{-7} n^{14.77} \text{ (m/s)} \qquad (4.14)$$

In relative terms, Equation 4.12 has higher $r^2$ when linearly correlating the logarithm of hydraulic conductivity with porosity. The performance in predicting the hydraulic conductivity for fine oil sand tailings is similar when using both Equations 4.13 and 4.14. Compared with the regression equations proposed in Section 4.4.2, it is concluded that the correlation of hydraulic conductivity versus porosity (k-n) is superior to that of hydraulic conductivity versus void ratio (k-e) for fine oil sand tailings. Thus, Equation 4.13 or 4.14 is preferred in predicting the hydraulic conductivity of fine oil sand tailings

### 4.4.3 Summary

In this section, two data regression models were proposed to correlate the hydraulic conductivity with a wide range of void ratios of fine oil sand tailings. The first set of models is more suitable for the mature fine tailings or similar geomaterials. According to the regression analysis, the k-n relationship is superior to the k-e relationship for the mature fine tailings. Thus, it is suggested that predictions of hydraulic conductivity for mature fine tailings should be based on the k-n relationship using Equation 4.7 or 4.8 in order to obtain more reliable results. The second set of models was developed based on the database presented in Section 4.3, except that the data published by Qiu (2001)

were excluded. Similarly, the correlation relationship of k-n is superior to the relationship of k-e for various fine oil sand tailings. Thus, it is suggested that, for fine oil sand tailings from northern Alberta, Canada, predictions or analyses of the hydraulic should be based on the k-n relationship using Equation 4.13 or 4.14.

**4.5 Evaluation and Comparison of Previous Empirical Equations**

Empirical equations (summarised in Chapter 2) have been proposed to predict the hydraulic conductivity for plastic soils. These equations are generally applicable for the specific geomaterials. However, the suitability and relative performances of these equations are uncertain in terms of predicting the hydraulic conductivity for fine oil sand tailings. Thus, it is desirable to assess and compare these equations using the data in the database (presented in Section 4.3). For this purpose, eight typical equations were selected from these empirical equations to estimate their suitability and performance for predicting the hydraulic conductivity for fine oil sand tailings.

The eight equations evaluated and presented in detail in this section were proposed by: Carrier (1984), Samarasinghe (1982) coupled with Sridharan and Nagaraj (2005), Suthaker (1995), Morris et al. (2000), Mbonimpa et al. (2002), Morris et al. (2003), Dolinar (2009) and Paul (2011).

To evaluate the predicting models or equations, the following two parameters are used: i) *a* is the mean value of R, calculated by Equation 4.15; ii) *b* is the root mean square error of R, calculated by Equation 4.16; where R is defined as the ratio of the predicted value of k ($k_{predicted}$) to the measured value of k ($k_{measured}$), and N is the total data number (Tang et al 2008; Deng et al 2011).

98

$$a = \frac{1}{N} \sum_{i=1}^{N} R_i \qquad (4.15)$$

$$b = \sqrt{\frac{1}{N} \sum_{i=1}^{N} (R_i - 1)^2} \qquad (4.16)$$

Figures 4.15 (a) to (h) show the measured hydraulic conductivity data of fine oil sand tailings coupled with the best fitted curve and the curve created by the eight equations. The predicted k values calculated by these equations versus measured k values are plotted in Figures 4.16 (a) to (h). The mean value of R and the root mean square error of R are shown in Table 4.9. The following can be concluded from Figures 4.15 and 4.16, and Table 4.9:

a) The equations, respectively proposed by Carrier (1984) and Morris et al. (2003), give poor estimates of k values with large deviations. The k-e relationship produced by Carrier (1984) equation does not conform to the measured k-e relationship for fine oil sand tailings. The equation by Morris et al. (2003) severely overestimates k values. Thus, these two equations are deemed not suitable for fine oil sand tailings.

b) Similar trends for the k-e relationship can be found between measured data and models by Samarasinghe et al. (1982) and Sridharan and Nagaraj (2005), Suthaker (1995), Morris et al. (2000), Mbonimpa et al. (2002), Morris et al. (2003), Dolinar (2009) and Paul (2011). Among them, the equations of Morris et al. (2000), Dolinar (2009) and Paul (2011) overestimate k values by about two orders of magnitude, whereas the equation of Samarasinghe et al. (1982) coupled with Sridharan and Nagaraj (2005) slightly underestimates k values

within one order of magnitude. The equations proposed by Suthaker (1995) and Mbonimpa et al. (2002) provide better prediction of k values for fine oil sand tailings mainly because they were initially developed based on data from mine tailings.

c) Although the equations of Morris et al. (2000), Dolinar (2009) and Paul (2011) produce similar trends with the data from this study, their predictive capacities are still much lower than the equations proposed by Samarasinghe et al. (1982) and Sridharan and Nagaraj (2005), Suthaker (1995) and Mbonimpa et al. (2002) due to relatively large a and b values, as shown in Table 4.9.

In summary, eight empirical equations were evaluated and compared in this section, in which the equations proposed by Samarasinghe et al. (1982) coupled with Sridharan and Nagaraj (2005), Suthaker (1995) and Mbonimpa et al. (2002) are shown to be relatively reliable in terms of predicting the hydraulic conductivity for fine oil sand tailings over a wide range of void ratios.

## 4.6 Summary

The experimental results obtained with three laboratory tests are presented first. The hydraulic conductivity of the MFT samples ranges from $9 \times 10^{-12}$ (m/s) to $1 \times 10^{-7}$ (m/s) within the void ratio of 0.5 to 7. The standard oedometer test is suitable for the measurement of hydraulic conductivity of MFT with the initial void ratio less than 1.6. For MFT with a natural water content of 171%, the falling head test can measure the hydraulic conductivity of MFT with the initial void ratio larger than 1.5. The Rowe cell tests cover the measurement range of both the standard oedometer tests and the falling

head tests. The hydraulic conductivity data obtained from the Rowe cell tests were higher than the data from the standard oedometer tests when the void ratio of the MFT sample was less than 1.5 and higher than the data from the falling head tests when the void ratio of the MFT sample was larger than 3. In addition, the initial void ratio affected the compressibility of MFT in low effective stress ($\sigma' < 10$ kPa) and this effect was diminished when the effective stress of MFT sample is larger than 10 kPa.

In Section 4.3, a hydraulic conductivity database for oil sand tailings is established by combining the data obtained from the literature (as summarized in Section 2.3) together with data obtained from this study. Then, a comparison of the hydraulic conductivity data for different oil sand tailings is presented, and the possible factors that may cause differences in hydraulic conductivity data are discussed. The samples used in Qiu's study (2001) are oil sand composite tailings (CT), which are sandy soils and classified as SM according to USCS (Qiu 2001), while the samples used in other studies are fine oil sand tailings. The hydraulic conductivity values published by Qiu are higher than others by up to two and a half orders of magnitude at the low void ratio, mainly because of the CT samples' lowest fine content, largest sand to fine ratio and non-plastic cohesionless characteristics. Except for the data published by Qiu, the hydraulic conductivity values (shown in Figure 4.9) are within two orders of magnitude at void ratios less than three. However, at void ratios larger than three, the data are spread over two orders of magnitude, and the widest spread occurs between the results of Suthaker and Miller.

In Section 4.4, two data regression models are proposed to correlate the hydraulic

conductivity with a wide range of void ratios of fine oil sand tailings (k-e relationship). The first set of models is developed based solely on the experimental results in this study. The second set of models is developed based on the database presented in Section 4.3. The data published by Qiu (2001) are excluded. According to the regression results, the correlation relationship of k-n is superior to the relationship of k-e for both mature fine tailings samples used in this study and various fine oil sand tailings used in previous studies. Thus, using Equation 4.7 or 4.8 to predict of the hydraulic conductivity of mature fine tailings, and using Equations 4.13 or 4.14. to the predict or analyze the hydraulic conductivity for various fine oil sand tailings are suggested.

In Section 4.5, the suitability and performances of eight empirical equations are assessed in terms of predicting hydraulic conductivity for fine oil sand tailings. The results show that equations proposed by Carrier (1984) and Morris et al. (2003) are not applicable for fine oil sand tailings to predict k values; equations proposed by Morris et al. (2000), Dolinar (2009) and Paul (2011) have relatively low predictive capacities; equations proposed by Samarasinghe et al. (1982) coupled with Sridharan and Nagaraj (2005), Suthaker (1995) and Mbonimpa et al. (2002) provide relatively accurate predictions of k values for fine oil sand tailings.

Table 4. 1 Results obtained form the Oedo-1 test and Oedo-2 test

| | Consolidation Pressure (kPa) | Final void ratio* e | Average void ratio* e | $C_v$ (m²/s) | $m_v$ (m²/kN.) | $a_v$ (m²/kN.) | K m/s |
|---|---|---|---|---|---|---|---|
| | 0 | 1.637 | n/a | n/a | n/a | n/a | n/a |
| | 5 | 1.401 | 1.519 | 1.29E-09 | 0.0187 | 0.0472 | 2.37E-10 |
| | 10 | 1.341 | 1.371 | 4.87E-10 | 0.00503 | 0.0119 | 1.22E-10 |
| Oedo-1 | 25 | 1.206 | 1.273 | 1.30E-09 | 0.00397 | 0.00903 | 5.07E-11 |
| test | 50 | 1.088 | 1.147 | 1.52E-09 | 0.00220 | 0.00473 | 3.29E-11 |
| | 100 | 0.961 | 1.024 | 2.08E-09 | 0.00125 | 0.00253 | 2.55E-11 |
| | 200 | 0.841 | 0.901 | 2.73E-09 | 0.000631 | 0.0012 | 1.69E-11 |
| | 400 | 0.728 | 0.784 | 3.66E-09 | 0.000317 | 0.000567 | 1.14E-11 |
| | 0 | 1.635 | n/a | n/a | n/a | n/a | n/a |
| | 5 | 1.469 | 1.552 | 2.25E-09 | 0.0130 | 0.0332 | 2.87E-10 |
| | 10 | 1.335 | 1.402 | 1.09E-08 | 0.000405 | 0.001 | 1.81E-10 |
| Oedo-2 | 25 | 1.184 | 1.260 | 1.71E-09 | 0.00803 | 0.0187 | 7.08E-11 |
| test | 50 | 1.085 | 1.135 | 3.09E-09 | 0.00186 | 0.00396 | 5.62E-11 |
| | 100 | 0.956 | 1.021 | 2.45E-09 | 0.00128 | 0.00258 | 3.07E-11 |
| | 200 | 0.834 | 0.895 | 2.36E-09 | 0.000644 | 0.00122 | 1.49E-11 |
| | 400 | 0.721 | 0.778 | 2.99E-09 | 0.000318 | 0.000565 | 9.32E-12 |

* Final void ratio refers to the void ratio of the sample after a loading step

* Average void ratio refers to the void ratio of samples during a loading step

Table 4. 2 Water content and sample height for four Rowe cell tests

| Test NO. | Initial Water Content (%) | Final Water Content (%) | Initial Sample Height (mm) | Final Sample Height (mm) |
|---|---|---|---|---|
| RC 1 | 177 | 74.1 | 13 | 7 |
| RC 2 | 129 | 88.3 | 15 | 4 |
| RC 3 | 210 | 165 | 20 | 15.6 |
| RC 4 | 76.7 | 43.4 | 16 | 11.3 |

Table 4. 3 Results obtained form the RC 1 Test

| Test NO. | Test Stage | Settlement (mm) | Sample Height (mm) | Effective Stress (kPa) | Void Ratio | Water Content (%) | ΔP (kPa) | Flow Rate (ml/min) | K (m/s) |
|---|---|---|---|---|---|---|---|---|---|
| 1 | C1* | 0.947 | n/a | 0-2 | n/a | n/a | n/a | n/a | n/a |
| | P1* | n/a | 11.901 | 2 | 4.04 | 160.9 | 1 | 0.553 | 5.84E-08 |
| 2 | C2 | 1.482 | n/a | 2-5 | n/a | n/a | n/a | n/a | n/a |
| | P2 | n/a | 10.42 | 5 | 3.41 | 135.9 | 2 | 0.489 | 2.34E-08 |
| 3 | C3 | 1.975 | n/a | 5-7 | n/a | n/a | n/a | n/a | n/a |
| | P3 | n/a | 8.44 | 7 | 2.58 | 102.6 | 2 | 0.1302 | 5.06E-09 |
| 4 | C4 | 1.688 | n/a | 7-10 | n/a | n/a | n/a | n/a | n/a |
| | P4 | n/a | 6.75 | 10 | 1.86 | 74.14 | 2 | 0.0403 | 1.25E-09 |

*C refers to consolidation test; C1 refers to the first consolidation stage;

*P refers to permeability test; P1 refers to the first permeability test;

Table 4. 4 Results obtained form the RC 2 Test

| Test NO. | Test Stage | Settlement (mm) | Sample Height (mm) | Effective Stress (kPa) | Void Ratio | Water Content (%) | ΔP (kPa) | Flow Rate (ml/min) | K (m/s) |
|---|---|---|---|---|---|---|---|---|---|
| 1 | C1* | 1.487 | n/a | 0-2 | n/a | n/a | n/a | n/a | n/a |
| | P1* | n/a | 13.41 | 2 | 2.83 | 112.8 | 1 | 0.0731 | 9.02E-09 |
| 2 | C2 | 0.735 | n/a | 2-3 | n/a | n/a | n/a | n/a | n/a |
| | P2 | n/a | 12.67 | 3 | 2.62 | 104.4 | 2 | 0.1003 | 5.85E-09 |
| 3 | C3 | 1.416 | n/a | 3-5 | n/a | n/a | n/a | n/a | n/a |
| | P3 | n/a | 11.25 | 5 | 2.22 | 88.28 | 2 | 0.0661 | 3.42E-09 |

*C refers to consolidation test; C1 refers to the first consolidation stage;

*P refers to permeability test; P1 refers to the first permeability test;

Table 4. 5 Results obtained form the RC 3 Test

| Test NO. | Test Stage | Settlement (mm) | Sample Height (mm) | Effective Stress (kPa) | Void Ratio | Water Content (%) | ΔP (kPa) | Flow Rate (ml/min) | K (m/s) |
|---|---|---|---|---|---|---|---|---|---|
| 1 | C1 | 1.962 | n/a | 0-2 | n/a | n/a | n/a | n/a | n/a |
| | P1 | n/a | 18.09 | 2 | 4.96 | 197.7 | 1 | 0.551 | 9.18E-08 |
| 2 | C2 | 0.892 | n/a | 2-3 | n/a | n/a | n/a | n/a | n/a |
| | P2 | n/a | 17.2 | 3 | 4.67 | 186 | 1 | 0.481 | 7.60E-08 |
| 3 | C3 | 0.813 | n/a | 3-4 | n/a | n/a | n/a | n/a | n/a |
| | P3 | n/a | 16.38 | 4 | 4.40 | 175.3 | 1 | 0.443 | 6.67E-08 |
| 4 | C4 | 0.775 | n/a | 4-5 | n/a | n/a | n/a | n/a | n/a |
| | P4 | n/a | 15.6 | 5 | 4.14 | 165.1 | 1 | 0.397 | 5.69E-08 |

Table 4. 6 Results obtained form the RC 4 Test

| Test NO. | Test Stage | Settlement (mm) | Sample Height (mm) | Effective Stress (kPa) | Void Ratio | Water Content (%) | ΔP (kPa) | Flow Rate (ml/min) | K (m/s) |
|---|---|---|---|---|---|---|---|---|---|
| 1 | C1 | 1.268 | n/a | 0-5 | n/a | n/a | n/a | n/a | n/a |
| | P1 | n/a | 14.56 | 5 | 1.69 | 67.37 | 2 | 0.00152 | 1.02E-09 |
| 2 | C2 | 0.931 | n/a | 5-10 | n/a | n/a | n/a | n/a | n/a |
| | P2 | n/a | 13.62 | 10 | 1.52 | 60.52 | 2 | 0.0123 | 7.71E-10 |
| 3 | C3 | 0.842 | n/a | 10-20 | n/a | n/a | n/a | n/a | n/a |
| | P3 | n/a | 12.78 | 20 | 1.36 | 54.3 | 2 | 0.0101 | 5.94E-10 |
| 4 | C4 | 1.476 | n/a | 20-40 | n/a | n/a | n/a | n/a | n/a |
| | P4 | n/a | 11.3 | 40 | 1.09 | 43.43 | 2 | 0.00716 | 3.72E-10 |

Table 4. 7 The hydraulic conductivity data obtained form four Rowe cell tests

| No. | Test | Void ratio | K (m/s) |
|-----|------|------------|---------|
| 1 | RC 4 | 1.09 | 3.72E-10 |
| 2 | RC 4 | 1.36 | 5.94E-10 |
| 3 | RC 4 | 1.52 | 7.71E-10 |
| 4 | RC 4 | 1.69 | 1.02E-09 |
| 5 | RC 1 | 1.86 | 1.25E-09 |
| 6 | RC 2 | 2.22 | 3.42E-09 |
| 7 | RC 1 | 2.58 | 5.06E-09 |
| 8 | RC 2 | 2.62 | 5.85E-09 |
| 9 | RC 2 | 2.83 | 9.02E-09 |
| 10 | RC 1 | 3.41 | 2.34E-08 |
| 11 | RC 1 | 4.04 | 5.84E-08 |
| 12 | RC 3 | 4.14 | 5.69E-08 |
| 13 | RC 3 | 4.40 | 6.67E-08 |
| 14 | RC 3 | 4.67 | 7.60E-08 |
| 16 | RC 3 | 4.96 | 9.18E-08 |

Table 4. 8 A comparison of the data shown in the database

| | Types of oil sand tailings | Specific gravity, $G_s$ | Liquid limit, $w_L$ (%) | Plastic limit, $w_p$ (%) | Plastic Index, $I_p$ | Major mineral composition | Grain size distribution | Bitumen content in dry mass (%) | USCS | Process water |
|---|---|---|---|---|---|---|---|---|---|---|
| This study | Mature fine oil sand tailings (MFT) | 2.51 | 51.6 | 29.1 | 22.5 | illite, kaolinite, and quartz | 0% sand, 80% silt and 20% clay sized solids. 100 % fines content. | 14.7 | MH | De-aired tap water |
| Suthaker (1995) | Mature fine oil sand tailings (MFT) | 2.1-2.5 | 40-60 | 20-25 | 20-35 | kaolinite and illite | 2-5% fine grained sand, 43-49% silt and 46-55% of clay size particles. 95-98% fines content | 6.5 | CH | Tailings pond water |
| Qiu (1998) | oil sand composite/ consolidated tailings (CT) | 2.6 | N/A | N/A | N/A | kaolinite and illite | 76% sand, 15% silt and 9% clay sized content. 24% fines content. | X* | SM | X |
| Jeeravipoolvarn (2008) | | 2.53 | 50 | 21 | 29 | kaolinite and quartz | 8% sand, 40% silt and 52% clay size solids. 92% fines content | 11 | CH | X |
| Miller (2010) | OreA–C (Extraction Process: C, caustic) | 2.55 | 50 | 26 | 24 | kaolinite and illite | 96% fines content | 3.9 | CH | syncrude recycled pond water |
| | OreA–NC (Extraction Process: NC, non-caustic) | 2.51 | 60 | 31 | 29 | kaolinite and illite | 100% fines content | 5 | CH | treated Athabasca river water |
| | Ore B–C | 2.48 | 52 | 27 | 25 | kaolinite and illite | 98% fines content | 5.9 | CH | syncrude recycled pond water |
| | Ore B–NC | 2.45 | 58 | 28 | 30 | kaolinite and illite | 98% fines content | 6.7 | CH | treated Athabasca river water |
| | Ore A–NC | 2.5 | 55 | 28 | 27 | kaolinite and illite | 99% fines content | 5.2 | CH | untreated Athabasca river water |
| Owolagba (2013) | centrifuged fine oil sand tailings | 2.39 | 41 | 20 | 21 | X | 52% clay size particles 95% fines content | X | CL | X |

*: X refers to not clearly mentioned in the literature

Table 4. 9 The mean value of R, a, and the root mean square error of R, b.

| No. | Studies | a | b |
|-----|---------|-----|------|
| 1 | Carrier and Beckman (1984, 1986) | 18.1 | 48.9 |
| 2 | Samarasinghe et al. (1982) and Sridharan and Nagaraj (2005) | 0.83 | 1.03 |
| 3 | Suthaker (1995) | 2.13 | 3.03 |
| 4 | Morris et al. (2000) | 41.5 | 77.1 |
| 5 | Mbonimpa et al. (2002) | 3.82 | 4.98 |
| 6 | Morris et al. (2003) | 346 | 1469 |
| 7 | Dolinar (2009) | 18.1 | 48.9 |
| 8 | Paul (2011) | 45.6 | 65.7 |

(a)



(b)

109

(c)



(d)

(e)



(f)

111
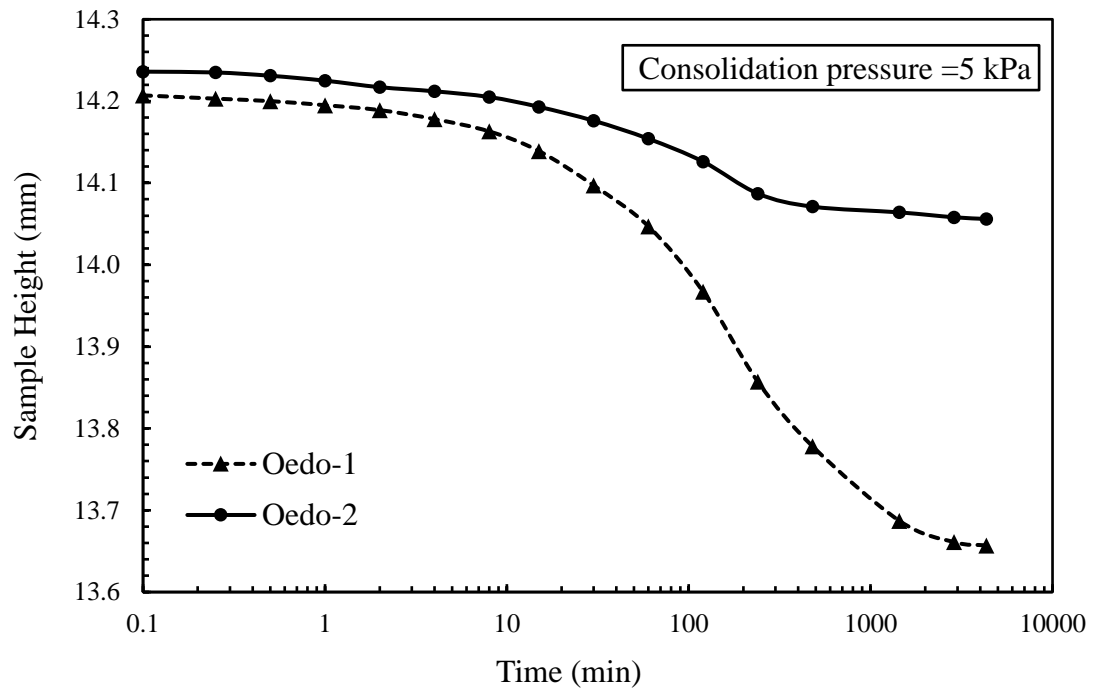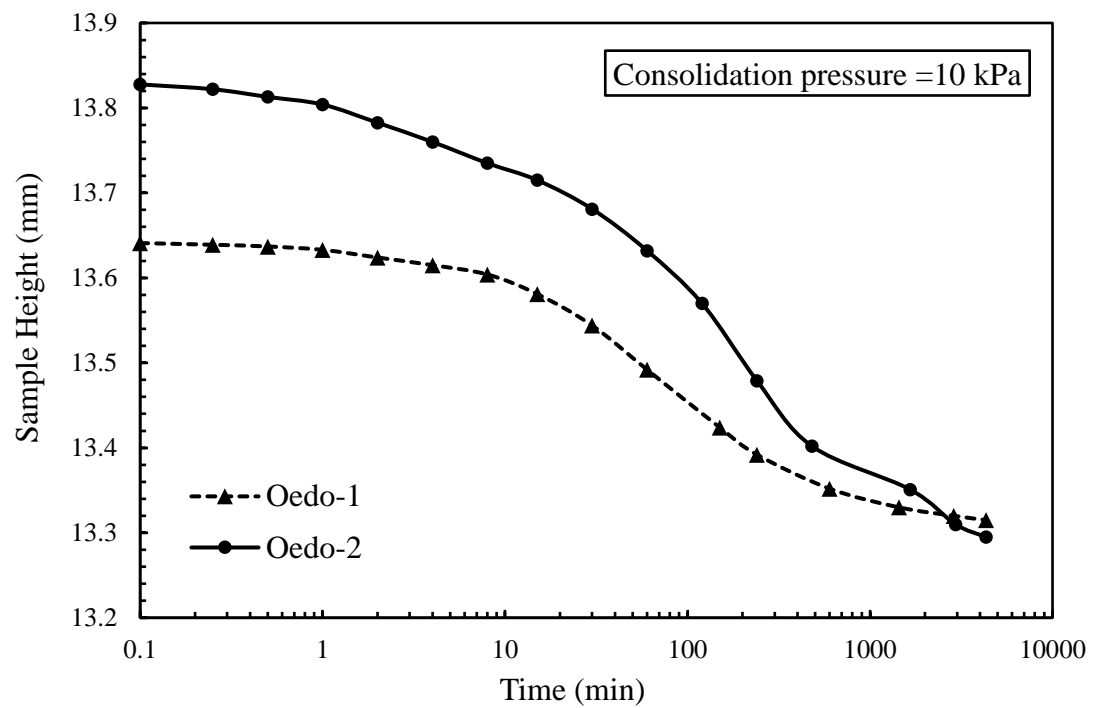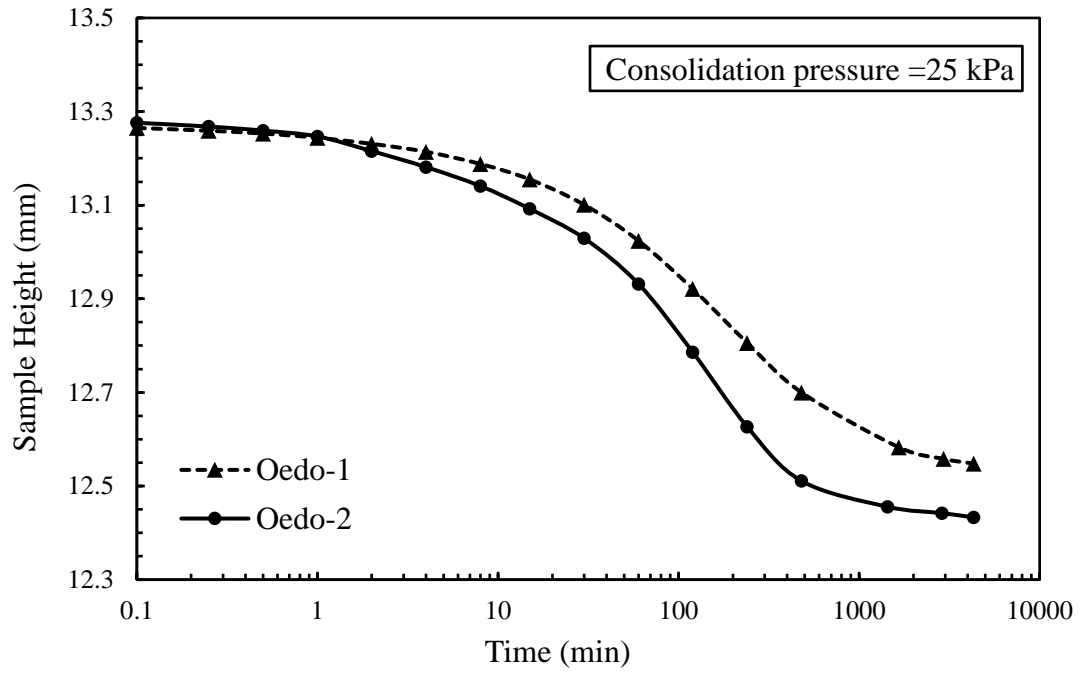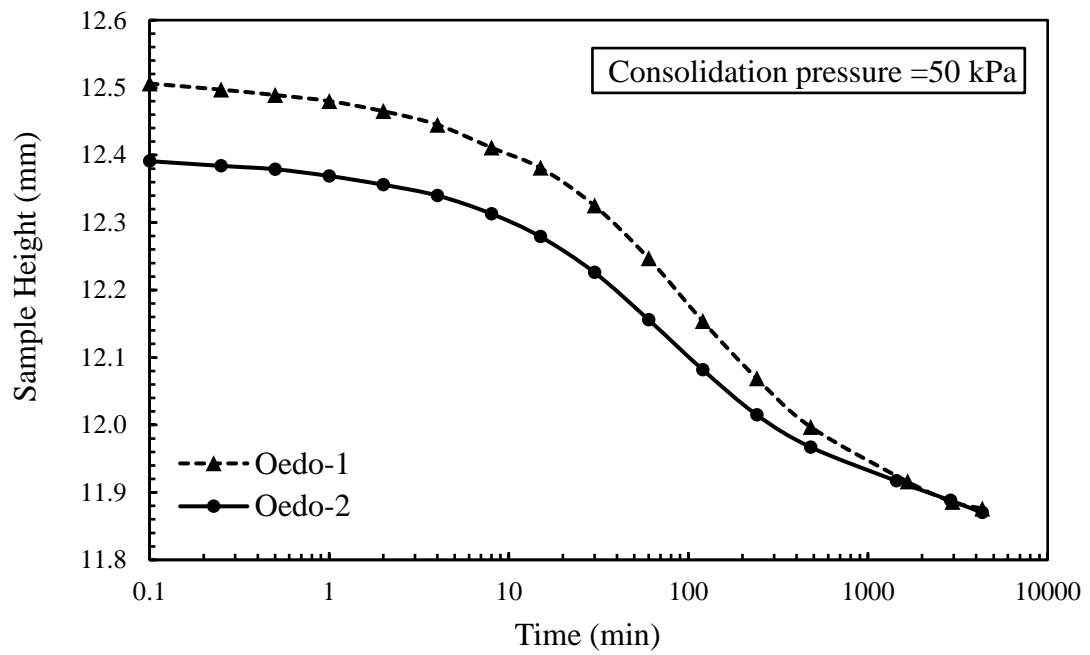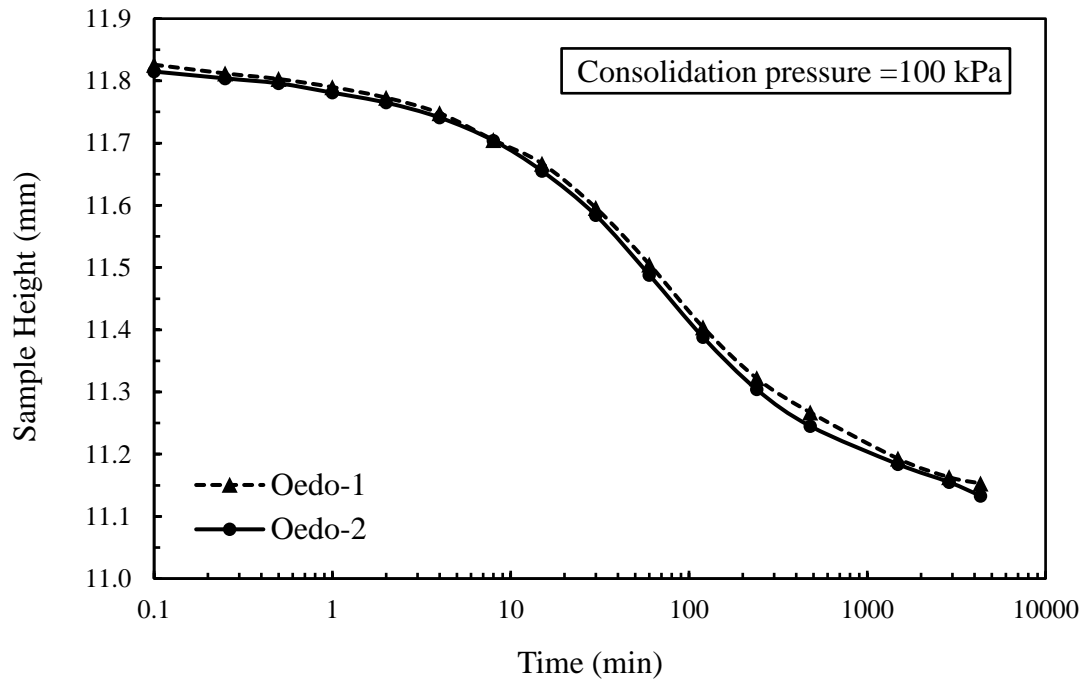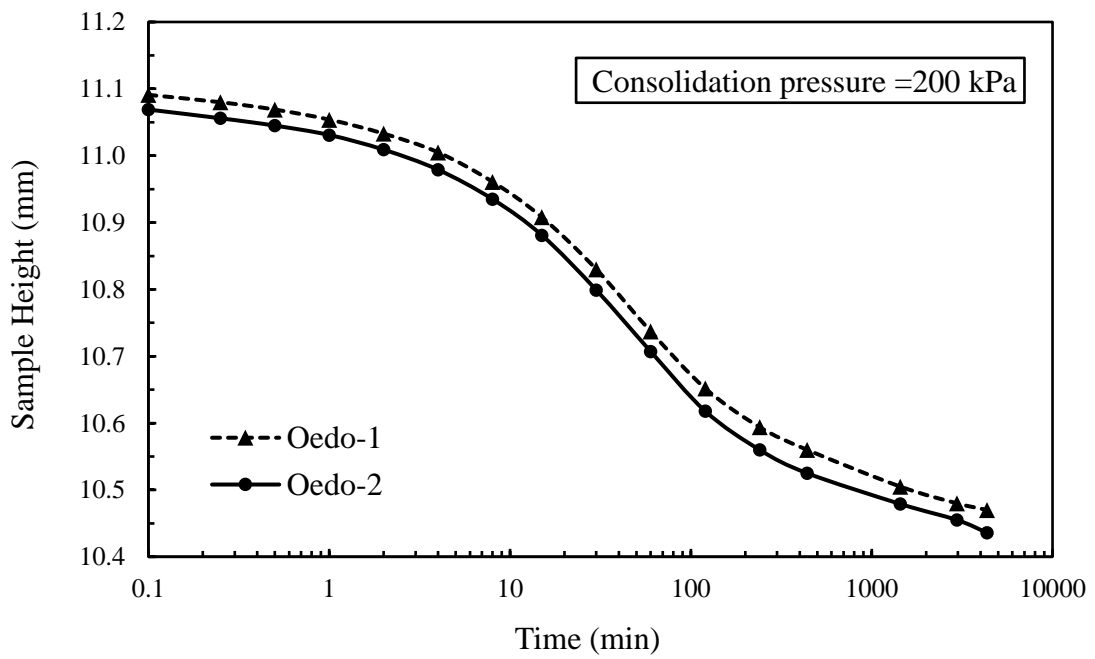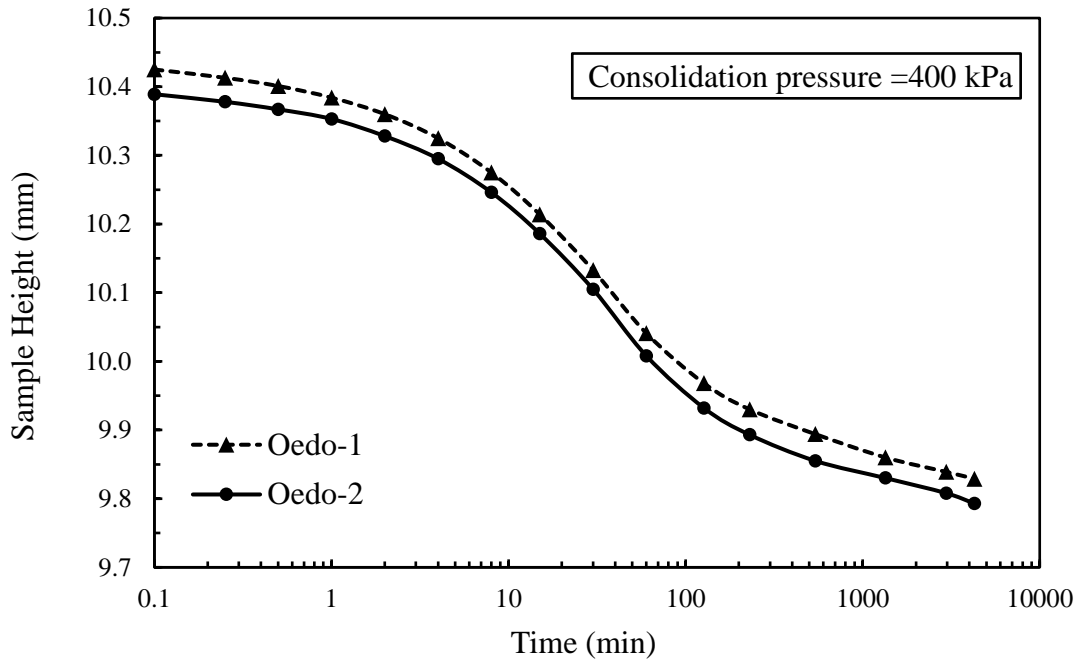
(g)

Figure 4. 1 Log time-settlement curves under each loading obtained from the Oedo-1 test and Oedo-2 test
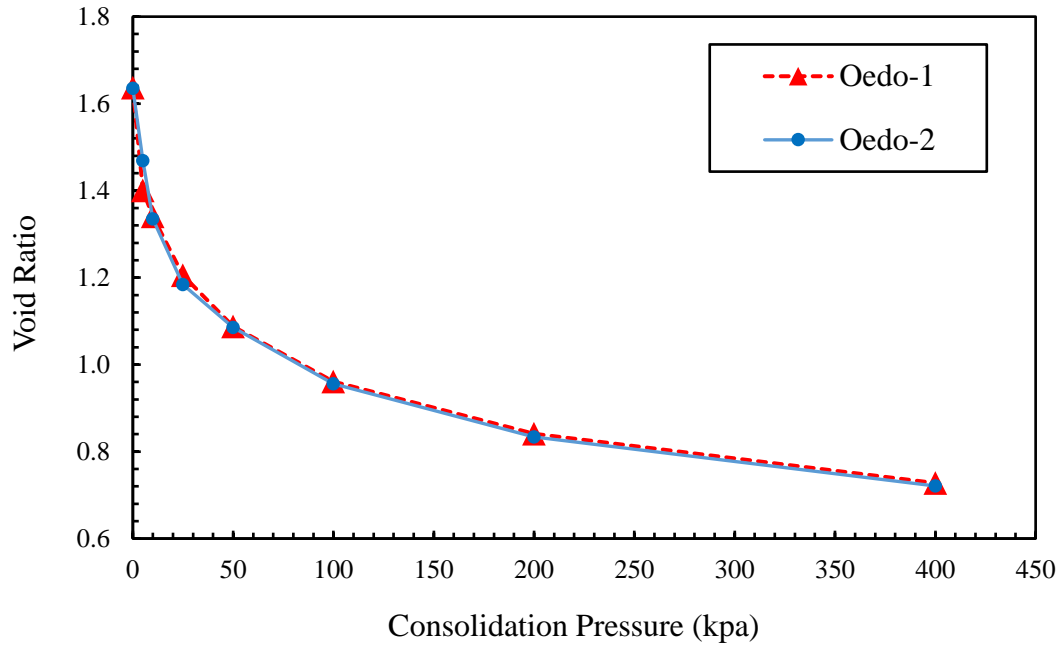


Figure 4. 2 Void ratio versus consolidation pressure obtained from the Oedo-1 test and Oedo-2 test

112
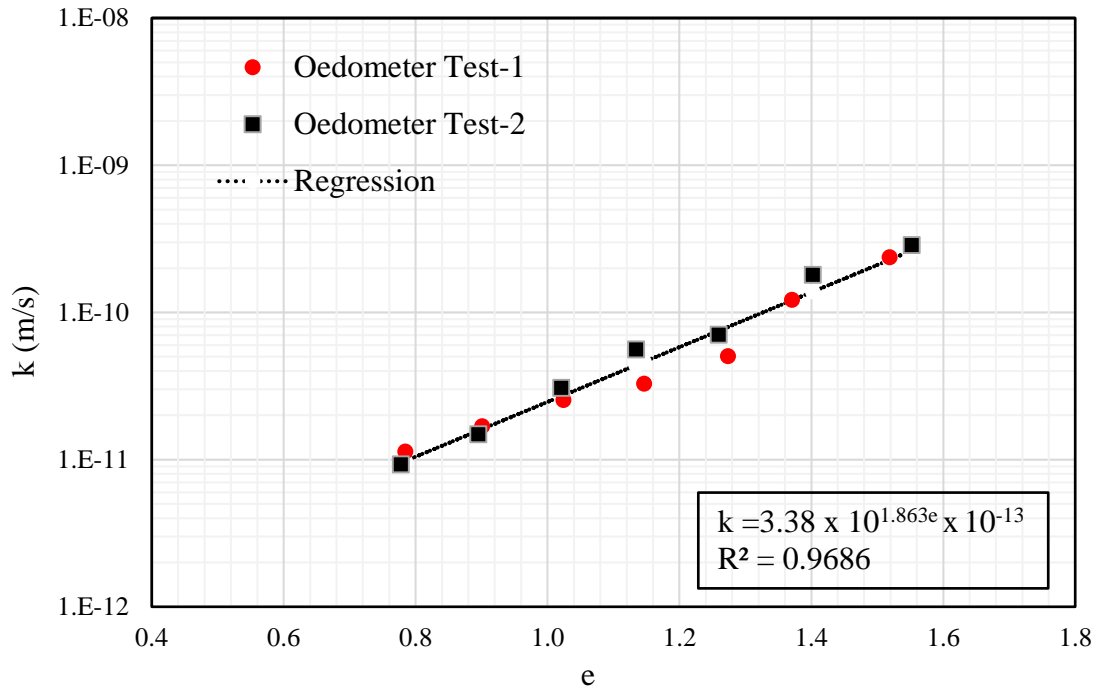
Figure 4. 3 Hydraulic conductivity versus void ratio

obtained from two oedometer tests
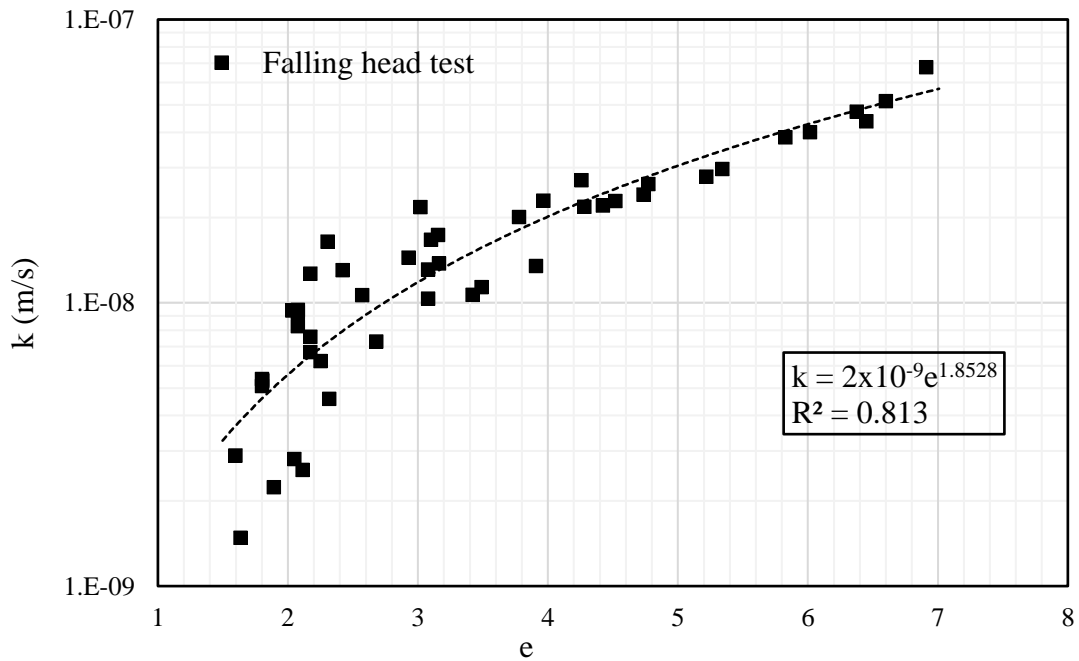


Figure 4. 4 Hydraulic conductivity versus void ratio

obtained from falling head tests
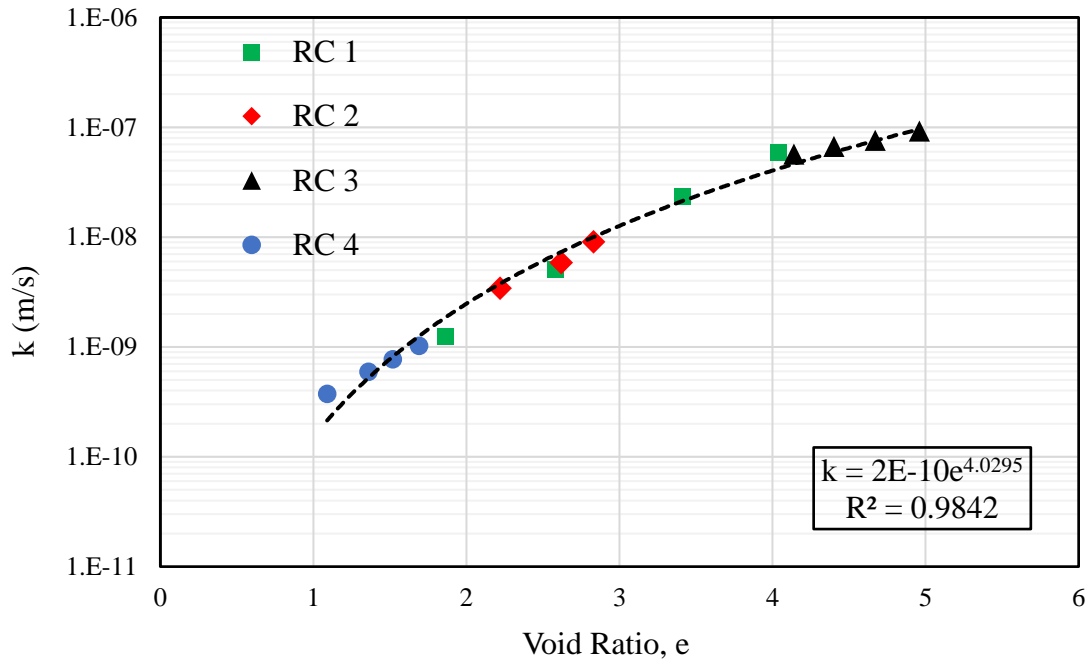
Figure 4. 5 Hydraulic conductivity versus void ratio obtained from Rowe cell tests
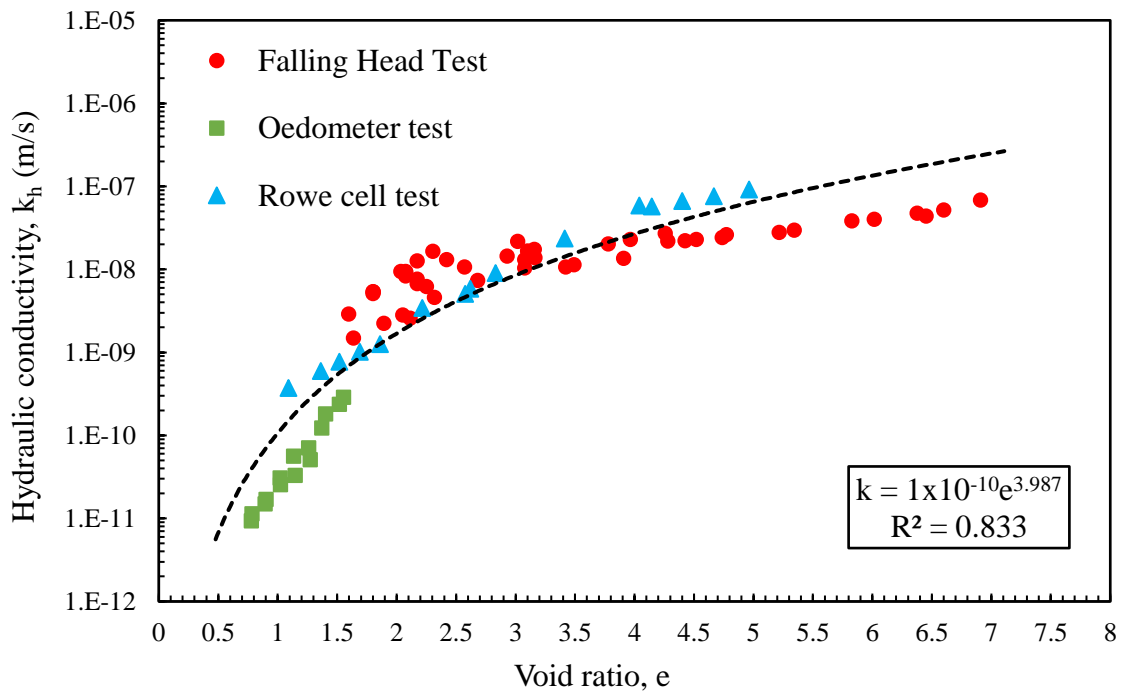


Figure 4. 6 Hydraulic conductivity versus void ratio obtained from three laboratory

tests
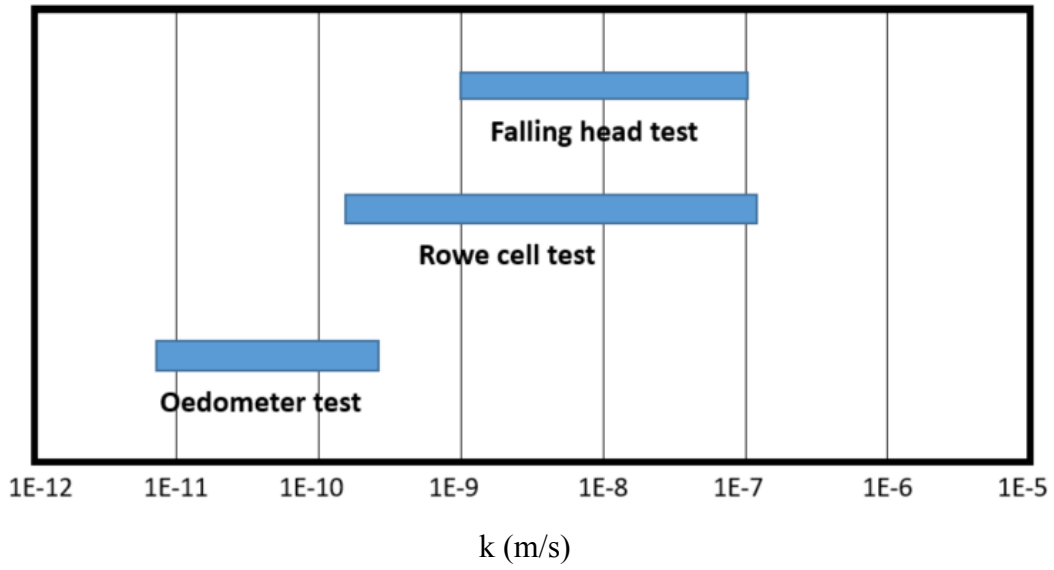
Figure 4. 7 The measurement range of three test methods
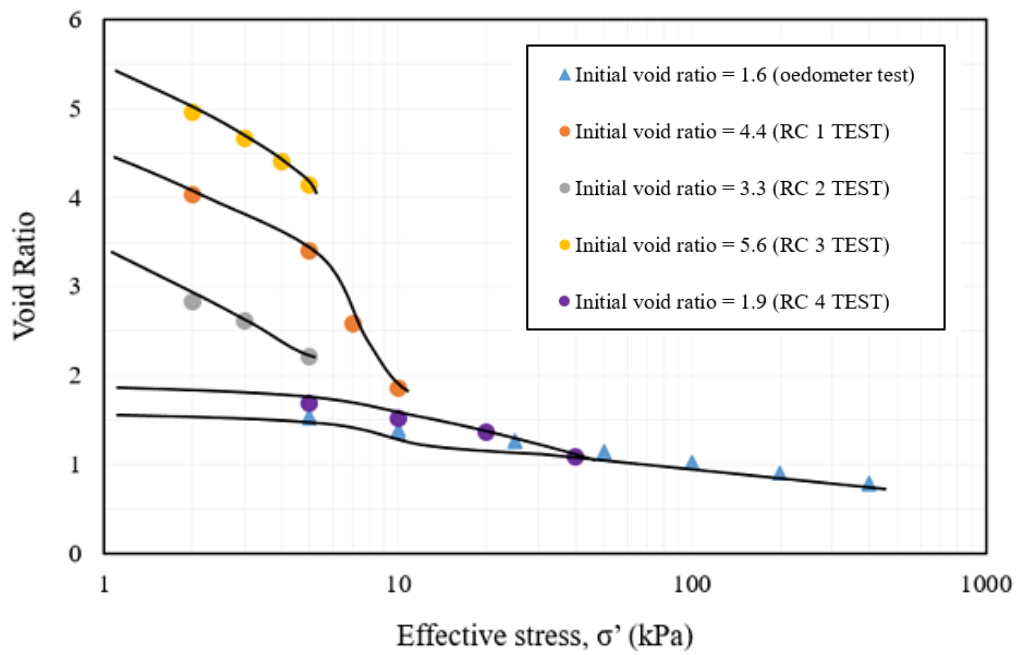


Figure 4. 8 The change of void ratio with effective stress (σ'-e)
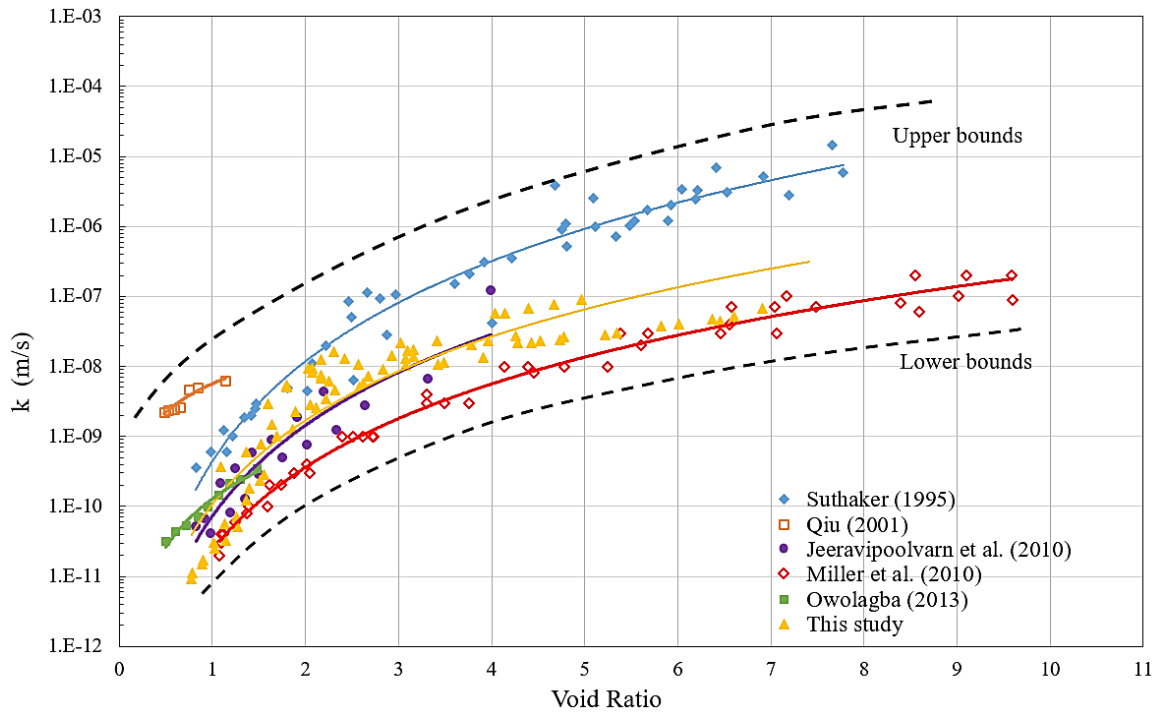
Figure 4. 9 Hydraulic conductivity database for oil sand tailings
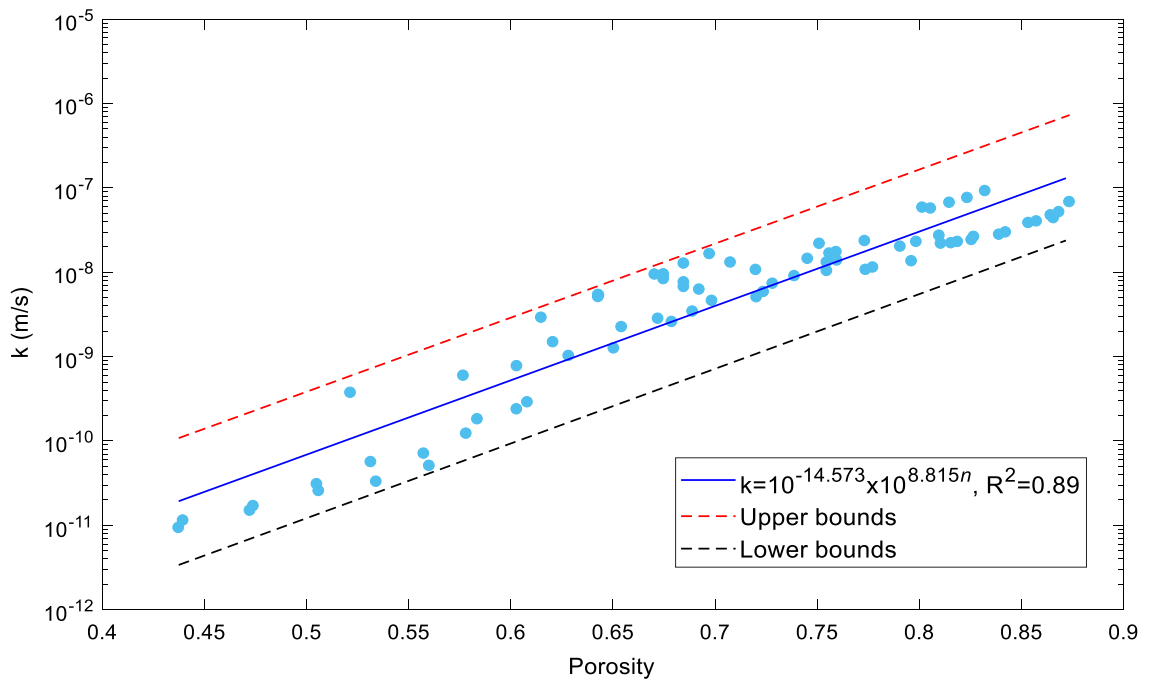


Figure 4. 10 Linear regression between the logarithm of hydraulic conductivity

and porosity for the mature fine tailings used in this study
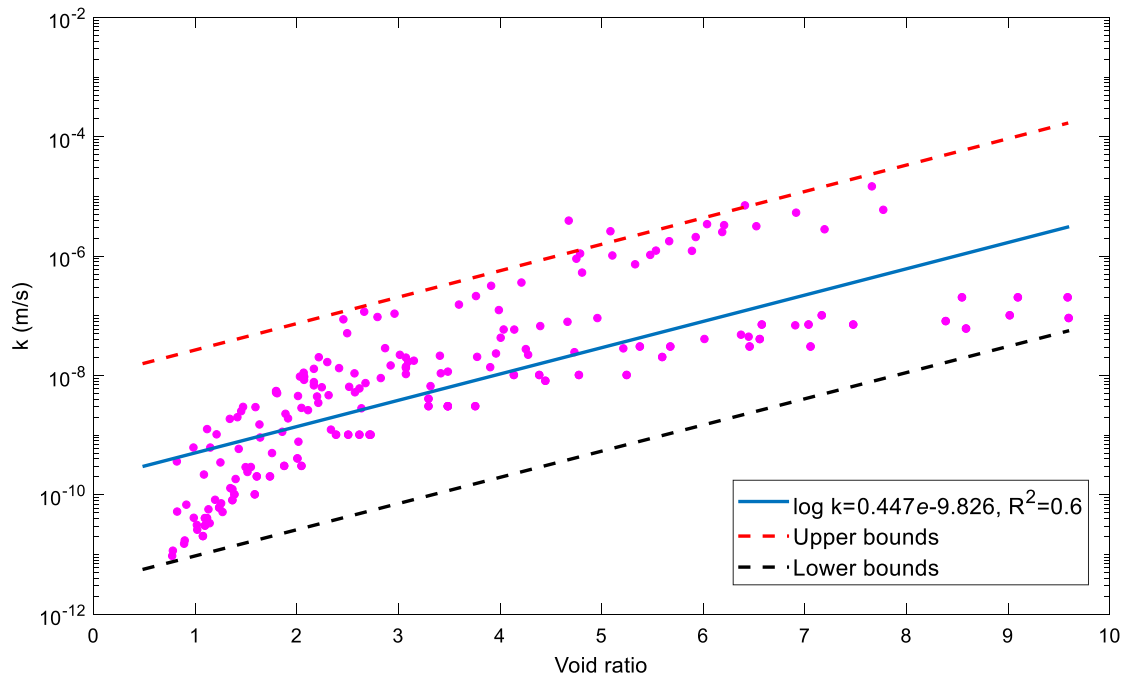
Figure 4. 11 Linear regression between the logarithm of hydraulic

conductivity and void ratio for oil sand tailings
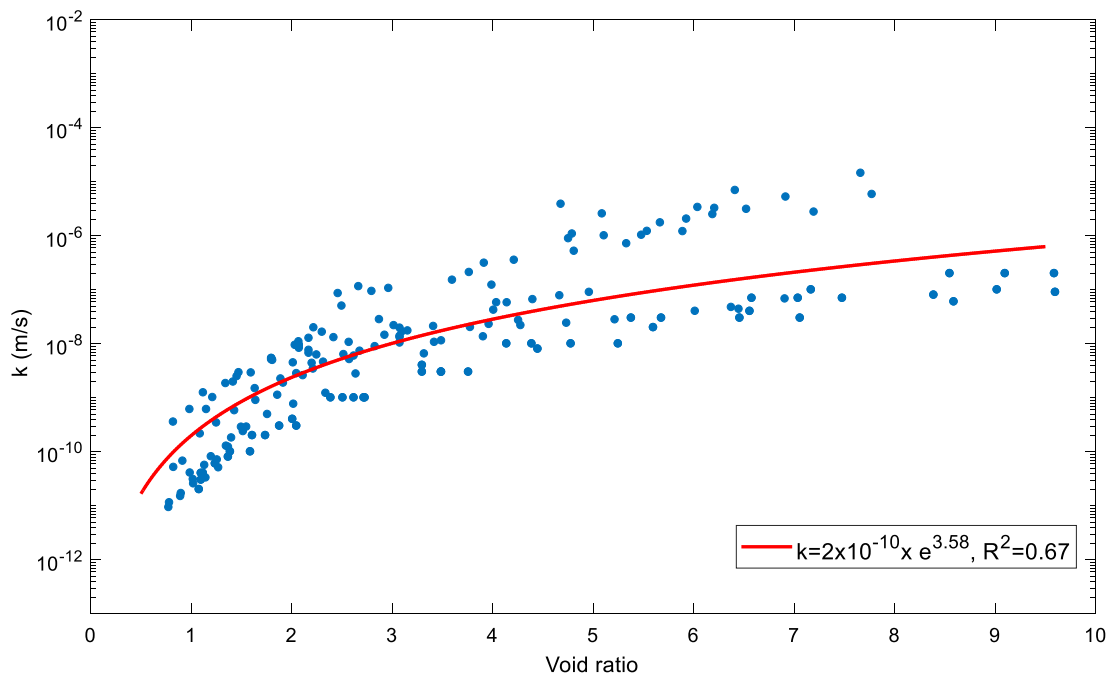


Figure 4. 12 Power regression between the hydraulic conductivity and void

ratio for oil sand tailings
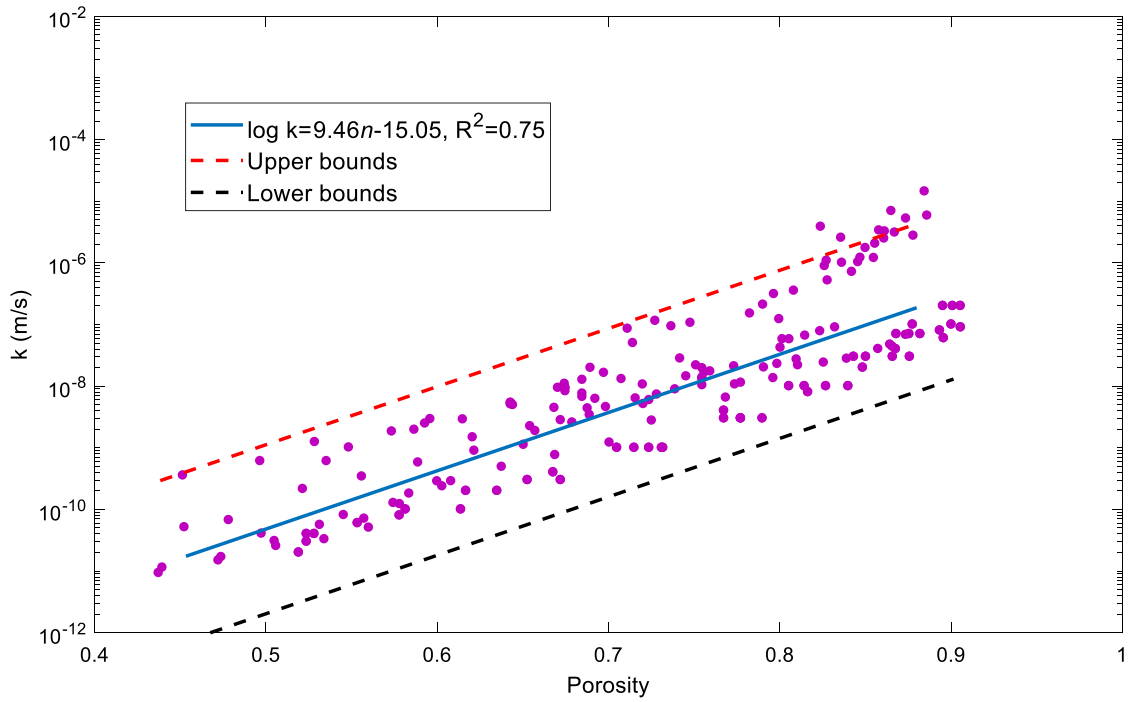
Figure 4. 13 Linear regression between the logarithm of hydraulic conductivity and porosity for oil sand tailings
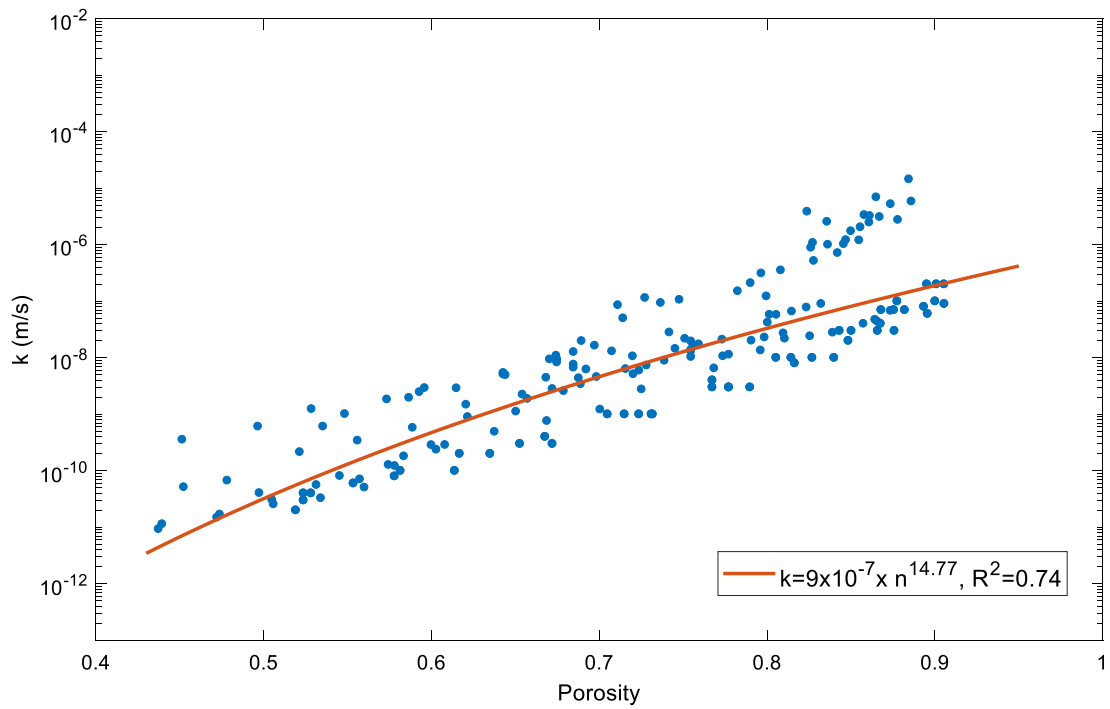


Figure 4. 14 Power regression between the hydraulic conductivity and porosity for oil sand tailings

(a)



(b)

(c)



(d)

120
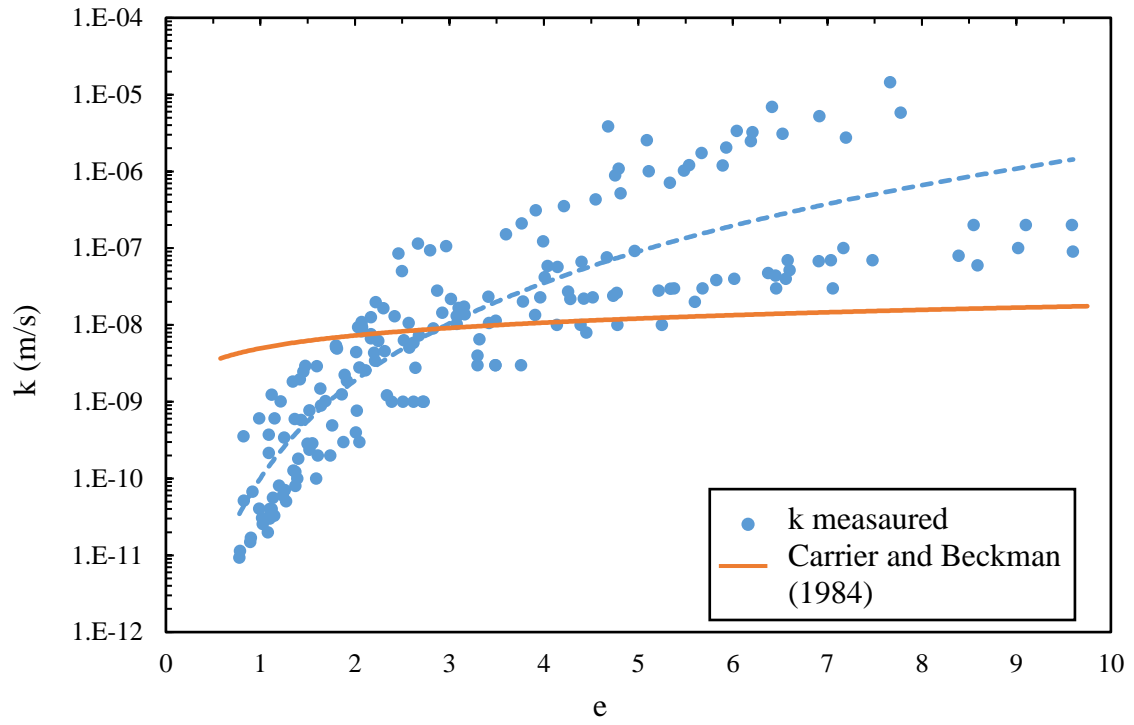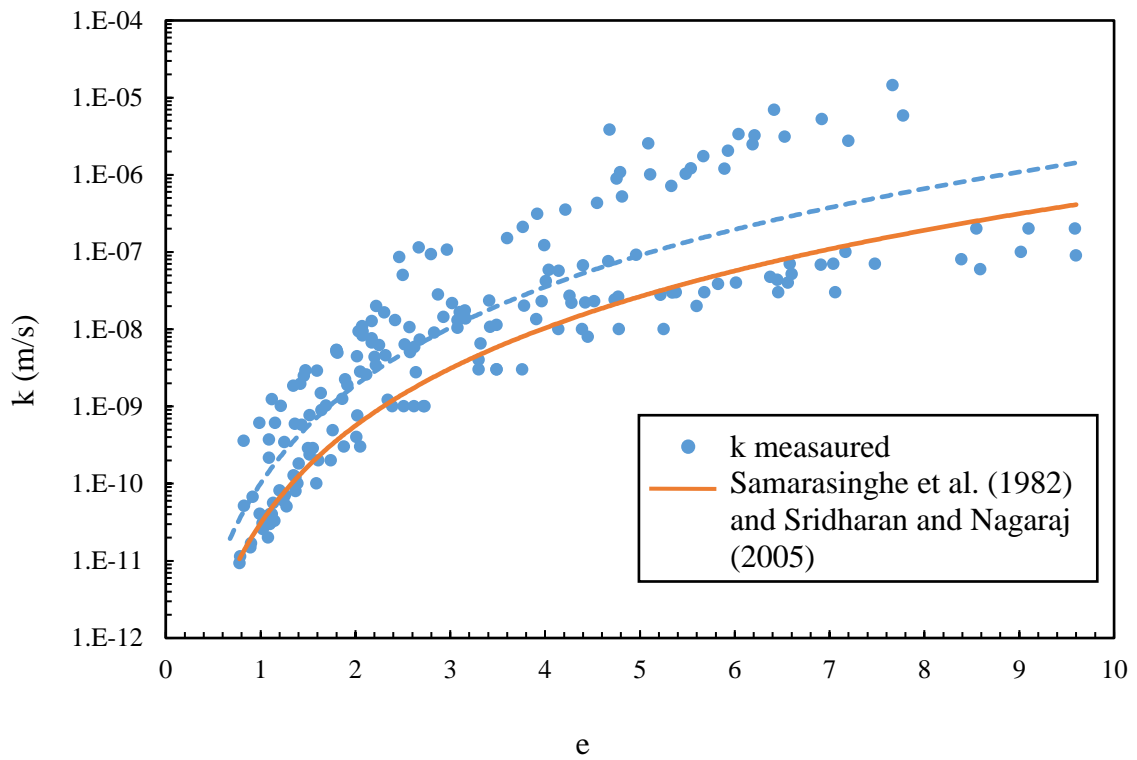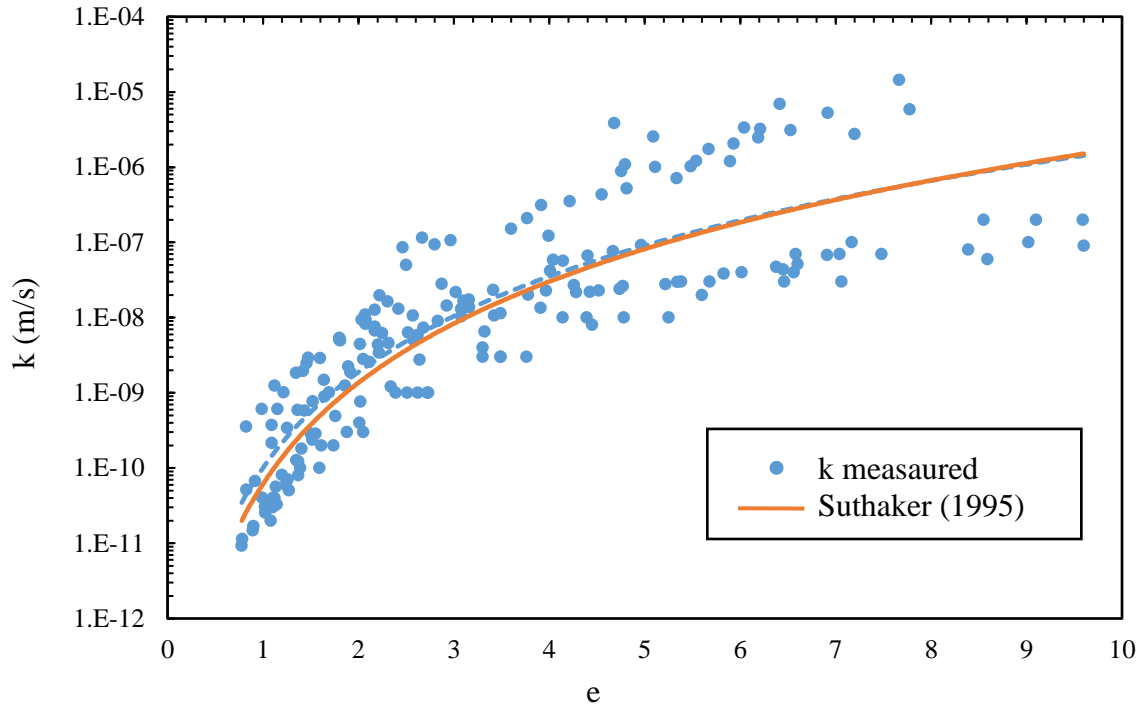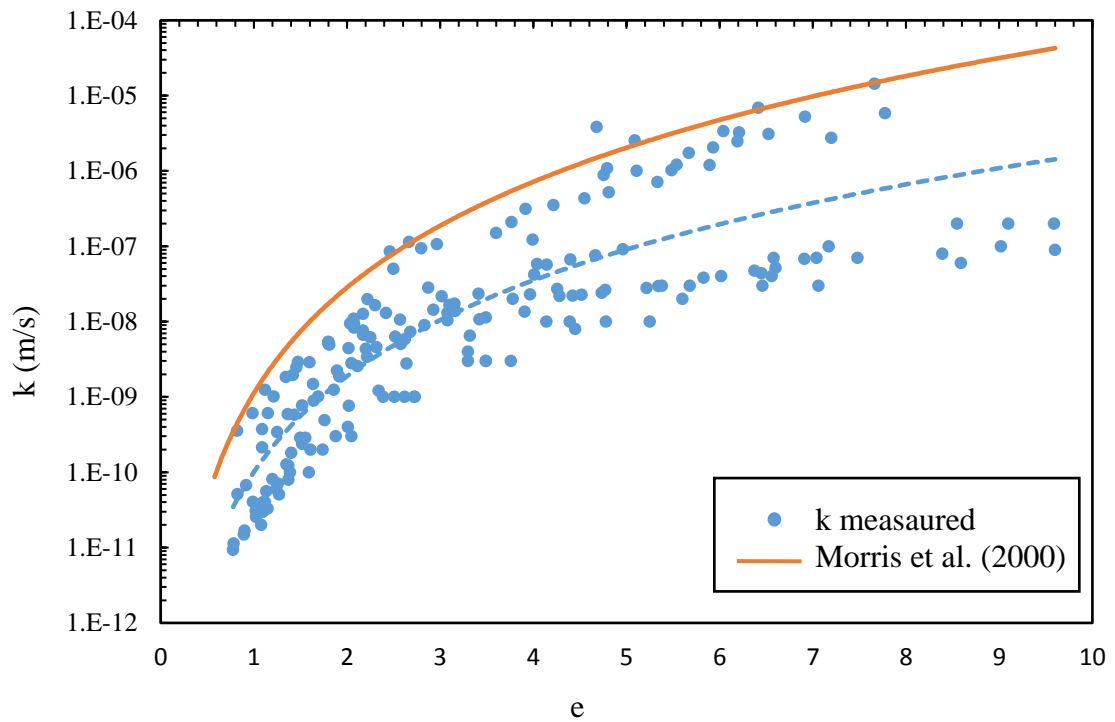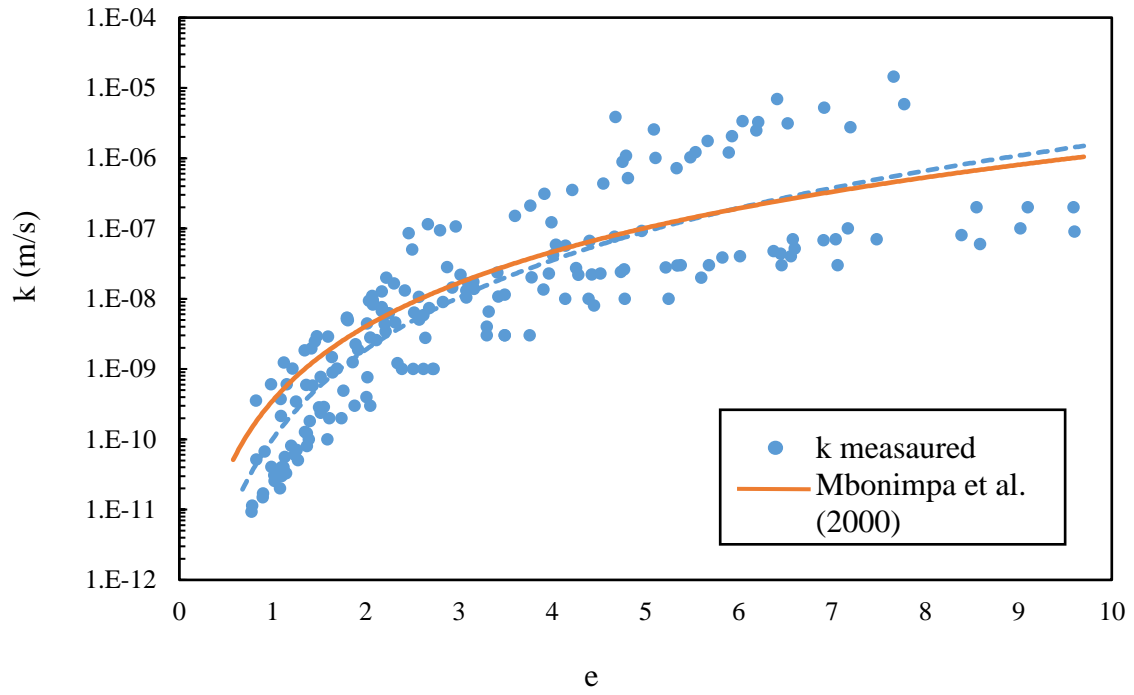
(e)
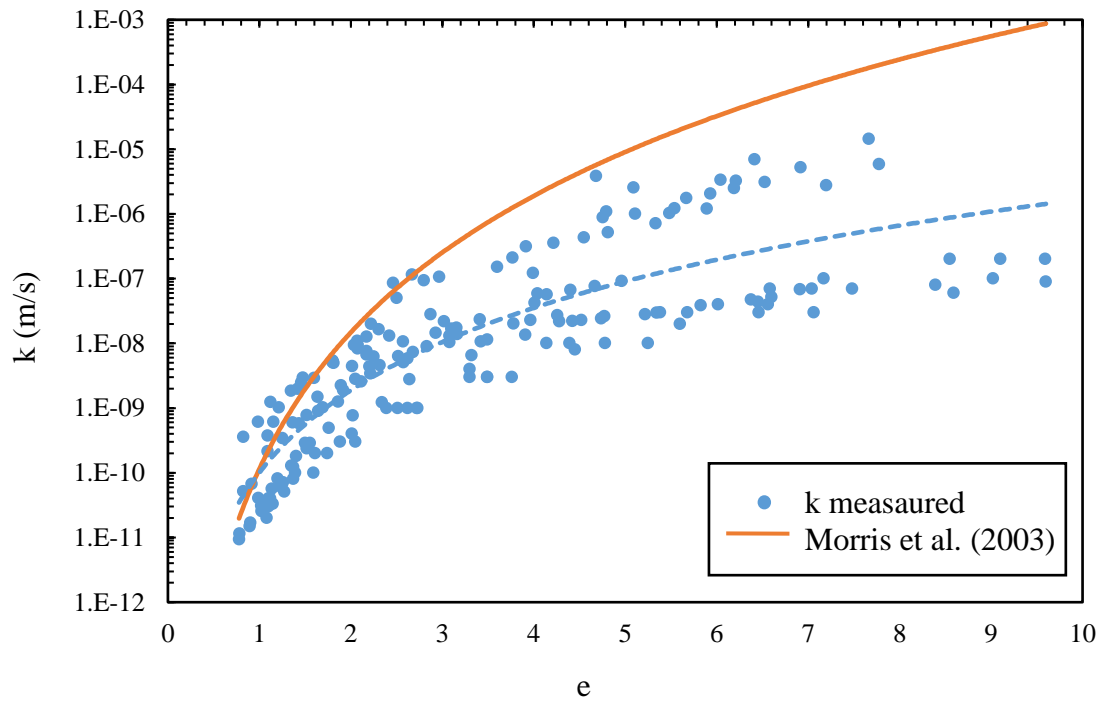


(f)

(g)
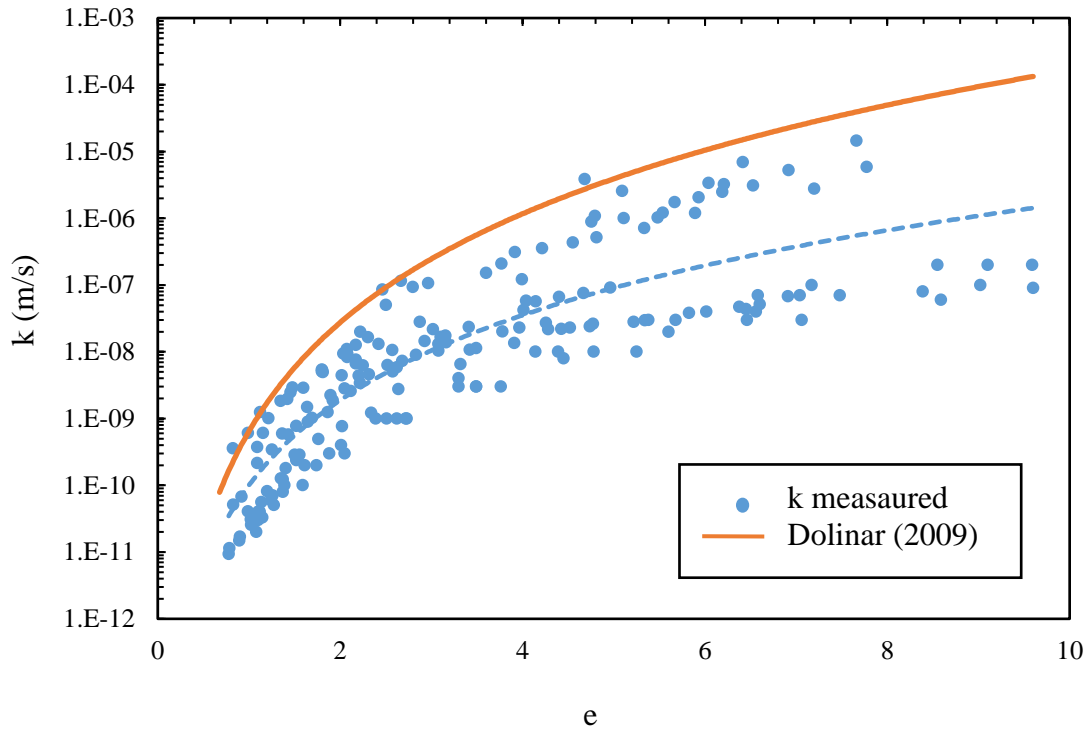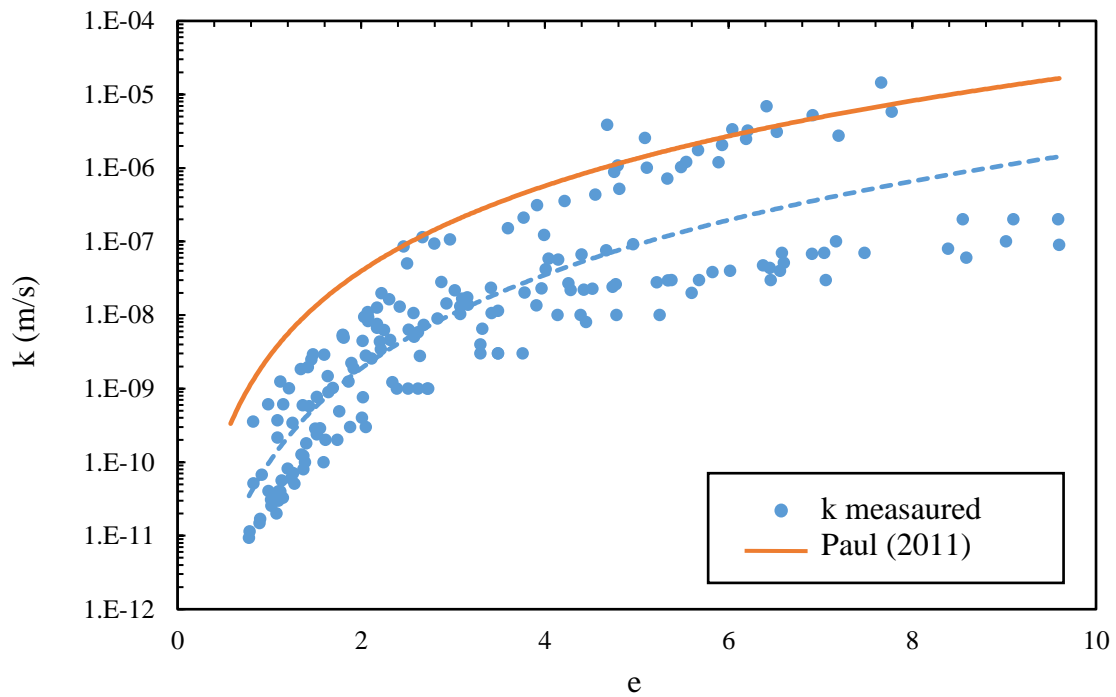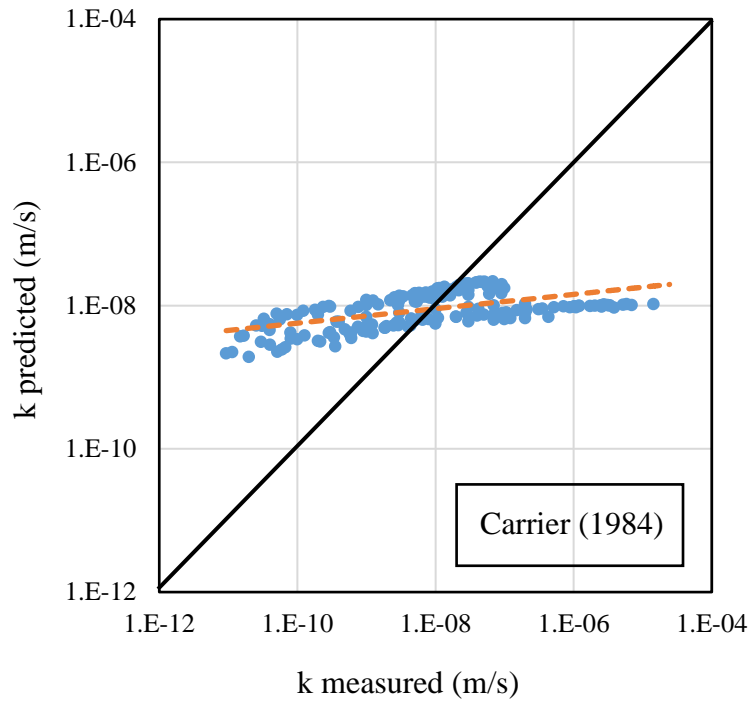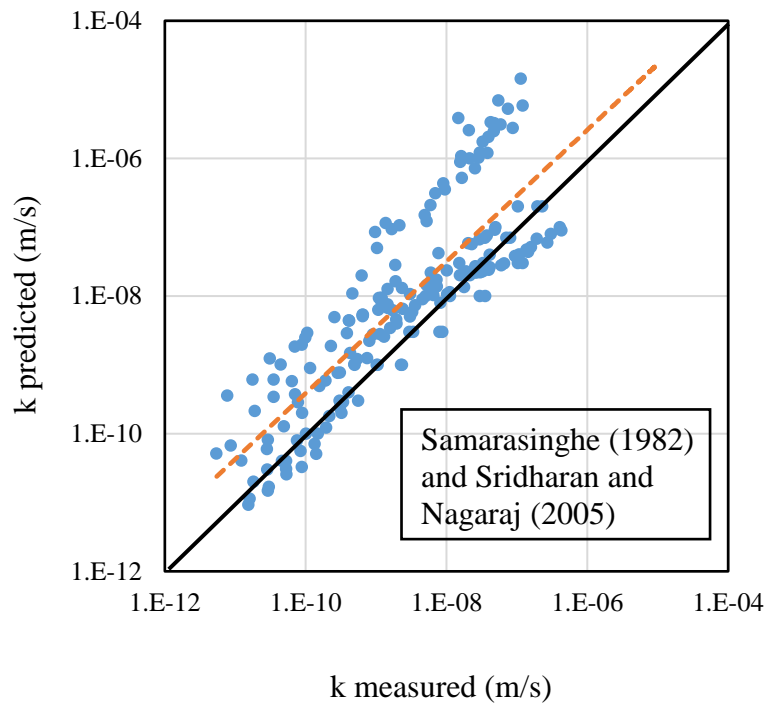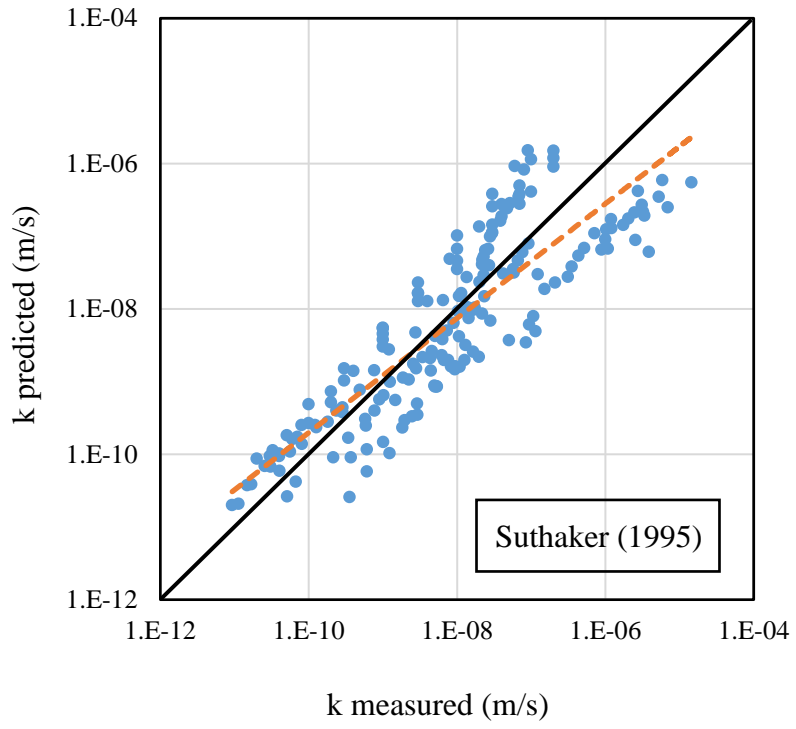


(h)

Figure 4. 15 The measured hydraulic conductivity data and the curve created by the 8 equations: a) Carrier and Beckman (1984, 1986); b) Samarasinghe et al. (1982) and Sridharan and Nagaraj (2005); c) Suthaker (1995); d) Morris et al. (2000); e) Mbonimpa et al. (2002); f) Morris et al. (2003); g) Dolinar (2009); h) Paul (2011).

(a)



(b)

(c)



(d)

124

(e)



(f)

(g)



(h)

Figure 4. 16 $k_{measured}$ versus $k_{predicted}$ calculated by the following equations： a) Carrier

and Beckman (1984, 1986); b) Samarasinghe et al. (1982) and Sridharan and Nagaraj (2005); c) Suthaker (1995); d) Morris et al. (2000); e) Mbonimpa et al. (2002); f) Morris et al. (2003); g) Dolinar (2009); h) Paul (2011).
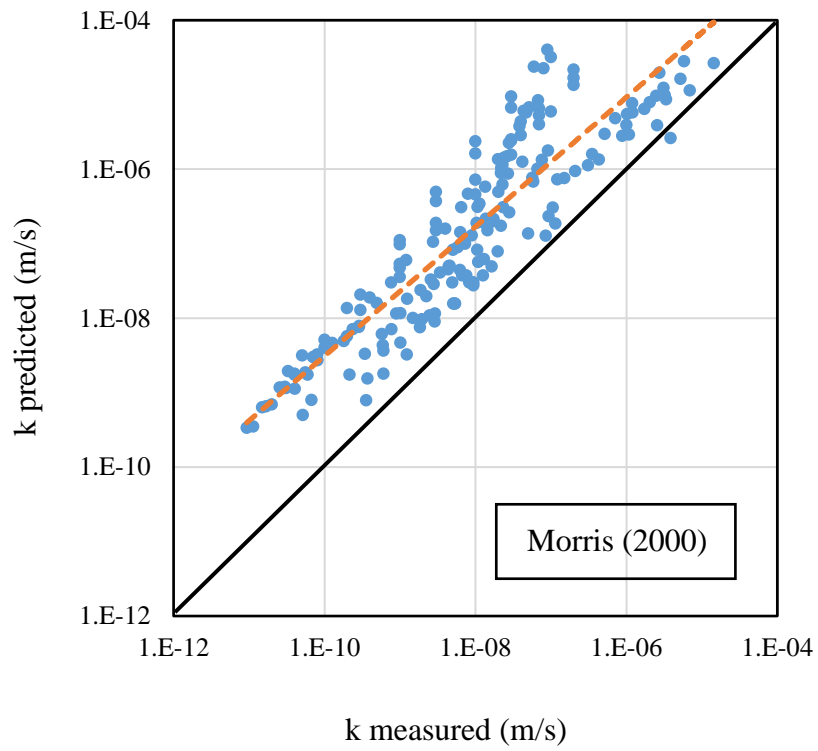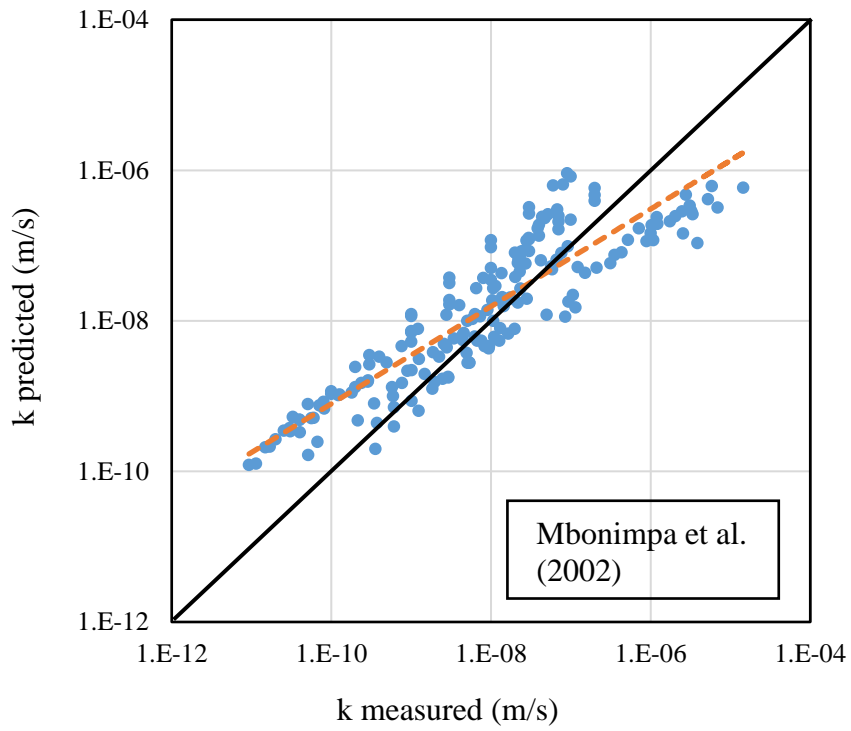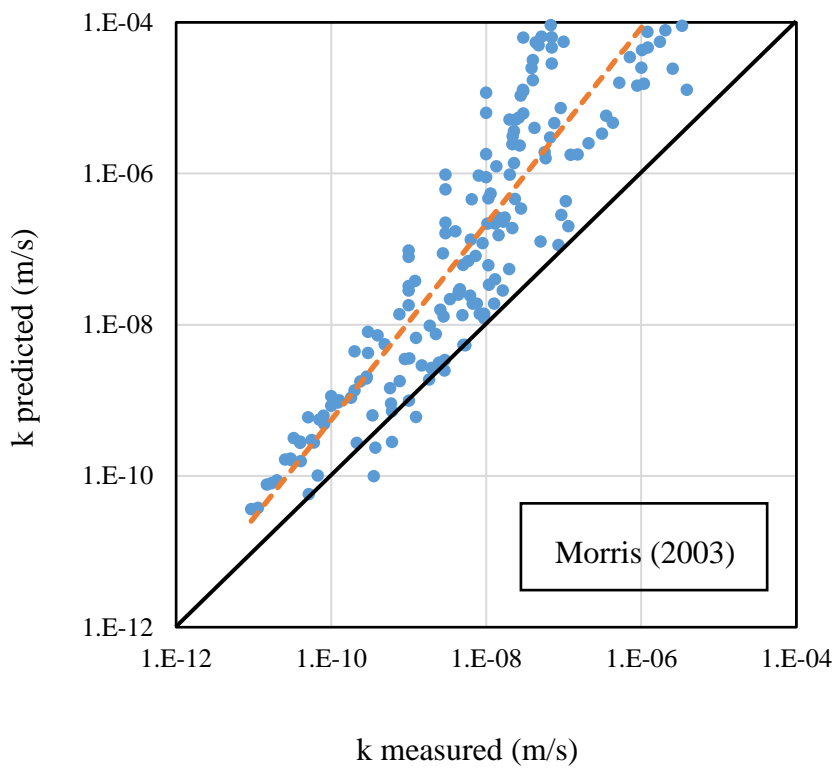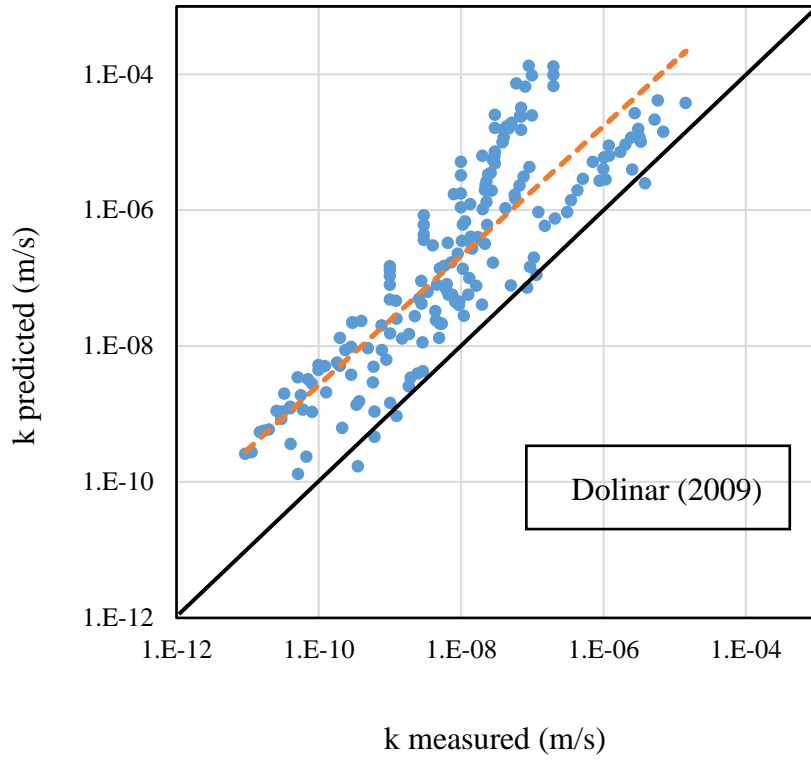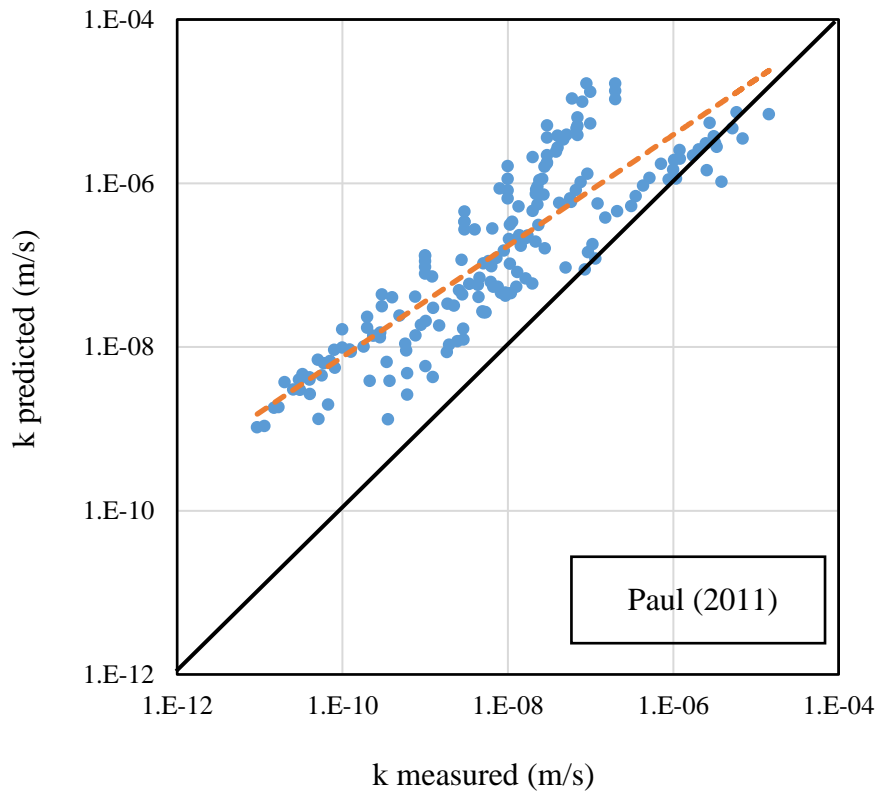
# CHAPTER 5    CONCLUSIONS AND RECOMMENDATIONS

## 5.1 Summary

In this thesis, the relationship between hydraulic conductivity and a wide range of void ratios for fine oil sand tailings is established. Three laboratory tests, the standard oedometer test, the falling head test and the Rowe cell test, are carried out to measure the hydraulic conductivity of MFT, and their results are presented. Based on the hydraulic conductivity data of this study together with the data reported in the literature, data regression models are developed to correlate the hydraulic conductivity with a wide range of void ratios (k-e relationship) for fine oil sand tailings. Empirical equations, which were proposed to predict the hydraulic conductivity for plastic soils, are evaluated for suitability and performance through the prediction of the hydraulic conductivity of fine oil sand tailings.

## 5.2 Conclusions

The main conclusions of the thesis are summarized as follows:

- According to the experimental results of three laboratory tests, the hydraulic conductivity of the MFT ranges from 9 x $10^{-12}$ (m/s) to 1 x $10^{-7}$ (m/s) within a void ratio range of 0.5 to 7. The ASTM-D2435 standard oedometer test is not applicable for MFT samples with an initial water content and void ratio higher than 65 % and 1.6, respectively. For MFT with a natural water content of 171%, the falling head test can measure the hydraulic conductivity for initial void ratios larger than 1.5. Rowe cell tests cover the measurement range of both the

standard oedometer tests and the falling head tests.

- The hydraulic conductivity measurements obtained from the Rowe cell tests are higher than the those from standard oedometer tests when the void ratio of MFT samples is less than 1.5 and higher than the measurements from falling head tests when the void ratio of MFT samples is larger than 3. Additionally, the initial void ratio affects the compressibility of MFT in low effective stress ($\sigma$'< 10 kPa) and this effect is diminished when the effective stress of MFT sample is larger than 10 kPa.

- The correlation relationship of k-n is superior to the relationship of k-e for both mature fine tailings samples and various fine oil sand tailings. It is suggested to use Equation 4.7 or 4.8 to predict the hydraulic conductivity of mature fine tailings, and Equations 4.13 or 4.14 to predict or analyze the hydraulic conductivity for various fine oil sand tailings.

- According to the evaluation results of empirical equations (presented in Chapter 4), equations proposed by Carrier (1984) and Morris et al. (2003), are not applicable for fine oil sand tailings to predict k values whereas equations proposed by Morris et al. (2000), Dolinar (2009) and Paul (2011) have relatively low predictive capacities and equations proposed by Samarasinghe et al. (1982) coupled with Sridharan and Nagaraj (2005), Suthaker (1995) and Mbonimpa et al. (2002) provide relatively accurate predictions of k values for fine oil sand tailings.

## 5.3 Engineering Significance

Compression of MFT appears to be very slow and MFT remains suspended in tailings pond for decades due to low permeability. Large volumes of MFT continually accumulate in tailings ponds, which produces the need for a large containment pond. This can lead to environmental concerns and MFT management challenges. Hydraulic conductivity is one of the most important properties of MFT as it controls consolidation behaviour. Clear understandings of hydraulic conductivity and its relationship with void ratio are essential to MFT management and treatment.

The practical significance of establishing the relationship between hydraulic conductivity and void ratio (k-e relationship) for fine oil sand tailings is to investigate the consolidation behaviour of these tailings, which undergo large settlement during consolidation (Suthaker 1995), based on large strain consolidation theories. These theories require explicit relationships between hydraulic conductivity and void ratio, as well as a relationship between void ratio and effective stress (Gibson et al. 1967). In addition, from a practical point of view, the k-e relationship can be used to quickly estimate the hydraulic conductivity in preliminary design stages for tailings disposal projects without excessive time or prohibitive testing costs.

## 5.4 Recommendations

The following recommendations are suggested for future studies:

- In order to countercheck the performance of the Rowe cell in terms of measuring the hydraulic conductivity of soft-fine grained geomaterials, additional testing using kaolinite or other general soils, placed in a slurry

consistency, should be performed in the Rowe cell test.

- A higher precision pressure equipment than the BK pressure panel used in this study is required for future research, particularly for soft fine-grained geomaterials where a low-pressure application is required.

- The possible factors which affect the hydraulic conductivity of fine oil sand tailings, particularly at the high void ratio, should be further investigated.

# BIBLIOGRAPHY

Adams, A. L. (2011). Laboratory evaluation of the constant rate of strain and constant head techniques for measurement of the hydraulic conductivity of fine grained soils (Doctoral dissertation, Massachusetts Institute of Technology).

Ahmed, S. I. (2013). A new approach for modeling the non-linear one dimensional consolidation behaviour of tailings (Doctoral dissertation, University of British Columbia).

Aiban, S. A., & Znidarčić, D. (1989). Evaluation of the flow pump and constant head techniques for permeability measurements. Geotechnique, 39(4), 655-666.

Al-Tabbaa, A., & Wood, D. M. (1987). Some measurements of the permeability of kaolin. Geotechnique, 37(4), 499-514.

Berilgen, S. A., Berilgen, M. M., & Ozaydin, I. K. (2006). Compression and permeability relationships in high water content clays. Applied Clay Science, 31(3), 249-261.

Bo, M. W., Arulrajah, A., & Choa, V. (1998). The hydraulic conductivity of Singapore marine clay at Changi. Quarterly Journal of Engineering Geology and Hydrogeology, 31(4), 291-299.

Bo, M. W., Sin, W. K., Choa, V., & Ing, T. C. (2003). Compression tests of ultra-soft soil using an hydraulic consolidation cell.

Bo, M. W., Choa, V., & Wong, K. S. (2010). Constant rate of loading test on ultra-soft soil.

BRAINARD.KILMAN Installation and operation instructions

Budhu, M. (2008). SOIL MECHANICS AND FOUNDATIONS, (With CD). John Wiley & Sons.

Casagrande, A., & Fadum, R. E. (1900). Notes on soil testing for engineering purposes.

Carman, P. C. (1937). Fluid flow through granular beds. Transactions-Institution of Chemical Engineeres, 15, 150-166.

Carrier, W. D., & Beckman, J. F. (1984). Correlations between index tests and the properties of remoulded clays. Geotechnique, 34(2), 211-228.

Carrier, W. D. (1986). Discussion: Consolidation parameters derived from index tests. Géotechnique, 36(2), 291-292.

Cao, Y. P., Wang, X. S., Du, L., Ding, J. W., & Deng, Y. F. (2014). A method of determining nonlinear large strain consolidation parameters of dredged clays. Water Science and Engineering, 7(2), 218-226.

Chapuis, R. P., & Aubertin, M. (2003). On the use of the Kozeny Carman equation to predict the hydraulic conductivity of soils. Canadian Geotechnical Journal, 40(3), 616-628.

Chapuis, R. P. (2012). Predicting the saturated hydraulic conductivity of soils: a review.

Bulletin of engineering geology and the environment, 71(3), 401-434.

Das, B. M., & Sobhan, K. (2013). Principles of geotechnical engineering. Cengage Learning.

Das, B. M. (2013). Advanced soil mechanics. CRC Press.

De Bruyn, C. M. A., Collins, L. F., & Williams, A. A. B. (1957). The specific surface, water affinity, and potential expansiveness of clays. Clay Minerals Bulletin, 3, 120-128.

Deng, Y. F., Tang, A. M., Cui, Y. J., & Li, X. L. (2011). Study on the hydraulic conductivity of Boom clay. Canadian Geotechnical Journal, 48(10), 1461-1470.

Dolinar, B. (2009). Predicting the hydraulic conductivity of saturated clays using plasticity-value correlations. Applied Clay Science, 45(1), 90-94.

Farrar, D. M., & Coleman, J. D. (1967). The correlation of surface area with other properties of nineteen British clay soils. Journal of Soil Science, 18(1), 118-124.

Fernandez, F., & Quigley, R. M. (1985). Hydraulic conductivity of natural clays permeated with simple liquid hydrocarbons. Canadian Geotechnical Journal, 22(2), 205-214.

Fernandez, F., & Quigley, R. M. (1991). Controlling the destructive effects of clay–organic liquid interactions, by application of effective stresses. Canadian Geotechnical Journal, 28(3), 388-398.

Gibson, R. E., England, G. L., & Hussey, M. J. L. (1967). The Theory of One-Dimensional Consolidation of Saturated Clays: 1. Finite Non-Linear Consildation of Thin Homogeneous Layers. Geotechnique, 17(3), 261-273.

Gofar, N., & Kassim, K. A. (2006). Determination of coefficient of rate of horizontal consolidation of peat soil.

Guo, Y. (2012). Electrokinetic Dewatering of Oil Sands Tailings (Doctoral dissertation, The University of Western Ontario London).

Guo, Y. (2017). Electrokinetic Consolidation of Oil Sands Tailings: An Experimental and Numerical Study.

Head, K. H. (1982). Manual of soil laboratory testing. volume 2: permeability, shear strength and compressibility tests. Manual of Soil Laboratory Testing, 48(10), 335-747.

Head, K. H., & Epps, R. (1986). Manual of soil laboratory testing (Vol. 3, pp. 1129-1196). London: Pentech Press.

Holtz, W.G. and Kovacs, W.D. (1981). An Introduction to Geotechnical Engineering. Prentice-Hall Inc., Englewood Cliffs, New Jersey

Islam, S. (2014). Thickening of Mature Fine Oil Sands Tailings (Doctoral dissertation, The University of Western Ontario).

Jeeravipoolvarn, S. (2005). Compression behaviour of thixotropic oil sands tailings

(Doctoral dissertation, University of Alberta).

Jeeravipoolvarn, S. (2010). Geotechnical Behavior of In-Line Thickened Oil Sands Tailings.

Jeeravipoolvarn, S (2015). Revisiting the large strain consolidation test for oil sands. Conference: Tailings and Mine Waste 2015, At Vancouver.

Krizek, R. J., & Somogyi, F. (1984). Perspectives on modelling consolidation of dredged materials. In Sedimentation Consolidation Models—Predictions and Validation: (pp. 296-332). ASCE.

Locat, J., Lefebvre, G., & Ballivy, G. (1984). Mineralogy, chemistry, and physical properties interrelationships of some sensitive clays from Eastern Canada. Canadian Geotechnical Journal, 21(3), 530-540.

Mandal, J. N., & Divshikar, D. G. (1995). Soil testing in civil engineering. AA Balkema.

Mbonimpa, M., Aubertin, M., Chapuis, R. P., & Bussière, B. (2002). Practical pedotransfer functions for estimating the saturated hydraulic conductivity. Geotechnical and Geological Engineering, 20(3), 235-259.

Mesri, G., Shahien, M., & Feng, T. W. (1995, May). Compressibility parameters during primary consolidation. In Proceedings of the international symposium on compression and consolidation of clayey soils, Hiroshima (Vol. 2, pp. 1021-1037).

Miller, W. G. (2010). Comparison of geoenvironmental properties of caustic and noncaustic oil sand fine tailings.

Morris, P. H., Lockington, D. A., & Apelt, C. J. (2000). Correlations for mine tailings consolidation parameters. International Journal of Surface Mining, Reclamation and Environment, 14(3), 171-182.

Morris, P. H. (2003). Compressibility and permeability correlations for fine-grained dredged materials. Journal of waterway, port, coastal, and ocean engineering, 129(4), 188-191.

Muhunthan, B. (1991). Liquid limit and surface area of clays. Geotechnique (United Kingdom).

Nagaraj, T. S., Pandian, N. S., & Narasimha Raju, P. S. R. (1991). An approach for prediction of compressibility and permeability behaviour of sand-bentonite mixes. Indian Geotechnical Journal, 21(3), 271-282.

Nagaraj, T. S., Pandian, N. S., & Narasimha-Raju, P. S. R. (1993). Stress state-permeability relationships for fine-grained soils. Geotechnique, 43(2).

Nagaraj, T. S., Pandian, N. S., & Raju, P. N. (1994). Stress-state—permeability relations for overconsolidated clays. Geotechnique, 44(2), 349-352.

Nishida, Y. O. S. H. I. C. H. I. K. A., & Nakagawa, S. (1969). Water permeability and plastic index of soils. In Proceedings of IASH-UNESCO Symposium Tokyo,

Pub (Vol. 89, pp. 573-578).

Olsen, H. W. (1966). Darcy's law in saturated kaolinite. Water Resources Research, 2(2), 287-295.

Olson, R. E., & Daniel, D. E. (1981). Measurement of the hydraulic conductivity of fine-grained soils. In Permeability and groundwater contaminant transport. ASTM International.

Olsen, H. W., Nichols, R. W., & Rice, T. L. (1985). Low gradient permeability measurements in a triaxial system. Geotechnique, 35(2), 145-157.

Owolagba, J. O. (2013). Dewatering Behavior of Centrifuged Oil Sand Fine Tailings for Surface Deposition (Doctoral dissertation, Faculty of Graduate Studies and Research, University of Regina).

Pane, V., & Schiffman, R. L. (1997). The permeability of clay suspensions. Geotechnique, 47(2), 273-288.

Paul, A. C. (2011). Statistical modeling for tailings consolidation using index properties (Doctoral dissertation, Faculty of Graduate Studies and Research, University of Regina).

Prakash, K., & Sridharan, A. (2002). Determination of liquid limit from equilibrium sediment volume. GEOTECHNIQUE-LONDON-, 52(9), 693-696.

Proskin, S., Sego, D., & Alostaz, M. (2010). Freeze–thaw and consolidation tests on

Suncor mature fine tailings (MFT). Cold Regions Science and Technology, 63(3), 110-120.

Qiu, Y., & Sego, D. C. (2001). Laboratory properties of mine tailings. Canadian Geotechnical Journal, 38(1), 183-190.

Standard, A. S. T. M. D2435/D2435M-11, 2011. Standard test method for one-dimensional consolidation properties of soils using incremental loading. Annual Book of ASTM (American Society of Testing Material) Standards, 04.08. ASTM International, West Conshohocken, PA.

Standard, A. S. T. M. (2007). D5856-95. Standard test method for measurement of hydraulic conductivity of porous material using a rigid-wall, compaction-mould permeameter. Annual book of ASTM (American Society of Testing Material) Standards, 4.

Samarasinghe, A. M., Huang, Y. H., & Drnevich, V. P. (1982). Permeability and consolidation of normally consolidated soils. Journal of the Geotechnical Engineering Division, 108(6), 835-850.

Sitharam, T. G., Sivapullaiah, P. V., & Subba Rao, K. S. (1995). Shrinkage behaviour of compacted unsaturated soils. In PROCEEDINGS OF THE FIRST INTERNATIONAL CONFERENCE ON UNSATURATED SOILS/ UNSAT'95/ PARIS/ FRANCE /6-8 SEPTEMBER 1995. VOLUME 1.

Sivapullaiah, P. V., Sridharan, A., & Stalin, V. K. (2000). Hydraulic conductivity of

bentonite-sand mixtures. Canadian Geotechnical Journal, 37(2), 406-413.

Somogyi, F. (1979). Analysis and prediction of phosphatic clay consolidation. Implementation Package.

Sridharan, A., Rao, S. M., & Murthy, N. S. (1986). Liquid limit of montmorillonite soils.

Sridharan, A., Rao, S. M., & Murthy, N. S. (1988). Liquid limit of kaolinitic soils. Geotechnique, 38(2), 191-198.

Sridharan, A., & Nagaraj, H. B. (2005). Hydraulic conductivity of remolded fine-grained soils versus index properties. Geotechnical and Geological Engineering, 23(1), 43-60.

Stepkowska, E. T., Thorborg, B., & Wichman, B. (1996). Stress state-permeability relationships for dredged sludge and their dependence on microstructure. In International Journal of Rock Mechanics and Mining Sciences and Geomechanics Abstracts (Vol. 3, No. 33, p. 121A).

Suthaker, N. N. (1995). Geotechnics of oil sand fine tailings.

Taylor, D. W. (1942). Research on consolidation of clays (Vol. 82). Massachusetts Institute of Technology.

Tanaka, H., & Locat, J. (1999). A microstructural investigation of Osaka Bay clay: the impact of microfossils on its mechanical behaviour. Canadian Geotechnical Journal, 36(3), 493-508.

Tavenas, F., Jean, P., Leblond, P., & Leroueil, S. (1983). The permeability of natural

soft clays. Part II: Permeability characteristics. Canadian Geotechnical Journal,

20(4), 645-660.

Tang, A. M., Cui, Y. J., & Le, T. T. (2008). A study on the thermal conductivity of

compacted bentonites. Applied Clay Science, 41(3), 181-189.

Xu, Y., Dabros, T., & Kan, J. (2008). Filterability of oil sands tailings. Process Safety

& Environmental Protection, 86(4), 268-276.

Yoshikuni, H., Okada, M., Ikegami, S., & Hirao, T. (1995). One-dimensional

consolidation analysis based on an elasto-viscous liquid model. Compression

and Consolidation of Clayey Soils, 505-512.

Zhang, R. (2016). Electrokinetics and Vacuum Combined Dewatering of Oil Sand
Tailings (Doctoral dissertation, The University of Western Ontario).

# VITAE

**NAME:**         Mingyue LIU

**Education:**     09/2011-07/2015 B.E.,

Department of Civil Engineering, Shandong University of Architecture

09/2015-08/2017 M.Esc.,

Department of Civil and Environmental Engineering. University of Western Ontario

**Employment**:   09/2015-08/2017, Research Assistant,

Department of Civil and Environmental Engineering. University of Western Ontario

09/2016-08/2017, Teaching Assistant,

Department of Civil and Environmental Engineering. University of Western Ontario